



CHORUS

This is the accepted manuscript made available via CHORUS. The article has been published as:

Jet measurements in heavy ion physics

Megan Connors, Christine Nattrass, Rosi Reed, and Sevil Salur

Rev. Mod. Phys. **90**, 025005 — Published 12 June 2018

DOI: [10.1103/RevModPhys.90.025005](https://doi.org/10.1103/RevModPhys.90.025005)

Review of Jet Measurements in Heavy Ion Collisions

Megan Connors,^{1,2} Christine Nattrass,³ Rosi Reed,⁴ and Sevil Salur⁵

¹Georgia State University, Atlanta, GA,
USA-30302.

²RIKEN BNL Research Center, Upton,
NY 11973-5000

³University of Tennessee, Knoxville, TN,
USA-37996.

⁴Lehigh University, Bethlehem, PA,
USA-18015.

⁵Rutgers University, Piscataway,
NJ USA-08854.

All authors contributed equally to this manuscript. Authors are listed alphabetically.

(Dated: December 19, 2017)

A hot, dense medium called a Quark Gluon Plasma (QGP) is created in ultrarelativistic heavy ion collisions. Early in the collision, hard parton scatterings generate high momentum partons that traverse the medium, which then fragment into sprays of particle called jets. Understanding how these partons interact with the QGP and fragment into final state particles provides critical insight into quantum chromodynamics. Experimental measurements from high momentum hadrons, two particle correlations, and full jet reconstruction at the Relativistic Heavy Ion Collider (RHIC) and the Large Hadron Collider (LHC) continue to improve our understanding of energy loss in the QGP. Run 2 at the LHC recently began and there is a jet detector at RHIC under development. Now is the perfect time to reflect on what the experimental measurements have taught us so far, the limitations of the techniques used for studying jets, how the techniques can be improved, and how to move forward with the wealth of experimental data such that a complete description of energy loss in the QGP can be achieved.

Measurements of jets to date clearly indicate that hard partons lose energy. Detailed comparisons of the nuclear modification factor between data and model calculations led to quantitative constraints on the opacity of the medium to hard probes. However, while there is substantial evidence for softening and broadening jets through medium interactions, the difficulties comparing measurements to theoretical calculations limit further quantitative constraints on energy loss mechanisms. Since jets are algorithmic descriptions of the initial parton, the same jet definitions must be used, including the treatment of the underlying heavy ion background, when making data and theory comparisons. We call for an agreement between theorists and experimentalists on the appropriate treatment of the background, Monte Carlo generators that enable experimental algorithms to be applied to theoretical calculations, and a clear understanding of which observables are most sensitive to the properties of the medium, even in the presence of background. This will enable us to determine the best strategy for the field to improve quantitative constraints on properties of the medium in the face of these challenges.

PACS numbers: 25.75.Dw

16	CONTENTS	33	H. Comparing different types of measurements	20	
17	I. Introduction	2	34	III. Overview of experimental results	20
18	A. Formation and evolution of the Quark Gluon Plasma	2	35	A. Cold nuclear matter effects	21
19	B. Jet definition	4	36	2. Reconstructed jets	21
20	C. Interactions with the medium	6	37	1. Inclusive charged hadrons	21
21	D. Separating the signal from the background	7	38	3. Dihadron correlations	22
			39	4. Summary of cold nuclear matter effects for jets	22
22	II. Experimental methods	8	40	B. Partonic energy loss in the medium	22
23	A. Detectors	8	41	1. Jet R_{AA}	24
24	B. Centrality determination	9	42	2. Dihadron correlations	25
25	C. Inclusive hadron measurements	10	43	3. Dijet imbalance	26
26	D. Dihadron correlations	11	44	4. γ -hadron, γ -jet and Z-jet correlations	27
27	1. Background subtraction methods	11	45	5. Hadron-jet correlations	29
28	E. Reconstructed jets	13	46	6. Path length dependence of inclusive R_{AA} and jet v_n	30
29	1. Jet-finding algorithms	13	47	7. Heavy quark energy loss	30
30	2. Dealing with the background	14	48	8. Summary of experimental evidence for partonic energy loss in the medium	32
31	F. Particle Flow	16	49		
32	G. Unfolding	17	50		

51	C. Influence of the medium on the jet
52	1. Fragmentation functions with jets
53	2. Boson tagged fragmentation functions
54	3. Dihadron correlations
55	4. Jet-hadron correlations
56	5. Dijets
57	6. Jet Shapes
58	7. Particle composition
59	8. LeSub
60	9. Jet Mass
61	10. Dispersion
62	11. Girth
63	12. Grooming
64	13. Subjettiness
65	14. Summary of experimental evidence for medium modification of jets
67	D. Influence of the jet on the medium
68	1. Evidence for out-of-cone radiation
69	2. Searches for Molière scattering
70	3. The rise and fall of the Mach cone and the ridge
71	4. Summary of experimental evidence for modification of the medium by jets
72	
73	E. Summary of experimental results
74	IV. Discussion and the path forward
75	A. Understand bias
76	B. Make quantitative comparisons to theory
77	C. More differential measurements
78	D. An agreement on the treatment of background in heavy ion collisions
79	

80 V. Acknowledgements

81 References

82 1

83 I. INTRODUCTION

84 In ultrarelativistic heavy ion collisions, the temper-
 85 ature is so high that the nuclei melt, forming a hot,
 86 dense liquid of quarks and gluons called the Quark Gluon
 87 Plasma (QGP). Hard quark and gluon scatterings occur
 88 early in the collision, prior to the formation of the QGP.

89 These quarks and gluons, known as partons, traverse
 90 the medium and then fragment into collimated sprays
 91 of particles called jets. These partons lose energy to the
 92 medium and the jets they produce are thus modified.
 93 This process, called jet quenching, is studied with exper-
 94 imental measurements of high momentum hadrons, two
 95 particle correlations, and jet reconstruction at the Rela-
 96 tivistic Heavy Ion Collider (RHIC) and the Large Hadron
 97 Collider (LHC). After nearly two decades of experimen-
 98 tal measurements have taught us so far, we reflect on the
 99 limitations of the techniques used for studying jets, how
 100 the techniques can be improved, and how to move for-
 101 ward with the wealth of experimental data such that a
 102 complete description of energy loss in the QGP can be
 103 achieved.

104 Our goal in the following sections is to provide an
 105 overview of what we have learned from jet measure-
 106 ments and what the field needs to do in order to im-
 107 prove our quantitative understanding of jet quenching

32 and the properties of the medium from RHIC energies
 33 ($\sqrt{s_{NN}} = 7.7\text{--}200$ GeV) to LHC energies ($\sqrt{s_{NN}} = 2.76\text{--}$
 34 5.02 TeV). We will discuss measurements using the AL-
 36 ICE, ATLAS, and CMS detectors at the LHC, and the
 38 BRAHMS, PHENIX, Phobos, and STAR detectors at
 39 RHIC. The main goal of this paper is to review experi-
 40 mental techniques and measurements. While we discuss
 41 some models and their interpretation, a full review of the
 42 theory of partonic interactions with the medium is out-
 43 side the scope of this paper. In this section, we provide
 44 an overview of the formation of the QGP and other pro-
 45 cesses which impact the measurement of jets and their
 46 interaction with the medium. One key factor in measur-
 47 ing jets in heavy ion collisions is accounting for the effect
 48 of the fluctuating background on different observables.
 48 Section II discusses the various measurement techniques
 49 and approaches to background subtraction and suppres-
 50 sion and how these techniques may impact the results
 50 and their interpretation. We include measurements of
 51 nuclear modification factors, dihadron and multi-hadron
 51 correlations, and reconstructed jets. We follow this with
 51 a discussion of results in Section III organized by what
 51 they tell us about the medium. Do jets lose energy in
 53 the medium? Is fragmentation modified in the medium?
 53 Do jets modify the medium? Are there cold nuclear mat-
 53 ter effects? We show that there is substantial evidence
 53 for both partonic energy loss and modified fragmenta-
 53 tion. The evidence for modification of the medium by
 53 jets is considerably more scant. Our understanding of
 53 cold nuclear matter effects is rapidly evolving, but cur-
 53 rently there do not appear to be substantial cold nuclear
 53 matter effects for jets.

140 We conclude with a discussion of what we have learned
 141 and the way forward for the field in Section IV. There
 142 are extensive detailed measurements of jets, benefited by
 143 improved detector technologies, high cross sections, and
 144 higher luminosities, and there have been dramatic im-
 145 provements in our theoretical understanding and capa-
 146 bilities. However, experimental techniques and the bias
 147 they may impose are frequently neglected, and it is not
 148 currently possible to apply experimental algorithms to
 149 most models. The current status of comparisons between
 150 models and data motivates our call for an agreement be-
 151 tween theorists and experimentalists on the appropriate
 152 treatment of the background, Monte Carlo generators
 153 that enable experimental algorithms to be applied to the-
 154 oretical calculations, and a clear understanding of which
 155 observables are most sensitive to the properties of the
 156 medium, even in the presence of background. This will
 157 enable us to quantitatively constrain properties of the
 158 medium.

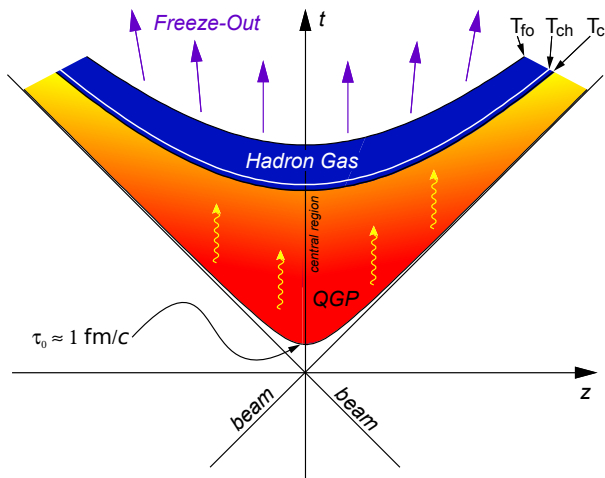


FIG. 1 A light cone diagram showing the stages of a heavy ion collision. The abbreviation T_{fo} is for the thermal freeze-out temperature, T_{ch} is for the chemical freeze-out temperature, and T_c is for the critical temperature where the phase transition between a hadron gas and a QGP occurs. τ_0 is the formation time of the QGP. Figure courtesy of Thomas Ullrich.

159 A. Formation and evolution of the Quark Gluon Plasma

160 Quarks and gluons become deconfined under extremely
161 high energy and density conditions. This deconfined
162 state became known as the QGP (Shuryak, 1980). With
163 the advancements in accelerator physics, it can be cre-
164 ated and studied in high energy heavy ion collisions.

165 The formation of the QGP requires energy densities
166 above $0.2\text{-}1\text{ GeV}/\text{fm}^3$ (Bazavov *et al.*, 2014; Karsch,
167 2002). These energy densities can currently be reached
168 in high energy heavy ion collisions at RHIC located at
169 Brookhaven National Laboratory in Upton, NY and the
170 LHC located at CERN in Geneva, Switzerland. Esti-
171 mates of the energy density indicate that central heavy
172 ion collisions with an incoming energy per nucleon pair as
173 low as $\sqrt{s_{NN}} = 7.7\text{ GeV}$, the lower boundary of collision
174 energies accessible at RHIC, can reach energy densities
175 above $1\text{ GeV}/\text{fm}^3$ (Adare *et al.*, 2016e) and that colli-
176 sions at 2.76 TeV , accessible at the LHC, reach energy
177 densities as high as $12\text{ GeV}/\text{fm}^3$ (Adam *et al.*, 2016i;
178 Chatrchyan *et al.*, 2012d). Contrary to initial naïve ex-
179 pectations of a gas-like QGP, the QGP formed in these
180 collisions was shown to behave like a liquid of quarks
181 and gluons (Adams *et al.*, 2005b; Adcox *et al.*, 2005; Ar-
182 sene *et al.*, 2005b; Back *et al.*, 2005; Heinz and Snellings,
183 2013).

184 The heavy ion collision and the evolution of the fireball,
185 as depicted in Figure 1, has several stages, and the mea-
186 surement of the final state particles can be affected by one
187 or all of these stages depending on the production mecha-
188 nism and interaction time within the medium. The initial

189 state of the incoming nuclei is not precisely known, but
190 its properties impact the production of final state parti-
191 cles. The incoming nuclei are often modeled as either an
192 independent collection of nucleons called a Glauber ini-
193 tial state (Miller *et al.*, 2007), or a wall of coherent gluons
194 called a Color Glass Condensate (Iancu *et al.*, 2001). In
195 either initial state model, both the impact parameter of
196 the nuclei and fluctuations in the positions of the incom-
197 ing quarks or gluons, called partons, lead to an asym-
198 metric nuclear overlap region. This asymmetric overlap
199 is shown schematically in Figure 2. The description of
200 the initial state most consistent with the data is between
201 these extremes (Moreland *et al.*, 2015). The proposed
202 electron ion collider is expected to resolve ambiguities
203 in the initial state of heavy ion collisions (Aprohmanian
204 *et al.*, 2015).

205 In all but the most central collisions, some fraction of
206 the incoming nucleons do not participate in the collision
207 and escape unscathed. These nucleons, called spectators,
208 can be observed directly and used to measure the impact
209 parameter of the collision. Before the formation of the
210 QGP, partons in the nuclei may scatter off of each other
211 just as occurs in $p+p$ collisions. An interaction with a
212 large momentum transfer (Q) is called a hard scattering,
213 a process which is, in principle, calculable with perturba-
214 tive quantum chromodynamics (pQCD). The majority of
215 these hard scatterings are $2\rightarrow 2$, which result in high mo-
216 mentum partons traveling 180° apart in the plane trans-
217 verse to the beam as they travel through the evolving
218 medium. These hard parton scatterings are the focus of
219 this paper.

220 As the medium evolves, it forms a liquid of quarks and
221 gluons. The liquid reaches local equilibrium, with tem-
222 perature fluctuations in different regions of the medium.
223 The liquid QGP phase is expected to live for $1\text{-}10\text{ fm}/c$,
224 depending on the collision energy (Harris and Muller,
225 1996). As the medium expands and cools, it reaches
226 a density and temperature where partonic interactions
227 cease, a hadron gas is formed, and the hadron fractions
228 are fixed. This point in the collision evolution is called
229 chemical freeze-out (Adam *et al.*, 2016j; Adams *et al.*,
230 2005b; Fodor and Katz, 2004). As the medium expands
231 and cools further, collisions between hadrons cease and
232 hadrons reach their final energies and momenta. This
233 stage of the collision, thermal freeze-out, occurs at a
234 somewhat lower temperature than the chemical freeze-
235 out.

236 Thermal photons, in a manner analogous to black
237 body radiation, reveal that the QGP may reach temper-
238 atures of $300\text{-}600\text{ MeV}$ in central collisions at both 200
239 GeV (Adare *et al.*, 2010a) and 2.76 TeV (Adam *et al.*,
240 2016g). The temperature can also be inferred from the
241 sequential melting of bound states of a bottom quark and
242 antiquark (Chatrchyan *et al.*, 2012g). The ratios of final
243 state hadrons are used to determine that the chemical
244 freeze-out temperature is around 160 MeV (Adam *et al.*,

245 2016j; Adams *et al.*, 2005b; Fodor and Katz, 2004) and
 246 that the thermal freeze out occurs at about 100–150 MeV,
 247 depending on the collision energy and centrality (Abelev
 248 *et al.*, 2013b; Adcox *et al.*, 2004; Arsene *et al.*, 2005a;
 249 Back *et al.*, 2007).

250 The properties of the medium are determined from
 251 the final state particles that are measured. The initial
 252 gluon density can be related to the final state hadron
 253 multiplicity through the concept of hadron-parton dual-
 254 ity (Van Hove and Giovannini, 1988), leading to estimates
 255 of gluon densities of around 700 per unit pseudorapidity
 256 at the top RHIC energy of $\sqrt{s_{NN}} = 200$ GeV (Adler *et al.*,
 257 2005) and 2000 per unit pseudorapidity at the top LHC
 258 energy of $\sqrt{s_{NN}} = 5.02$ TeV (Aad *et al.*, 2012, 2016c;
 259 Aamodt *et al.*, 2010; Adam *et al.*, 2016d; Chatrchyan
 260 *et al.*, 2011a).

261 The azimuthal anisotropy in the momentum distribu-
 262 tion of final state hadrons is the result of the initial state
 263 anisotropy. The survival of these anisotropies provides
 264 evidence that the medium flows in response to pres-
 265 sure gradients (Aad *et al.*, 2014b; Adam *et al.*, 2016a;
 266 Adler *et al.*, 2001, 2003c; Alver *et al.*, 2007; Chatrchyan
 267 *et al.*, 2014b). This asymmetry is illustrated schemat-
 268 ically in Figure 2. The shape and magnitude of these
 269 anisotropies can be used to constrain the viscosity to
 270 entropy ratio, revealing that the QGP has the lowest
 271 viscosity to entropy ratio ever observed (Adams *et al.*,
 272 2005b; Adcox *et al.*, 2005; Arsene *et al.*, 2005b; Back
 273 *et al.*, 2005). Hadrons containing strange quarks are en-
 274 hanced in heavy ion collisions above expectations from
 275 $p+p$ collisions (Abelev *et al.*, 2013f, 2014b; Khachatryan
 276 *et al.*, 2017d). This is due to a combination of the sup-
 277 pression of strangeness in $p+p$ collisions due to the lim-
 278 ited phase space for the production of strange quarks,
 279 and the higher energy density available for the produc-
 280 tion of strange quarks in heavy ion collisions. Corre-
 281 lations between particles may provide evidence for in-
 282 creased production of strangeness due to the decreased
 283 strange quark mass in the medium (Abelev *et al.*, 2009c;
 284 Adam *et al.*, 2016f). Baryon production is enhanced for
 285 both light (Abelev *et al.*, 2006; Adler *et al.*, 2004; Arsene
 286 *et al.*, 2010) and strange quarks (Abelev *et al.*, 2013f,
 287 2014b, 2008; Khachatryan *et al.*, 2017d), an observation
 288 generally interpreted as evidence for the direct produc-
 289 tion of baryons through the recombination of quarks in
 290 the medium (Dover *et al.*, 1991; Fries *et al.*, 2003; Greco
 291 *et al.*, 2003; Hwa and Yang, 2003).

292 Hard parton scattering occurs early in the collision evo-
 293 lution, prior to the formation of the QGP, so that their
 294 interactions with the QGP probe the entire medium evo-
 295 lution. Therefore, they can be used to reveal the prop-
 296 erties of the medium, such as its stopping power and
 297 transport coefficients. Since the differential production
 298 cross section of these hard parton scatterings is calcula-
 299 ble in pQCD, and these calculations have been validated
 300 over many orders of magnitude in proton-proton colli-

301 sions, in principle they form a well calibrated probe. The
 302 initial production must scale by the number of nucleon
 303 collisions, which means that their interactions with the
 304 medium would cause deviations from this scaling. Since
 305 the majority of these hard partons are produced in pairs,
 306 they can be used both as a probe and a control. Particle
 307 jets of this nature are formed in e^+e^- and proton-proton
 308 ($p+p$) collisions as well and are observed to fragment sim-
 309 ilarly in e^+e^- and $p+p$ collisions.

310 In a heavy ion collision, where a QGP is formed, the
 311 hard scattered quarks and gluons are expected to inter-
 312 act strongly with the hot QCD medium due to their color
 313 charges, and lose energy, either through collisions with
 314 medium partons, or through gluon bremsstrahlung. The
 315 energy loss of high momentum partons due to strong
 316 interactions is a process called jet quenching, and re-
 317 sults in modification of the properties of the result-
 318 ing jets in heavy ion collisions compared to expecta-
 319 tions from proton-proton collisions (Baier *et al.*, 1995;
 320 Bjorken, 1982; Gyulassy and Plumer, 1990). This en-
 321 ergy loss was first observed in the suppression of high
 322 momentum hadrons produced in heavy ion collisions at
 323 RHIC (Adams *et al.*, 2003b; Adler *et al.*, 2003b; Back
 324 *et al.*, 2004) and later also observed at the LHC (Aamodt
 325 *et al.*, 2011b; Chatrchyan *et al.*, 2012e). The modification
 326 can be observed through measurements of jet shapes, par-
 327 ticle composition, fragmentation, splitting functions and
 328 many other observables. Detailed studies of jets to char-
 329 acterize how and why partons lose energy in the QGP
 330 require an understanding of how evidence for energy loss
 331 may be manifested in the different observables, and the
 332 effect of the large and complicated background from other
 333 processes in the collision.

334 Early studies of the QGP focused on particles produced
 335 through soft processes, measuring the bulk properties of
 336 the medium. With the higher cross sections for hard pro-
 337 cesses with increasing collision energy, higher luminosity
 338 delivered by colliders, and detectors better suited for jet
 339 measurements, studies of jets are enabling higher preci-
 340 sion measurements of the properties of the QGP (Akiba
 341 *et al.*, 2015). The 2015 nuclear physics Long Range Plan
 342 (LRP) (Aprohmanian *et al.*, 2015) highlighted the partic-
 343 ular need to improve our quantitative understanding of
 344 jets in heavy ion collisions. Here we assess our current
 345 understanding of jet production in heavy ion collisions in
 346 order to inform what shape future studies should take in
 347 order to optimize the use of our precision detectors.

348 B. Jet definition

349 In principle, using a jet finding algorithm to cluster all
 350 of the daughter particles of a given parton will give access
 351 to the full energy and momentum of the parent parton.
 352 However, even in e^+e^- collisions, the definition of a jet
 353 is ambiguous, even on the partonic level. For instance,

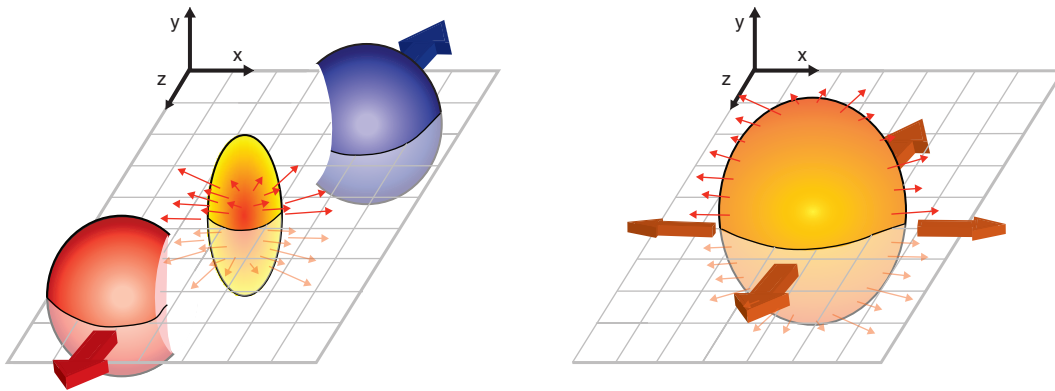


FIG. 2 Schematic diagrams showing the initial overlap region (left) and the spatial anisotropy generated by this anisotropic overlap region. This anisotropy can be quantified using the Fourier coefficients of the momentum anisotropy. Figure courtesy of Boris Hippolyte.

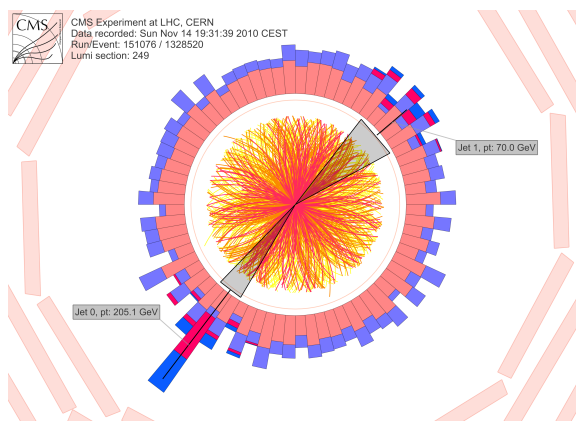


FIG. 3 Event display showing a dijet event in a Pb+Pb collision at $\sqrt{s_{NN}} = 2.76$ TeV (CMS, 2010). This shows the large background for jet measurements in heavy ion collisions.

354 in $e^+e^- \rightarrow q\bar{q}$, the quark may emit a gluon. If this gluon
 355 is emitted at small angles relative to the quark, it is usu-
 356 ally considered part of the jet, whereas if it is emitted at
 357 large angles relative to the parent parton, it may be con-
 358 sidered a third jet. This ambiguity led to the Snowmass
 359 Accord, which stated that in order to be comparable, exper-
 360 imental and theoretical measurements had to use the
 361 same definition of a jet and that the definition should be
 362 theoretically robust (Huth *et al.*, 1990).

363 The choice of which final state particles should be in-
 364 cluded in the jet is also somewhat arbitrary and more
 365 difficult in $A+A$ collisions than in $p+p$ collisions. Fig-
 366 ure 3 shows an event display from a Pb+Pb collision at
 367 $\sqrt{s_{NN}} = 2.76$ TeV, showing the large background in the
 368 event. If a hard parton emits a soft gluon and that gluon
 369 thermalizes with the medium, are the particles from the
 370 hadronization of that soft gluon part of the jet or part

371 of the medium? Any interaction between daughters of
 372 the parton and medium particles complicates the defini-
 373 tion of what should belong to the jet and what should
 374 not. This ambiguity in the definition of the observable
 375 itself makes studies of jets qualitatively different from,
 376 e.g., measurements of particle yields. These aspects of
 377 jet physics need to be taken into account in the choice
 378 of a jet finding algorithm and background subtraction
 379 methods in order to be able to interpret the resulting
 380 measurements.

381 One of the main motivations for studies of jets in heavy
 382 ion collisions was to provide measurements of observables
 383 with a production cross-section that can be calculated
 384 using pQCD, which yields a well calibrated probe. In
 385 certain limits, this is feasible, although it is worth noting
 386 that many observables are sensitive to non-perturbative
 387 effects. One such non-perturbative effect is hadroniza-
 388 tion, which can affect even the measurements of relatively
 389 simple observables such as the jet momentum spectra.

390 In addition to the ambiguities inherent in the definition
 391 of what is and is not a jet, there is the question of how
 392 to deal with the large background in heavy ion collisions.
 393 For example, measurements of reconstructed jets usually
 394 have a minimum momentum threshold for constituents
 395 in order to suppress the background contribution. If the
 396 corrections for these analysis techniques are insensitive
 397 to assumptions about the background and hadronization,
 398 the results may still be perturbatively calculable. How-
 399 ever, these techniques for dealing with the background
 400 may also bias the measured jet sample, for instance by
 401 selecting gluon jets at a higher rate than quark jets. In
 402 the context of jets in a heavy ion collision, these analysis
 403 cuts are part of the definition of the jet and can not be
 404 ignored.

405 The interpretation of the measurement of any observ-
 406 able cannot be fully separated from the techniques used
 407 to measure it because both measurements and theoretic-

cal calculations of jet observables must use the same definition of a jet. As we review the literature, we discuss how the jet definitions and techniques used in experiment may influence the interpretation of the results. Even though our goal is an understanding of partonic interactions within the medium, a detailed understanding of soft particle production is necessary to understand the methods for suppressing and subtracting the contribution of these particles to jet observables.

C. Interactions with the medium

There are several models used to describe interactions between hard partons and the medium, however, a full review of theoretical calculations is beyond the scope of this paper. We briefly summarize theoretical frameworks for interactions of hard partons with the medium here and refer readers to (Burke *et al.*, 2014; Qin and Wang, 2015) and the references therein for details. The production of final state particles in nuclear collisions is described by assuming that these processes can be factorized (Majumder, 2007a; Majumder and Van Leeuwen, 2011). The nuclear parton distribution functions $x_a f_a^A(x_a)$ and $x_b f_b^B(x_b)$ describe the probability of finding partons with momentum fraction x_a and x_b , respectively. The differential cross sections for partons a and b interacting with each other to produce a parton c with a momentum p can be described using pQCD. The production of a final state hadron h is then given by fragmentation function $D_c^h(z)$ where $z = p^h/p$ is the fraction of the parton's momentum carried by the final state hadron. The differential cross section for the production of hadrons as a function of their transverse momenta p_T and rapidity y at leading order is then given by

$$\frac{d^3\sigma^h}{dyd^2p_T} = \frac{1}{\pi} \int dx_a \int dx_b f_a^A(x_a) f_b^B(x_b) \frac{d\sigma_{ab \rightarrow cX}}{d\hat{t}} \frac{D_c^h(z)}{z}. \quad (1)$$

where $\hat{t} = (\hat{p} - x_a P)^2$, \hat{p} is the four-momentum of parton, c , and P is the average momentum of a nucleon in nucleus A . The nuclear parton distribution functions and the fragmentation functions cannot be calculated perturbatively. The parton distribution functions describe the initial state of the incoming nuclei. Any differences between the nuclear and proton parton distribution functions, which describe the distribution of partons in a nucleon, are considered cold nuclear matter effects. Cold nuclear matter effects may include coherent multiple scattering within the nucleus (Qiu and Vitev, 2006), gluon shadowing and saturation (Gelis *et al.*, 2010), or partonic energy loss within the nucleus (Bertocchi and Treleani, 1977; Vitev, 2007; Wang and Guo, 2001). Most models for interactions of partons with a QGP factorize this process and only modify the fragmentation functions (Majumder, 2007a). One goal of studies of high momentum particles in heavy ion collisions is to study the modification of these fragmentation functions, which will allow us to understand how and why partons lose energy within the QGP and to determine the microscopic

structure of the medium. We note that the theoretical definition in Equation 1 associates the production of a final state hadron with a particular parton. This is not possible experimentally, so the experimentally measured quantity also referred to as a fragmentation function is not the same as $D_c^h(z)$ in Equation 1.

Medium-induced gluon radiation (bremsstrahlung) and collisions with partons in the medium cause the partons to lose energy to the medium, often described as a modification of the fragmentation functions in Equation 1. There are four major approaches to describing these interactions. The GLV model (Djordjevic and Gyulassy, 2004; Djordjevic *et al.*, 2005; Djordjevic and Heinz, 2008; Vitev and Gyulassy, 2002; Wicks *et al.*, 2007) and its CUJET implementation (Buzzatti and Gyulassy, 2012) assumes that the scattering centers in the medium are nearly static and that the mean free path of a parton is much larger than the color screening length in the medium. This assumption is valid for a thinner medium.

The Higher Twist (Majumder, 2012) framework assumes medium modified splitting functions during fragmentation calculated by including higher twist corrections to the differential cross sections for deep inelastic scattering off of nuclei. These corrections are enhanced by the length of the medium. The higher twist model has also been adapted to include multiple gluon emissions (Collins *et al.*, 1985; Majumder, 2012; Majumder and Van Leeuwen, 2011).

In the BDMPS (Baier *et al.*, 1997, 1998, 2000) approach and its equivalents (Albacete *et al.*, 2005; Armesto *et al.*, 2012; Eskola *et al.*, 2005; Wiedemann, 2000b, 2001; Zakharov, 1996) the effect of multiple parton scatterings is evaluated using a path integral over a path ordered Wilson line (Wiedemann, 2000a,b). This assumes infinite coherence of the radiated gluons and a thick medium. YAJEM (Renk, 2008, 2013a) and JEWEL (Zapp, 2014a,b) are Monte Carlo implementations of the BDMPS framework.

The energy loss mechanism in the AMY model is similar to BDMPS but the rate equations for partonic energy loss are solved numerically and convoluted with differential pQCD cross sections and fragmentation functions to determine the final state differential hadronic cross sections (Arnold *et al.*, 2002; Jeon and Moore, 2005; Qin *et al.*, 2009, 2008). This is applied in a realistic hydrodynamical environment (Qiu and Heinz, 2012; Qiu *et al.*, 2012; Song and Heinz, 2008a,b). The MARTINI model (Qin *et al.*, 2008; Schenke *et al.*, 2011) is a Monte Carlo model implementation of the AMY formalism which uses PYTHIA (Sjostrand *et al.*, 2006) to describe the hard scattering and a Glauber initial state (Miller *et al.*, 2007). Partonic energy loss occurs in the medium, taking temperature and hydrodynamical flow into account (Nonaka and Bass, 2007; Schenke *et al.*, 2010, 2011).

There are additional approaches, including embedding

495 jets into a hydrodynamical fluid (Tachibana *et al.*, 2017) 551
 496 and using the correspondence between Anti-deSitter 552
 497 space and conformal field theories (Gubser, 2007). There 553
 498 is a new description of jet quenching in which coherent 554
 499 parton branching plays a central role to the jet-medium 555
 500 interactions (Casalderrey-Solana *et al.*, 2013; Mehtar- 556
 501 Tani and Tywoniuk, 2015). In this work it is assumed 557
 502 that the hierarchy of scales governing jet evolution allow 558
 503 the jet to be separated into a hard core, which interacts 559
 504 with the medium as a single coherent antenna, and softer 560
 505 structures that will interact in a color decoherent fash- 561
 506 ion. In order for this to be valid, there must be a large 562
 507 separation of the intrinsic jet scale and the characteristic 563
 508 momentum scale of the medium. While this certainly is
 509 valid for the highest momentum jets at the LHC, it is
 510 not clear at which scales in collision energy and jet en-
 511 ergy this assumption breaks down. We refer readers to
 512 a recent theoretical review for a more complete picture
 513 of theoretical descriptions of partonic energy loss in the
 514 QGP (Qin and Wang, 2015).

515 Medium-induced bremsstrahlung occurs when the 564
 516 medium exchanges energy, color, and longitudinal mo- 565
 517 mentum with the jet. Since both the energy and longi- 566
 518 tudinal momentum of the hard partons exceeds that of 567
 519 the medium partons, these exchanges cause the parton 568
 520 as a whole to lose energy. Additionally, since the hard 569
 521 partons have much higher transverse momentum than the 570
 522 medium partons, any collision will reduce the momentum 571
 523 of the jet as a whole. Both of these effects will broaden 572
 524 the resulting jet and soften the average final state parti- 573
 525 cles produced from the jet. Collisional energy loss simi- 574
 526 larly broadens and softens the jet. Partonic energy loss 575
 527 in the medium is quantified by the jet transport coeffi- 576
 528 cients $\hat{q} = Q^2/L$, where Q is the transverse momentum 577
 529 lost to the medium and L is the path-length traversed; \hat{e} , 578
 530 the longitudinal momentum lost per unit length; and \hat{e}_2 , 579
 531 the fluctuation in the longitudinal momentum per unit 580
 532 length (Majumder, 2013; Muller, 2013).

533 The JET collaboration systematically compared each 581
 534 of these models to data to determine how well the trans- 582
 535 port properties of partons in the medium can be con- 583
 536 strained (Burke *et al.*, 2014). This substantially im- 584
 537 proved our quantitative understanding of partonic en- 585
 538 ergy loss in the medium, but only used a small fraction 586
 539 of the available data. The Jetscape collaboration (Col- 587
 540 laboration", 2017) has formed to develop a Monte Carlo 588
 541 framework which enables combinations of different mod-
 542 els of the initial state, the hydrodynamical evolution of
 543 medium, and partonic energy loss to be used within the
 544 same framework. The goal is a Bayesian analysis compar-
 545 ing models to data to quantitatively determine properties
 546 of the medium, similar to (Bernhard *et al.*, 2016; Novak
 547 *et al.*, 2014). Jetscape will incorporate many of the avail-
 548 able jet observables into this Bayesian analysis. Part of
 549 the motivation for this paper is to evaluate which exper-
 550 imental observables might provide effective input for this

effort and what factors need to be considered for these
 comparisons.

In light of the ambiguities in the jet definition dis-
 cussed above, we note that whether or not the energy
 is lost depends on this definition. The functional exper-
 imental definition of lost energy is any energy which no
 longer retains short-range correlations with the parent
 parton, meaning that it is further than about half a unit
 in pseudorapidity and azimuth. Energy which retains
 short-range correlations with the parent parton is still
 considered part of the jet and any short-range modifica-
 tions are considered modifications of the fragmentation
 function.

564 D. Separating the signal from the background

565 Hard partons traverse a medium which is flowing and
 566 expanding, with fluctuations in the density and temper-
 567 ature. Since the mean transverse momentum of uniden-
 568 tified hadrons in Pb+Pb collisions at $\sqrt{s_{NN}} = 2.76$ TeV
 569 is 680 MeV/c (Abelev *et al.*, 2013g), sufficiently high
 570 p_T hadrons are expected to be produced dominantly in
 571 jets and production from soft processes is expected to be
 572 negligible. It is unclear precisely at which momentum the
 573 particle yield is dominated by jet production rather than
 574 medium production. Moreover, most particles produced
 575 in jets are at low momenta even though the jet momen-
 576 tum itself is dominated by the contribution of a few high
 577 p_T particles. Particularly if jets are modified by processes
 578 such as recombination, strangeness enhancement, or hy-
 579 drodynamical flow, these low momentum particles pro-
 580 duced in jets may carry critical information about their
 581 parent partons' interactions with the medium. Methods
 582 employed to suppress and subtract background from jet
 583 measurements are dependent on assumptions about the
 584 background contribution and can change the sensitivity
 585 of measurements to possible medium modifications. The
 586 resulting biases in the measurements can be used as a tool
 587 rather than treated as a weakness in the measurement;
 588 however, they must be first understood.

The largest source of correlated background is due to
 collective flow. The azimuthal distribution of particles
 created in a heavy ion collision can be written as

$$\frac{dN}{d(\phi - \psi_R)} \propto 1 + \sum_{n=1}^{\infty} 2v_n \cos(n(\phi - \psi_R)) \quad (2)$$

589 where N is the number of particles, ϕ is the angle of a
 590 particle's momentum in azimuth in detector coordinates
 591 and ψ_R is the angle of the reaction plane in detector coor-
 592 dinates (Poskanzer and Voloshin, 1998). The Fourier co-
 593 efficients v_n are thought to be dominantly from collective
 594 flow at low momenta (Adams *et al.*, 2005b; Adcox *et al.*,
 595 2005; Arsene *et al.*, 2005b; Back *et al.*, 2005), although
 596 equation 2 is valid for any correlation because any distri-
 597 bution can be written as its Fourier decomposition. The

magnitude of the Fourier coefficients v_n decreases with increasing order. The sign of the flow contribution to the first order coefficient v_1 is dependent on the incoming direction of the nuclei and changes sign when going from positive to negative pseudorapidities. For most measurements, which average over the direction of the incoming nuclei, v_1 due to flow is zero, although we note that there may be contributions to v_1 from global momentum conservation.

The even v_n arise mainly from anisotropies in the average overlap region of the incoming nuclei, considering the nucleons to be smoothly distributed in the nucleus with the density depending only on the radius. The odd v_n for $n > 1$ are generally understood to arise from the fluctuations in the positions of the nucleons within the nucleus. These fluctuations also contribute to the even v_n , though these coefficients are dominated by the overall geometry. Jets themselves can lead to non-zero v_n through jet quenching, complicating background subtraction for jet studies. At high momenta ($p_T \gtrsim 5\text{-}10$ GeV/ c) the v_n are thought to be dominated by jet production. Furthermore, the v_n fluctuate event-by-event even for a given centrality class. This means that independent measurements, which differ in their sensitivity to jets, averaged over several events cannot be used blindly to subtract the correlated background due to flow.

To measure jets, experimentalists have to make some assumptions about the interplay between hard and soft particles and about the form of the background. Without such assumptions, experimental measurements are nearly impossible. Some observables are more robust to assumptions about the background than others, however, these measurements are not always the most sensitive to energy loss mechanisms or interactions of jets with the medium. An understanding of data requires an understanding of the measurement techniques and assumptions about the background. We therefore discuss the measurement techniques and their consequences in great detail in Section II before discussing the measurements themselves in Section III.

II. EXPERIMENTAL METHODS

This section focuses on different methods for probing jet physics including inclusive hadron measurements, di-hadron correlations, jet reconstruction algorithms and jet-particle correlations and a brief description of relevant detectors. In addition to explaining the measurement details and how the effect of the background on the observable is handled for each, this section highlights strengths and weaknesses of these different methods which are important for interpreting the results. We emphasize background subtraction and suppression techniques because of potential biases they introduce.

TABLE I Collision systems, collision energies (\sqrt{s}) for $p+p$ collisions, collision energies per nucleon ($\sqrt{s_{NN}}$) for $A+A$ collisions, charged particle multiplicities ($dN/d\eta$) for central collisions, energy densities for central collisions, and the temperature compared to the critical temperature for formation of the QGP T/T_c for both RHIC and the LHC.

Collider	RHIC	LHC
Collisions	$p+p$, $d+Au$, $Cu+Cu$, $Au+Au$, $U+U$	$p+p$, $p+Pb$, $Pb+Pb$
\sqrt{s}	62–500 GeV	0.9–14 TeV
$\sqrt{s_{NN}}$	7.7–500 GeV	2.76–5.02 TeV
$dN/d\eta$	192.4 ± 16.9 687.4 ± 36.6 (Adare <i>et al.</i> , 2016e)	– 1584 ± 76 (Aamodt <i>et al.</i> , 2010), 1943 ± 54 (Adam <i>et al.</i> , 2016d)
ϵ	1.36 ± 0.14 GeV/fm^3 (Adare <i>et al.</i> , 2016e) – 4.9 ± 0.3 GeV/fm^3 (Adams <i>et al.</i> , 2004b)	12.3 ± 1.0 GeV/fm^3 (Adam <i>et al.</i> , 2016i)
T/T_c^a	1.3	1.8–1.9

^a Calculated using $T = 196$ MeV at $\sqrt{s_{NN}} = 200$ GeV, $T = 280$ MeV at $\sqrt{s_{NN}} = 2.76$ TeV, and $T = 292$ MeV at $\sqrt{s_{NN}} = 5.02$ TeV from (Srivastava *et al.*, 2016) assuming that $T_c = 155$ MeV from the extrapolation of the chemical freeze-out temperature using comparisons of data to statistical models in (Floris, 2014).

A. Detectors

Measurements of heavy ion collisions often focus on midrapidity, with precision, particle identification, and tracking in a high multiplicity environment. Some measurements, such as those of single particles, are not significantly impacted by a limited acceptance, while the acceptance corrections for reconstructed jets are more complicated when the acceptance is limited. We briefly summarize the colliders, RHIC and the LHC, and the most important features of each of their detectors for measurements of jets, referring readers to other publications for details.

The properties of the medium are slightly different at RHIC and the LHC, with the LHC reaching the highest temperatures and energy densities and RHIC providing the widest range of collision energies and systems. The relevant properties of each collider are summarized in Table I. Some properties of each detector are summarized in Table II.

The BRAHMS (Adameczyk *et al.*, 2003), PHENIX (Adcox *et al.*, 2003), and PHOBOS (Back *et al.*, 2003) experiments are experiments which have completed their taking data at RHIC. The STAR (Ackermann *et al.*, 2003) experiment is taking data at RHIC and sPHENIX (Adare *et al.*, 2015) is a proposed upgrade at RHIC to be built in the existing PHENIX hall. STAR has full azimuthal acceptance and nominally covers pseudorapidities $|\eta| < 1$ with a silicon inner tracker and a time projection chamber (TPC), surrounded by an electromagnetic calorime-

TABLE II Summary of acceptance of detectors at RHIC and the LHC and when detectors took data. When not otherwise listed, azimuthal acceptance is 2π .

Collider	Detector	EMCal	HCal	Tracking	Taking data
RHIC	BRAHMS	N/A	N/A	$0 < \eta < 4$	2000–2006
	PHENIX	$ \eta < 0.35$	N/A	$ \eta < 0.35, 2 \times \Delta\phi = 90^\circ$	2000–2016
	PHOBOS	N/A	N/A	$0 < \eta < 2, 2 \times \Delta\phi = 11^\circ$	2000–2005
	STAR	$ \eta < 1.0$	N/A	$ \eta < 1.0$	2000–
	sPHENIX	$ \eta < 1.0$	$ \eta < 1.0$	$ \eta < 1.0$	future
LHC	ALICE	$ \eta < 0.7, \Delta\phi = 107^\circ$ and $\Delta\phi = 60^\circ$	N/A	$ \eta < 0.9$	2009–
	ATLAS	$ \eta < 4.9$	$ \eta < 4.9$	$ \eta < 2.5$	2009–
	CMS	$ \eta < 3.0$	$ \eta < 5.2$	$ \eta < 2.5$	2009–
	LHCb	N/A	N/A	$ \eta < 0.35$	2009–

ter (Ackermann *et al.*, 2003). An inner silicon detector was installed before the 2014 run. Particle identification is possible both through energy loss in the TPC and a time of flight (TOF) detector. STAR also has forward tracking and calorimetry. The PHENIX central arms cover $|\eta| < 0.35$ and are split into two 90° azimuthal regions (Adcox *et al.*, 2003). They consist of drift and pad chambers for tracking, a TOF for particle identification, and precision electromagnetic calorimeters. There are both midrapidity and forward silicon for precision tracking and forward electromagnetic calorimeters. PHENIX also has two muon arms at forward rapidities ($-1.15 < |\eta| < -2.25$ and $1.15 < |\eta| < 2.44$) with full azimuthal coverage. The PHOBOS detector consists of a large acceptance scintillator with wide acceptance for multiplicity measurements ($|\eta| < 3.2$) and two spectrometer arms capable of both particle identification and tracking covering $0 < |\eta| < 2$ and split into two 11° azimuthal regions (Back *et al.*, 2003). The BRAHMS detector has a spectrometer arm capable of particle identification with wide rapidity coverage ($0 \lesssim y \lesssim 4$) (Adamczyk *et al.*, 2003). sPHENIX will have full azimuthal acceptance and acceptance in pseudorapidity of approximately $|\eta| < 1$ with a TPC combined with precision silicon tracking and both electromagnetic and hadronic calorimeters (Adare *et al.*, 2015). sPHENIX is optimized for measurements of jets and heavy flavor at RHIC.

The LHC has four main detectors, ALICE, ATLAS, CMS, and LHCb. ALICE, which is primarily devoted to studying heavy ion collisions at the LHC, has a TPC, silicon inner tracker, and TOF covering $|\eta| < 0.9$ and full azimuth (Aamodt *et al.*, 2008). It has an electromagnetic calorimeter (EMCal) covering $|\eta| < 0.7$ with two azimuthal regions covering 107° and 60° in azimuth and a forward muon arm. Both ATLAS and CMS are multipurpose detectors designed to precisely measure jets, leptons and photons produced in pp and heavy ion collisions. The ATLAS detector's precision tracking is performed by a high-granularity silicon pixel detector, followed by the silicon microstrip tracker and complemented by the transition radiation tracker for the $|\eta| < 2.5$ region. The hadronic and electromagnetic calorimeters provide her-

metic azimuthal coverage in the $|\eta| < 4.9$ range. The muon spectrometer surrounds the calorimeters covering $|\eta| < 2.7$ with full azimuthal coverage (Aad *et al.*, 2008). The main CMS detectors are silicon trackers which measure charged particles within the pseudorapidity range $|\eta| < 2.5$, an electromagnetic calorimeter partitioned into a barrel region ($|\eta| < 1.48$) and two endcaps ($|\eta| < 3.0$), and hadronic calorimeters covering the range $|\eta| < 5.2$. All CMS detectors listed here have full azimuthal coverage (Chatrchyan *et al.*, 2008). LHCb focuses on measurements of charm and beauty at forward rapidities. The LHCb detector consists of a single spectrometer covering $1.6 < |\eta| < 4.9$ and full azimuth (Alves *et al.*, 2008). This spectrometer arm is capable of tracking and particle identification, however, tracking is limited to low multiplicity collisions.

B. Centrality determination

The impact parameter b , defined as the transverse distance between the centers of the two colliding nuclei, cannot be measured directly. Glancing interactions with a large impact parameter generally produce fewer particles while collisions with a small impact parameter generally produce more particles, with the number of final state particles increasing monotonically with the overlap volume between the nuclei. This correlation can be used to define the collision centrality as a fraction of the total cross section. High multiplicity events have a low average b and low multiplicity events have a large average b . The former are called central collisions and the latter are called peripheral collisions. In large collision systems, the variations in the number of particles produced due to fluctuations in the energy production by individual soft nucleon-nucleon collisions is small compared to the variations due to the impact parameter. The charged particle multiplicity, N_{ch} , can then be used to constrain the impact parameter.

Usually the correlation between the impact parameter and the multiplicity is determined using a Glauber model (Miller *et al.*, 2007). The distribution of nucleons

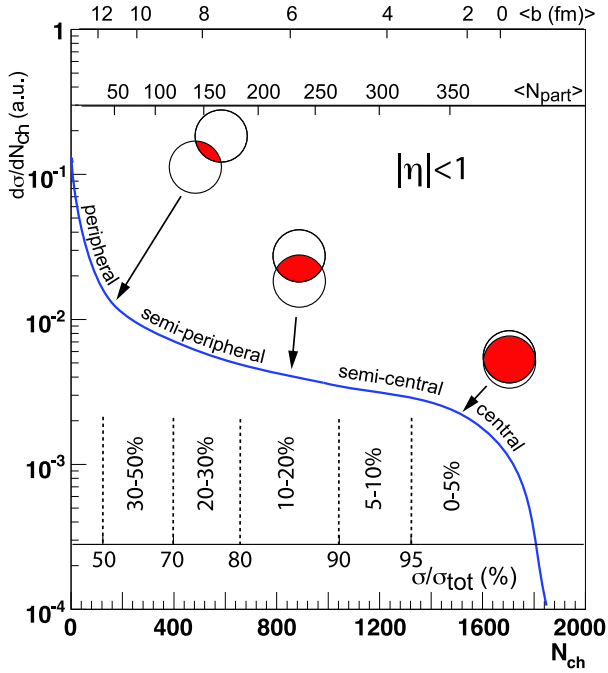


FIG. 4 Cartoon showing the correlation between the multiplicity N_{ch} , the impact parameter b , the number of binary nucleon-nucleon collisions N_{bin} , and the number of participating nucleons N_{part} . Figure from (Miller *et al.*, 2007) courtesy of Thomas Ullrich.

in the nucleus is usually approximated as a Fermi distribution in a Woods-Saxon potential and the multiplicity is assumed to be a function of the number of participating nucleons (N_{part}) and the binary number of interactions between nucleons (N_{bin}). The experimentally observed multiplicity is fit to determine a parametric description of the data and the data are binned by the fraction of events. For example, the 10% of all events with the highest multiplicity are referred to as 0-10% central. There are a few variations in technique which generally lead to consistent results (Abelev *et al.*, 2013c). Figure 4 illustrates this schematically. Centralities determined assuming that the distribution of impact parameters at a fixed multiplicity is Gaussian are consistent with those using a Glauber model (Das *et al.*, 2017).

The largest source of uncertainty from centrality determination in heavy ion collisions is due to the normalization of the multiplicity distribution at low multiplicities. In general an experiment identifies an anchor point in the distribution, such as identifying the N_{ch} where 90% of all collisions produce at least that multiplicity. Because the efficiency for detecting events with low multiplicity is low, the distribution is not measured well for low N_{ch} , so identification of this anchor point is model dependent. This inefficiency does not directly impact measurements of jets in 0-80% central collisions because these events are typically high multiplicity, however, it can lead to a

significant uncertainty in the correct centrality. This uncertainty is largest at low multiplicities, corresponding to more peripheral collisions.

As the phenomena observed in heavy ion collisions have been observed in increasingly smaller systems, this approach to determining centrality has been applied to these smaller systems as well. While the term “centrality” is still used, this is perhaps better understood as event activity, since the correlation between multiplicity and impact parameter is weaker in these systems and other effects may become relevant (Alvioli *et al.*, 2016, 2014; Alvioli and Strikman, 2013; Arnesen *et al.*, 2015; Bzdak *et al.*, 2016; Coleman-Smith and Muller, 2014). The interpretation of the “centrality” dependence in small systems should therefore be done carefully.

C. Inclusive hadron measurements

Single particle spectra at high momenta, which are dominated by particles resulting from hard scatterings, can be used to study jets. To quantify any modifications to the hadron spectra in nucleus-nucleus ($A+A$) collisions, the nuclear modification factor was introduced. The nuclear modification factor in $A+A$ collisions is defined as

$$R_{AA} = \frac{\sigma_{NN}}{\langle N_{bin} \rangle} \frac{d^2 N_{AA}/dp_T d\eta}{d^2 \sigma_{pp}/dp_T d\eta} \quad (3)$$

where η is the pseudorapidity, p_T is the transverse momentum, $\langle N_{bin} \rangle$ is the average number of binary nucleon-nucleon collisions for a given range of impact parameter, and σ_{NN} is the integrated nucleon-nucleon cross section. N_{AA} and σ_{pp} in this context are the yield in AA collision and cross section in $p+p$ collisions for a particular observable. If nucleus-nucleus collisions were simply a superposition of nucleon-nucleon collisions, the high p_T particle cross-section should scale with the number of binary collisions and therefore $R_{AA} = 1$. An $R_{AA} < 1$ indicates suppression and an $R_{AA} > 1$ indicates enhancement. R_{AA} is often measured as a function of p_T and centrality class. Measurements of inclusive hadron R_{AA} are relatively straightforward as they only require measuring the single particle spectra and a calculation of the number of binary collisions for each centrality class based on a Glauber model (Miller *et al.*, 2007). Theoretically, hadron R_{AA} can be difficult to interpret, particularly at low momenta, because different physical processes that are not calculable in pQCD, such as hadronization, can change the interpretation of the result. Interpretation of R_{AA} usually focuses on high p_T , where calculations from perturbative QCD (pQCD) are possible. An alternative to R_{AA} is R_{CP} , where peripheral heavy ion collisions are used as the reference instead of $p+p$ collisions

$$R_{CP} = \frac{\langle N_{bin}^{peri} \rangle}{\langle N_{bin}^{cent} \rangle} \frac{d^2 N_{AA}^{cent}/dp_T d\eta}{d^2 N_{AA}^{peri}/dp_T d\eta} \quad (4)$$

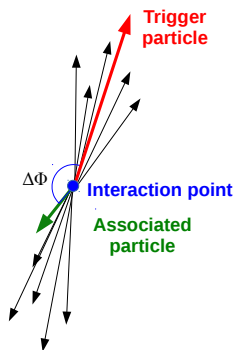


FIG. 5 Schematic diagram showing the identification of a high- p_T hadron in a $p+p$ collision and its use to define a coordinate system for dihadron correlations.

where *cent* and *peri* denote the values of $\langle N_{bin} \rangle$ and N_{AA} for central and peripheral collisions, respectively. This is typically done either when there is no $p+p$ reference available or the $p+p$ reference has much larger uncertainties than the $A+A$ reference. It does have the advantage that other nuclear effects could be present in the R_{CP} cross-section and cancel in the ratio, and that these collisions are recorded at the same time and thus have the same detector conditions. However, there can be QGP effects in peripheral collisions so this can make the interpretation difficult. The pQCD calculations used to interpret these results are sensitive in principle to hadronization effects, however, if the R_{AA} of hard partons does not have a strong dependence on p_T , the R_{AA} of the final state hadrons will not have a strong dependence on p_T . R_{AA} will therefore be relatively insensitive to the effects of hadronization and more theoretically robust.

D. Dihadron correlations

A hard parton scattering usually produces two partons that are separated by 180° in the transverse plane (commonly stated as back-to-back). In a typical dihadron correlation study (Aamodt *et al.*, 2012; Abelev *et al.*, 2009b; Adler *et al.*, 2003a, 2006d; Alver *et al.*, 2010), a high- p_T hadron is identified and used to define the coordinate system because its momentum is assumed to be a good proxy for the jet axis of the parton it arose from. This hadron is called the trigger particle. The azimuthal angle of other hadrons' momenta in the event is calculated relative to the momentum of this trigger particle. These hadrons are commonly called the associated particles. This is illustrated schematically in Figure 5. The associated particle is typically restricted to a fixed momentum range, also typically higher than the $\langle p_T \rangle$ of tracks in the event and lower than the momenta of trigger particles. The distribution of associated particles relative

to the trigger particle can be measured in azimuth ($\Delta\phi$), pseudorapidity ($\Delta\eta$), or both.

Figure 6 shows a sample dihadron correlation in $\Delta\phi$ and $\Delta\eta$ and its projection onto $\Delta\phi$ for trigger momenta $10 < p_T^t < 15$ GeV/ c within pseudorapidities $|\eta| < 0.5$ and associated particles within $|\eta| < 0.9$ with momenta and $1.0 < p_T^a < 2.0$ GeV/ c in $p+p$ collisions at $\sqrt{s} = 2.76$ TeV in PYTHIA (Sjostrand *et al.*, 2006). The peak near 0° , called the near-side, is narrow in both $\Delta\phi$ and $\Delta\eta$ and results from associated particles from the same parton as the trigger particle. The peak near 180° , called the away-side, is narrow only in $\Delta\phi$ and is roughly independent of pseudorapidity. This peak arises from associated particles produced by the parton opposing the one which generated the trigger particle. The partons are back-to-back in the frame of the partons, but the rest frame of the partons is not necessarily the same as the rest frame of the incoming nuclei because the incoming partons may not carry the same fraction of the parent nucleons' momentum, x . Since most of the momenta of both the partons and the nucleons are in the direction of the beam (which is universally taken to be the z axis), a difference in pseudorapidity is observed, while the influence on the azimuthal position is negligible. This causes the away-side to be broad in $\Delta\eta$ without requiring modified fragmentation or interaction with the medium, as evident in Figure 6.

1. Background subtraction methods

Dihadron correlations typically have a low signal to background ratio, often less than 1:25. The raw signal in dihadron correlations is typically assumed to arise from only two sources, particles from jets and particles from the underlying event, which are correlated with each other due to flow. The production mechanisms of the signal and the background are assumed to be independent so they can be factorized. These assumptions are called the two source model (Adler *et al.*, 2006b). The correlation of two particles in the background due to flow is given by (Adler *et al.*, 2003a; Bielcikova *et al.*, 2004)

$$\frac{dN}{\pi d\Delta\phi} = B \left(1 + \sum_{n=1}^{\infty} 2v_n^t v_n^a \cos(n\Delta\phi) \right) \quad (5)$$

where B is a constant which depends on the normalization and the multiplicity of trigger and associated particles in an event, the v_n^t are the v_n for the trigger particle, the v_n^a are the v_n for the associated particle, and $\Delta\phi$ is the difference in azimuthal angle between the associated particle and the trigger. The v_n for the trigger particle may arise either from flow, if the trigger particle is not actually from a jet, or from jet quenching, since the path length dependence of partonic energy loss leads to a suppression of jets out-of-plane. Because dihadron cor-

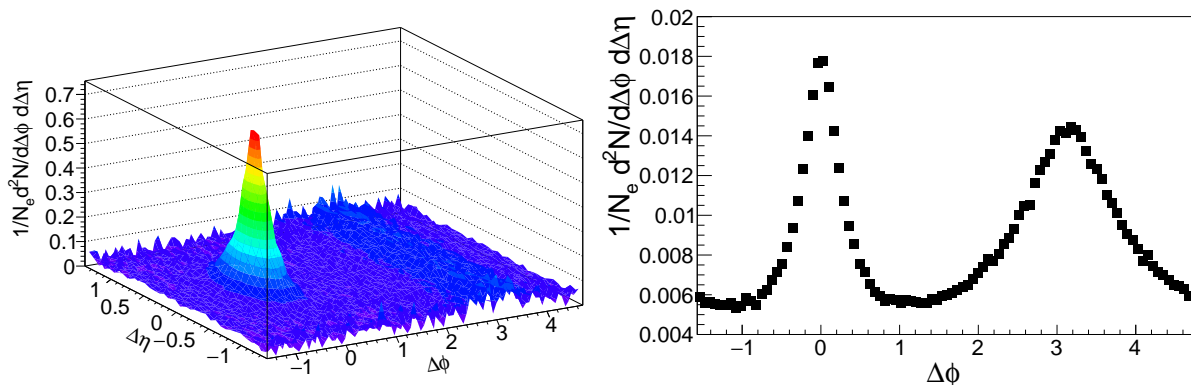


FIG. 6 Dihadron correlations for trigger momenta $10 < p_T^\dagger < 15$ GeV/c and $1.0 < p_T^a < 2.0$ GeV/c within pseudorapidities $|\eta| < 0.5$ and associated particles within $|\eta| < 0.9$ in $p+p$ collisions at $\sqrt{s} = 2.76$ TeV in PYTHIA (Sjostrand *et al.*, 2006). The signal is normalized by the number of equivalent Pb+Pb collisions. Left: Correlation function as a function of $\Delta\phi$ and $\Delta\eta$. Right: Projection onto $\Delta\phi$.

relations are typically measured by averaging over positive and negative pseudorapidities, the average v_1 due to flow is zero and the $n = 1$ term is usually omitted. Global momentum conservation also leads to a v_1 signal which is approximately inversely proportional to the particle multiplicity (Borghini *et al.*, 2000). The momentum conservation term is typically assumed to be negligible, which may be valid for higher multiplicity events. The pseudorapidity range for both trigger and associated particles is typically restricted to a region where the v_n do not change dramatically so that the pseudorapidity dependence of $\frac{dN}{d\phi}$ is negligible. The azimuthal dependence of any additional sources of long range correlations could be expanded in terms of their Fourier coefficients without loss of generality.

There are two further assumptions commonly used in order to subtract this background: that the appropriate v_n are the same as the v_n measured in other analyses and that there is a region in $\Delta\phi$ near $\Delta\phi \approx 1$ where the signal is zero. The latter assumption is called the Zero-Yield-At-Minimum (ZYAM) method (Adams *et al.*, 2005a). Early studies of dihadron correlations fit the data near $\Delta\phi \approx 1$ to determine the background level (Adams *et al.*, 2004a; Adare *et al.*, 2007b,b; Adler *et al.*, 2003a, 2006c). Later studies typically use a few points around the minimum (Adler *et al.*, 2006b; Agakishiev *et al.*, 2010; Aggarwal *et al.*, 2010). An alternative to ZYAM for determining the background level, B in Equation 5, is the absolute normalization method (Sickles *et al.*, 2010). This method makes no assumption about the background level based on the shape of the underlying background but rather estimates the level of combinatorial pairs from the mean number of trigger and mean number of associated particles in all events as a function of event multiplicity.

It has been suggested that Hanbury-Brown-Twiss (HBT) correlations (Lisa and Pratt, 2008; Lisa *et al.*,

2005), quantum correlations between identical particles from the same source, may contribute to the near-side peak in some momentum regions. If the momenta of the trigger and associated particles are sufficiently different, these contributions are expected to be negligible. Distinguishing resonances from jet-like correlations is more difficult. A high momentum resonance can itself be considered a jet or part of a jet. The appropriate classification for lower momentum resonances is less clear, but functionally any short range correlations are considered part of the signal in dihadron correlations.

The background is then dominated by contributions from flow. However, this does not mean that the v_n measured in other analyses are necessarily the Fourier coefficients of the background for dihadron correlations. Methods for measuring v_n have varying sensitivities to non-flow (such as jets) and fluctuations (Voloshin *et al.*, 2008). Fluctuations in v_n may either increase or decrease the effective v_n , depending on their physical origin and its correlation with jet production. The correct v_n in equation 5 is also complicated by proposed decorrelations between the reaction planes for soft and hard processes, which would change the effective v_n (Aad *et al.*, 2014a; Jia, 2013). A recent method uses the reaction plane dependence of the background in equation 5 to extract the background level and shape from the correlation itself (Sharma *et al.*, 2016).

The majority of measurements of dihadron correlations in heavy ion collisions in the literature omit odd v_n since these studies were done before the odd v_n were observed and understood to arise due to collective flow. The first direct observation of the odd v_n was in high- p_T dihadron correlations, where subtraction of only the even v_n led to two structures called the ridge (on the near-side) (Abelev *et al.*, 2009b; Alver *et al.*, 2010) and the shoulder or Mach cone (on the away-side) (Abelev *et al.*,

2009b; Adare *et al.*, 2008a,a,d; Afanasiev *et al.*, 2008; Agakishiev *et al.*, 2010). This means that the majority of studies of dihadron correlations at low and intermediate momenta ($p_T \lesssim 3$ GeV/c) do not take the odd v_n into account and therefore include distortions due to flow. Exceptions are studies which used the $\Delta\eta$ dependence on the near-side to subtract the ridge and focused on the jet-like correlation (Abelev *et al.*, 2009b, 2010a, 2016; Agakishiev *et al.*, 2012c). An understanding of the low momentum jet components is important because many of the medium modifications of the jet manifest as differences in distributions at low momenta. While some of the iconic RHIC results showing jet quenching did not include odd v_n (Adams *et al.*, 2004a) and the complex structures at low and intermediate momenta are now understood to arise due to flow rather than jets (Nattrass *et al.*, 2016), some of the broad conclusions of these studies are robust and studies at sufficiently high momenta ($p_T \gtrsim 3$ GeV/c) are still valid because the impact of the higher order v_n is negligible. Section III focuses on results robust to the omission of the odd v_n and more recent results.

E. Reconstructed jets

A jet is defined by the algorithm used to group final state particles into jet candidates. In QCD any parton may fragment into two partons, each carrying roughly half of the energy and moving in approximately the same direction. This is a difficult process to quantify theoretically and leads to divergencies in theoretical calculations. A robust jet finding algorithm would find the same jet with the same p_T regardless of the details of the fragmentation and would thus be *collinear safe*. Additionally, QCD allows for an infinite number of very soft partons to be produced during the fragmentation of the parent parton. All experiments have low momentum thresholds for their acceptance so these particles cannot generally be observed and the production of soft partons leads to theoretical divergencies as well. A robust jet finding algorithm will find the same jets, even in the presence of a large number of soft partons and would thus be *infrared safe*. In order for the jet definition to be robust, the jet-finding algorithm must be both infrared and collinear safe (Salam, 2010).

Jet finding algorithms are generally characterized by a resolution parameter. In the case of a conical jet, this is the radius of the jets

$$R = \sqrt{\Delta\phi^2 + \Delta\eta^2} \quad (6)$$

where $\Delta\phi$ is the distance from the jet axis in azimuth and $\Delta\eta$ is the distance from the jet axis in pseudorapidity. A conical jet is symmetric in $\Delta\phi$ and $\Delta\eta$, although it is not theoretically necessary for jets to be symmetric. We will focus the discussion on conical jets, since they are

the most intuitive to understand. The most common jet-finding algorithm in heavy ion collisions, anti- k_T , usually reconstructs conical jets. The majority of jet measurements include corrections up to the energy of all particles in the jet, whether or not they are observed directly. The ALICE experiment also measures charged jets, which are corrected only up to the energy contained in charged constituents.

We emphasize that a measurement of a jet is not a direct measurement of a parton. A jet is a composite object comprising several final state hadrons. If the jet reconstruction algorithm applied to theoretical calculations and data is the same, experimental measurements of jets can be comparable to theoretical calculations of jets. However, even theoretically, it is unclear which final state particles should be counted as belonging to one parton. What the original parton's energy and momentum were before it fragmented is therefore an ill-posed question. The only valid comparisons between theory and experiment are between jets comprised of final state hadrons and reconstructed with the same algorithm. This understanding was the conclusion of the Snowmass Accord (Huth *et al.*, 1990). Ideally both the jet reconstruction algorithms and the treatment of the combinatorial background in heavy ion collisions would also be the same for theory and experiment.

1. Jet-finding algorithms

Infrared and collinear safe sequential recombination algorithms such as the k_T , anti- k_T and Cambridge/Aachen (CAMB) are encoded in *FastJet* (Cacciari *et al.*, 2011, 2008a,b, 2012; Salam, 2010). The *FastJet* (Cacciari *et al.*, 2012) framework takes advantage of advanced computing algorithms in order to decrease computational times for jet-finding. This is essential for jet reconstruction in heavy ion collisions due to the large combinatorial background. Due to the ubiquity of the anti- k_T jet-finding algorithm in studies of jets in heavy ion collisions, it is worth describing this algorithm in detail. The anti- k_T algorithm is a sequential recombination algorithm, which means that a series of steps for grouping particles into jet candidates is repeated until all particles in an event are included in a jet candidate. The steps are:

1. Calculate

$$d_{ij} = \min(1/p_{T,i}^2, 1/p_{T,j}^2) \frac{(\eta_i - \eta_j)^2 + (\phi_i - \phi_j)^2}{R^2} \quad (7)$$

and

$$d_i = 1/p_{T,i}^2 \quad (8)$$

for every pair of particles where $p_{T,i}$ and $p_{T,j}$ are the momenta of the particles, η_i and η_j are the

pseudorapidities of the particles, and ϕ_i and ϕ_j are the azimuthal angles of the particles.

2. Find the minimum of the d_{ij} and d_i . If this minimum is a d_{ij} , combine these particles into one jet candidate, adding their energies and momenta, and return to the first step.

3. If the minimum is a d_i , this is a final state jet candidate. Remove it from the list and return to the first step. Iterate until no particles remain.

The original implementation of the anti- k_T used rapidity rather than pseudorapidity (Cacciari *et al.*, 2008a), however, in practice most experiments cannot identify particles to high momenta and the difference is negligible at high momenta so pseudorapidity is used in practice.

The anti- k_T algorithm has a few notable features for jet reconstruction in heavy ion collisions. Since d_{ij} is smallest for pairs of high- p_T particles, the anti- k_T algorithm starts clustering high- p_T particles into jets first and forms a jet around these particles. The anti- k_T algorithm creates jets which are approximately symmetric in azimuth and pseudorapidity, at least for the highest energy jets. Particularly in heavy ion collisions, it must be recognized that the “jets” from a jet-finding algorithm are not necessarily generated by hard processes. Since all final state particles are grouped into jet candidates, some jet candidates will comprise only particles whose production was not correlated because they were created in the same hard process but which randomly happen to be in the same region in azimuth and pseudorapidity. These jet candidates are called fake or combinatorial jets. Particles that are correlated through a hard process will be grouped into jet candidates, which will also contain background particles. Care must therefore be used when interpreting the results of a jet-finding algorithm as it is possible to have jet candidates in an analysis that come from processes that may not be included in the calculation used to interpret the results.

There are two important additional points to be made with regard to jet-finding algorithms as applied to heavy ion collisions. While jet-finding algorithms have been optimized for measurements in small systems such as e^+e^- and $p+p$ collisions, these algorithms are computationally efficient and well-defined both theoretically and experimentally. Although we may want to consider how we use these algorithms, there is no need for further development of jet-finding algorithms for use in heavy ion collisions. However, there is a difference between jet-finding in principle and in practice. While these jet-finding algorithms are infrared and collinear safe *if all particles are input into the jet-finding algorithm*, most experimental measurements restrict the momenta and energies of the tracks and calorimeter clusters input into the jet-finding algorithms. Some apply other selection criteria to the population of jets, such as requiring a high

momentum track, which are not infrared or collinear safe. These techniques are not necessarily avoidable, especially in the high background environment of heavy ion collisions, however, they must be considered when interpreting the results.

2. Dealing with the background

Combinatorial jets and distortions in the reconstructed jet energy due to background need to be taken into account in order to interpret a measured observable. This can be done either in the measurement, or in theoretical calculations that are compared to the measurement. The latter is particularly difficult in a heavy ion environment because the background has contributions from all particle production processes.

While it is impossible to know which particles in a jet candidate come from hard processes and which come from the background, and indeed it is even ambiguous to make this distinction on theoretical level, differences between particles in the signal and the background on average can be used to reduce the impact of particles from the background and calculate the impact of the remaining background on an ensemble of jet candidates. As mentioned in Section I, the average momentum of particles in the background is much lower than that of those in the signal. Figure 7 shows a comparison of HYDJET to STAR data (Lokhtin *et al.*, 2009b) and the particles produced by hard and soft processes in HYDJET. At sufficiently high p_T , particle production is dominated by hard processes. HYDJET has been tuned to match fluctuations and v_n from heavy ion collisions, so this qualitative conclusion should be robust. Jets themselves can contribute to background for the measurement of other jets, however, the probability of multiple jets overlapping spatially and fragmenting into several high momentum particles is low. Therefore, introducing a minimum momentum for particles to be used in jet-finding reduces the number of background particles in the jet candidates. This also reduces the number of combinatorial jets, since there are very few high momentum particles which were not created from a hard process. While this selection criterion reduces the background contribution, it is not collinear safe. Additionally, as most of the modification of the jet fragmentation function is observed for constituents with $p_T < 3$ GeV, this could remove the modification signature for particular observables.

The effect of the background can also be reduced by focusing on smaller jets or higher energy jets. For a conical jet, the jet area is $A_{jet} = \pi R^2$. The average number of background particles in the jet candidate is proportional to the area. The background energy scales with the area of the jet, but is independent of the jet energy (assuming that the signal and background are independent), so the fractional change in the reconstructed jet energy due to

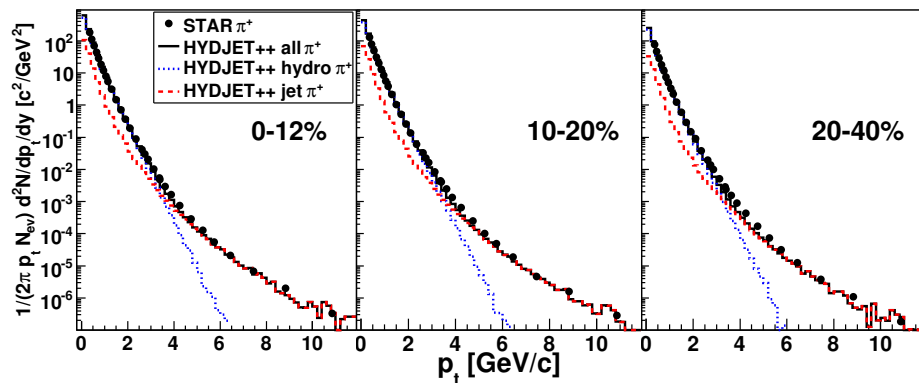


FIG. 7 Figure from (Lokhtin *et al.*, 2009b) comparing HYDJET (Lokhtin *et al.*, 2009a) calculations to STAR data (Abelev *et al.*, 2006). Particle production in HYDJET is separated into those from hard and soft processes. This shows that at sufficiently high momenta, particle production is dominated by hard processes.

1149 background is smaller for higher energy jets as the ma- 1187
 1150 jority of the jet energy is focused in the core of the jet. 1188
 1151 Furthermore, in elementary collisions, the distribution of 1189
 1152 final state particles in the jet as a function of the fraction 1190
 1153 of the jet energy carried by the particle is approximately 1191
 1154 independent of the jet energy. This means that the differ- 1192
 1155 ence in the average momentum for signal particles versus 1193
 1156 background particles is larger for high energy jets. Since 1194
 1157 jets that interact with the medium are expected to lose 1195
 1158 energy and become broader, studies of high momentum, 1196
 1159 narrow jets alone cannot give a complete picture of par- 1197
 1160 tonic energy loss in the QGP. Furthermore, even in $p+p$
 1161 collisions, theoretical calculations are more difficult for
 1162 jets with smaller cone sizes because they are sensitive to
 1163 the details of the hadronization (Abelev *et al.*, 2013d). 1198

1164 The fraction of combinatorial jet candidates can also 1200
 1165 be reduced by requiring additional evidence of a hard 1201
 1166 process, such as requiring that the candidate jet has at 1202
 1167 least one particle above a minimum threshold, requiring 1203
 1168 that the jet candidate have a hard core, or identifying 1204
 1169 a heavy flavor component within the jet candidate. We 1205
 1170 note that the distinction between fake jets and the back- 1206
 1171 ground contribution in jets from hard processes is am- 1207
 1172 biguous, particularly for low momentum jets, however, 1208
 1173 the corrections for these effects are generally handled sep- 1209
 1174 arately. Below we review methods for addressing the im- 1210
 1175 pact of background particles on the jet energy and corre- 1211
 1176 sponding methods for dealing with any remaining combi- 1212
 1177 natorial jets. Each of these methods have strengths and 1213
 1178 weaknesses, and may lead to biases in the surviving jet 1214
 1179 population. 1215

1180 There are five classes of methods for background sub- 1216
 1181 traction in the four experiments which have published 1217
 1182 jet measurements in heavy ion collisions. ALICE and 1218
 1183 STAR use measurements of the average background en- 1219
 1184 ergy/momentum density in the event to subtract the 1220
 1185 background contribution from jet candidates. ATLAS 1221
 1186 uses an iterative procedure, first finding jet candidates, 1222

then omitting them from the calculation of the back-
 ground energy distribution, and then using this back-
 ground distribution to find new jet candidates. CMS
 subtracts background before jet finding, omitting jet can-
 didates from the background subtraction. In addition,
 an event mixing method was recently applied to STAR
 data to estimate the average contribution from the back-
 ground to both the jet energy and combinatorial jets.
 Constituent subtraction refers to corrections to account
 for background before jet finding. Each of these are de-
 scribed in greater detail below.

ALICE/STAR In this method the background contribu-
 tion to a jet candidate is assumed to be proportional to
 the area of that candidate. The area of each jet is es-
 timated by filling an event with many very soft, small
 area particles (ghost particles), rerunning the jet-finder,
 and then counting how many are clustered into a given
 jet. The background energy/momentum density per unit
 area (ρ) is measured by either using randomly oriented jet
 cones or the k_T jet-finding algorithm and calculating the
 momentum over the area of the cone or k_T jet. The me-
 dian of the energy per unit area of the collection is used
 to reduce the impact from real jets in the event on the de-
 termination of the background density. The two highest
 energy jets in the event are omitted from the distribution
 of jets used to determine the background energy density.
 Since the background has a p_T modulation that is corre-
 lated with the reaction plane, an event plane dependent
 ρ can be determined as well (Adam *et al.*, 2016b).

This method was proposed in (Cacciari *et al.*, 2008b)
 for measurements in $p+p$ collisions under conditions with
 high pile up and its feasibility in heavy ion collisions
 demonstrated in (Abelev *et al.*, 2012a). The strength of
 this method is that it can be used even with jets clustered
 with low momentum constituents. However, the energy
 of individual jets is not known precisely since only the

average background contribution is subtracted, but the background itself could fluctuate which smears the measurement of the jet energy and momentum. Additionally measurements of the background energy density can include some contribution from real jets. Subtracting the average contribution to a jet candidate due to the background may not fully take into account the tendency of jet-finding algorithms to form combinatorial jets around hot spots in the background.

ATLAS We outline the approach in (Aad *et al.*, 2013b). We note that the details of the analysis technique are optimized for each observable. ATLAS measures both calorimeter and track jets. Track jets are reconstructed using charged tracks with $p_T > 4$ GeV/ c . The high momentum constituent cut strongly suppresses combinatorial jets, and ATLAS estimates that a maximum of only 4% of all $R = 0.4$ anti- k_T track jet candidates in 0-10% central Pb+Pb collisions contain a 4 GeV/ c background track. For calorimeter jet measurements, ATLAS estimates the average background energy per unit area and the v_2 using an iterative procedure (Aad *et al.*, 2013b). In the first step, jet candidates with $R = 0.2$ are reconstructed. The background energy is estimated using the average energy modulated by the v_2 calculated in the calorimeters, excluding jet candidates with at least one tower with $E_T > \langle E_T \rangle$. Jets from this step with $E_T > 25$ GeV and track jets with $p_T > 10$ GeV/ c are used to calculate a new estimate of the background and a new estimate of v_2 , excluding all clusters within $\Delta R < 0.4$ of these jets. This new background modulated by the new v_2 and jets with $E_T > 20$ GeV were considered for subsequent analysis.

Combinatorial jets are further suppressed by an additional requirement that they match a track jet with high momentum (e.g. $p_T > 7$ GeV/ c (Aad *et al.*, 2013b)) or a high energy cluster (e.g. $E_T > 7$ GeV (Aad *et al.*, 2013b)) in the electromagnetic calorimeter. These requirements strongly suppress the combinatorial background, however, they may lead to fragmentation biases and may suppress the contribution from jets which have lost a considerable fraction of their energy in the medium. These biases are likely small for the high energy jets which have been the focus of ATLAS studies, however, the bias is stronger near the 20 GeV lower momentum threshold of ATLAS studies.

CMS In measurements by CMS the background is subtracted from the event before the jet-finding algorithm is run. The average energy and its dispersion is calculated as a function of η . Tower energies are recalculated by subtracting the mean energy plus the mean dispersion. Negative energies after this step are set to zero. These tower energies are input into a jet-finding algorithm and the

background is recalculated, omitting towers contained in the jets. The tower energies are again calculated by subtracting the mean energy plus the dispersion and setting negative values to zero.

Event Mixing The goal of event mixing is to generate the combinatorial background – in the case of jet studies, fake jets. In STAR, the fraction of combinatorial jets in an event class is generated by creating a mixed event where every track comes from a different event (Adamczyk *et al.*, 2017c). The data are binned in classes of multiplicity, reconstructed event plane, and z-vertex position so that the mixed event accurately reflects the distribution of particles in the background. Jet candidates are reconstructed using this algorithm in order to calculate the contribution from combinatorial jets, which can then be subtracted from the ensemble. This is a very promising method, particularly for low momentum jets, but we note that it is sensitive to the details of the normalization at low momenta. It is also computationally intensive, which may make it impractical, and it is unclear how to apply it to all observables.

Constituent Subtraction The constituent background subtraction method was first developed to remove pile-up contamination from LHC based experiments, where it is not unusual to have contributions from multiple collisions in a single event. Unlike the area based subtraction methods described above, the constituent method subtracts the background constituent-by-constituent. The intention is to correct the 4-momentum of the particles, and thus correct the 4-momentum of the jet (Berta *et al.*, 2014). It is necessary to consider the jet 4-momentum for some of the new jet observables that will be described in this paper, such as jet mass. The process is an iterative scheme that utilizes the ghost particles, which are nearly zero momentum particles with a very small area on the order of 0.005 which are embedded into the event by many jet finding algorithms. The jet finder is then run on the event, and the area is determined by counting the number of ghost particles contained within the jet. Essentially the local background density is determined and then subtracted from the constituents, which are thrown out if they reach zero momentum. The effect of this background scheme on the applicable observables is under study and it is not clear as of yet what its effect is compared to the more traditional area based background subtraction schemes.

F. Particle Flow

The particle flow algorithm was developed in order to use the information from all available sub-detectors

in creating the objects that are then clustered with a jet-finding algorithm. Many particles will leave signals in multiple sub-detectors. For instance a charged pion will leave a track in a tracker and shower in a hadronic calorimeter. If information from both detectors is used, this would double count the particle. However, excluding a particular sub-detector would remove information about the energy flow in the collision as well. Tracking detectors generally provide better position information while hadronic calorimeters are sensitive to more particles but whose positions are altered by the high magnetic field necessary for tracking. The goal is to use the best information available to determine a particle's energy and position simultaneously.

The particle flow algorithm operates by creating stable particles from the available detectors. Tracks from the tracker are extrapolated to the calorimeters – in the case of CMS, an electromagnetic calorimeter and a hadronic calorimeter (CMS, 2009). If there is a cluster in the associated calorimeter, it is linked to the track in question. Only the closest cluster to the track is kept as a charged particle should only have a single track. The energy and momentum of the cluster and track are compared. If the energy is low enough compared to the momentum, only a single hadron with momentum equal to a weighted average of the track and calorimeter is created. The exact threshold should depend on the details of the detector and its energy resolution. If the energy is above a certain threshold, neutral particles are then created out of the excess energy. If that excess is only in an electromagnetic calorimeter, the neutral particle is assumed to be a photon. If the excess is in a hadronic calorimeter, the neutral particle is assumed to be a hadron. If there is some combination, multiple neutral particles may be created, with the photon given preference in terms of "using up" the excess energy.

By grouping the information into individual particles, the particle flow algorithm reduces the sensitivity of the measurement of the jet energy to the jet fragmentation pattern. This is a correction that can be done prior to unfolding, which is described below. The particle flow algorithm can be a powerful tool, however, it depends on the details of the sub-detectors that are available, their energy resolution, and their granularity. For example, the ALICE detector has precision tracking detectors and an electromagnetic calorimeter but no hadronic calorimeter. The optimal particle flow algorithm for the ALICE detector is to use the tracking information when available and only use information from the electromagnetic calorimeter if there is no information from the tracking detectors. Additionally, the magnetic field strength plays a role, as this will dictate how much the charge particle paths diverge from one another before reaching the calorimeter and how far charged particles are deflected before reaching the calorimeters. To fully utilize this algorithm, the energy resolution of all calorimeters must

be known precisely, and the distribution of charged and neutral particles must be known.

G. Unfolding

Before comparing measurements to theoretical calculations or other measurements, they must be corrected for both detector effects and smearing due to background fluctuations. Both the jet energy scale (JES) and the jet energy resolution (JER) need to be considered in any correction procedure. The jet energy scale is a correction to the jet to recover the true 4-vector of the original jet (and not of the parton that created it). The background subtraction methods described above are examples of corrections to the jet energy scale due to the addition of energy from the underlying background. Precision measurements of the energy scale, as done by the ATLAS collaboration (ATL, 2015a), are an important step in understanding the detector response and necessary to reduce the systematic uncertainties. The jet energy resolution is a measure of the width of the jet response distribution. An example from the ALICE experiment can be seen in Figure 8. In heavy-ion collisions there are two components, the increase in the distribution due to the fluctuating background that will be clustered into the jet, and due to detector effects.

In most measurements of reconstructed jets, the jet energy resolution is on the order of 10-20% for the high momentum jets, where detector effects dominate. This can be understood because even a hadronic calorimeter is not equally efficient at observing all particles. In particular, the measurement of neutrons, antineutrons, and the K_L^0 is difficult. The high magnetic field necessary for measuring charged particle momentum leads to a lower threshold on the momenta of reconstructed particles and can sweep charged particles in or out of the jet. As a result, even an ideal detector has a limited accuracy for measuring jets. The large fluctuations in the measured jet energy due to these effects distort the measured spectrum. This is qualitatively different from measurements of single particle observables, where the momentum resolution is typically 1% or better, often negligible compared to other uncertainties. This means that measurements of jet observables must be corrected for fluctuations due to the finite detector resolution if they will be compared to theoretical calculations or to measurements of the same observable in a different detector, or even from the same detector with different running conditions. Fluctuations in the background in $A+A$ collisions lead to further distortions in the reconstructed jet energy. Correcting for these effects is generally referred to as unfolding in high energy physics, although it is called unsmearing or deconvolution in other fields.

Here we summarize unfolding methods, based on the discussion in (Ade, 2011; Cowan, 2002). If the true value

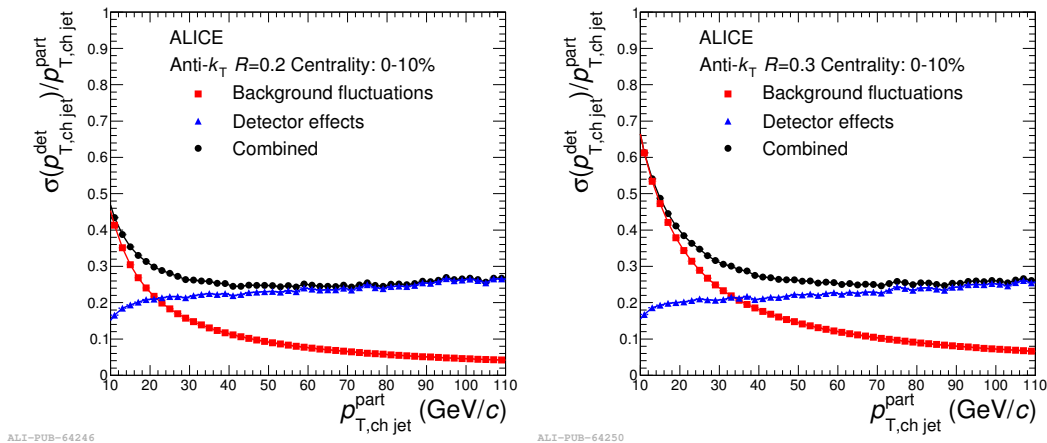


FIG. 8 Figure from ALICE (Abelev *et al.*, 2014a). On the left is the standard deviation of the combined jet response (black circles) for $R=0.2$ anti- k_T jets, including background fluctuations (red squares) and detector effects (blue triangles) for 0-10% central Pb+Pb events. On the right is the standard deviation of the combined jet response (black circles) for $R=0.3$ anti- k_T jets, including background fluctuations (blue triangles) and detector effects (red squares) for 0-10% central Pb-Pb events. The background effects increase the jet energy resolution more for larger jets, as can be seen from the difference in the background distributions in both plots. For high momentum jets, where the momentum of the jet is much larger than background fluctuations, the jet energy resolution will be dominated by detector effects.

of an observable in a bin i is given by y_i^{true} , then the observed value in bin j , y_j^{reco} , is given by

$$y_j^{reco} = \sum_{i=0}^N R_{ij} y_i^{true} \quad (9)$$

where R_{ij} is the response matrix relating the true and reconstructed values.

The response matrix is generally determined using Monte Carlo models including particle production, propagation of those particles through the detector material and simulation of its response, and application of the measurement algorithm, although sometimes data-driven corrections are incorporated into the response matrix. As an example, we consider the analysis of jet spectra. The truth result (y_i^{true}) is usually generated by an event generator such as PYTHIA (Sjostrand *et al.*, 2006) or DPMJET (Ranft, 1999). The jet finding algorithm to be used in the analysis is run on this truth event, which generates the particle level jets comprising y_i^{true} . The truth event is then run through a simulation of the detector response. It is common to include a simulated background from a generator such as HIJING (X.-N. Wang, and M. Gyu-lassy, 1991), but not required. This creates the reconstructed event, and as before, the jet finding algorithm used in the analysis is run on this event to create the detector level jets that make up y_j^{reco} . Next, the particle level jets must be matched to detector level jets to build the response matrix, with unmatched jets determining the reconstruction efficiency. There are several ambiguities in this method. The first is that it comes with an assumption of the spectra shape and fragmentation pat-

tern of the jets from the simulation. The second is that there is not always a one-to-one correspondence between the truth and detector level jets. The detector response may cause the energy of a particular truth jet to be split into two detector level jets. However, the response matrix requires a one-to-one correspondence, which necessitates a choice.

If one could simply invert the response matrix, it would be possible to determine $y_i^{true} = \sum_{i=0}^N R_{ij}^{-1} y_j^{reco}$. However, response matrices for jet observables are generally ill-conditioned and not invertible. The further the jet response matrix is from a diagonal matrix, the more difficult the correction procedure is. This is one reason the background subtraction methods outlined in the preceding section are employed. By correcting the jet energy scale on a jet-by-jet basis, the response matrix is much closer to a diagonal matrix, however this is not a sufficient correction. The process of unfolding is thus required to determine y_i^{true} given the information in Equation 9.

One of the main challenges in unfolding is that it is an ill-posed statistical inverse problem which means that even though the mapping of y_i^{true} to y_j^{reco} is well-behaved, the inverse mapping of y_j^{reco} to y_i^{true} is unstable with respect to statistical fluctuations in the smeared observations. This is a problem even if the response matrix is known with precision. The issue is that within the statistical uncertainties, the smeared data can be explained by the actual physical solution, but also by a large family of wildly oscillating unphysical solutions. The smeared observations alone cannot distinguish among these alternatives, so additional a priori information about physically plausible solutions needs to

1489 be included. This method of imposing physically plau- 1538
 1490 sible solutions is called regularization, and it essentially 1539
 1491 is a method to reduce the variance of the unfolded truth 1540
 1492 points by introducing a bias. The bias generally comes 1541
 1493 in the form of an assumption about the smoothness of 1542
 1494 the observable, however, this assumption always results 1543
 1495 in a loss of information. 1544

If an observable is described well by models, it may 1545
 be possible to correct the measurement using the ratio of 1546
 the observed to the true value in Monte Carlo: 1547

$$\gamma_j^{true} = \frac{\gamma_j^{true,MC}}{y_j^{reco,MC}} y_j^{reco} \quad (10) \quad 1548$$

1496 where γ_j^{true} is the estimate of the true value, $\gamma_j^{true,MC}$ is 1551
 1497 the true value in the Monte Carlo model, and $y_j^{reco,MC}$ is 1552
 1498 the measurement predicted by the model. This approach 1553
 1499 is called a bin-by-bin correction. It is also satisfactory 1554
 1500 when the response matrix is nearly diagonal which is gen- 1555
 1501 erally true when the bin width is wider than the resolu- 1556
 1502 tion in the bin. In this circumstance, the inversion of the 1557
 1503 response matrix is generally stable and the measurement 1558
 1504 is not affected significantly by statistical fluctuations in 1559
 1505 the measurement or the response matrix. For example, 1560
 1506 bin-by-bin efficiency corrections to measurements of sin- 1561
 1507 gle particle spectra may be adequate as long as the mo- 1562
 1508 mentum resolution is fairly good and the input spectra 1563
 1509 have roughly the same shape as the true spectra. This 1564
 1510 approach can work for measurements of reconstructed 1565
 1511 jets in systems such as $p+p$ collisions [e.g. fragmentation 1566
 1512 function measurements]. Unfortunately, for typical jet 1567
 1513 measurements, the desired binning is significantly nar- 1568
 1514 rower than the jet energy resolution, and fluctuations in 1569
 1515 the response matrix then lead to instabilities if the re- 1570
 1516 sponse matrix is inverted. Additionally, the high back- 1571
 1517 ground environment of heavy ion collisions leads to lower 1572
 1518 energy resolution, and Monte Carlo models generally do 1573
 1519 not describe the data well. Bin-by-bin corrections are 1574
 1520 therefore usually inadequate for measurements in heavy 1575
 1521 ion collisions. 1576

1522 Several algorithms have been developed to solve equa- 1577
 1523 tion 9. The two most commonly used algorithms are 1578
 1524 Single Value Decomposition (SVD) (Hocker and Kartvel- 1579
 1525 ishvili, 1996) and Bayesian Unfolding (D’Agostini, 1995). 1580
 1526 Bayesian unfolding uses a guess, which is called the prior 1581
 1527 of the true distribution, usually from a Monte Carlo 1582
 1528 model, as the start of an iterative procedure. This 1583
 1529 method is regularized by choosing how many iterations 1584
 1530 to use, where choosing an early iteration will result in 1585
 1531 a distribution that is closer to the prior, and thus more 1586
 1532 regularized. As the number of iterations increase there 1587
 1533 is a positive feedback which is driven by fluctuations in 1588
 1534 the response matrix and spectra, that makes the asymp- 1589
 1535 totically unfolded spectrum diverge sharply from reality. 1590
 1536 The SVD formalism is a way by which to factorize a ma- 1591
 1537 trix into a set of matrices. This is used to write the

’unfolding’ equation as a set of linear equations, with the
 assumption that the response matrix R can be decom-
 posed into three matrices such that $R = USV^T$ where U
 and V are orthogonal and S is diagonal. The regulariza-
 tion method for using SVD formalism in unfolding uses
 a dampened least squares method to couple all the linear
 equations that come out of the process and solve them.
 One then chooses a parameter, k , which corresponds to
 the k^{th} singular value of the decomposed matrix, and
 suppresses the oscillatory divergences in the solution.

It is worth noting that for any approach, there is a
 trade off between potential bias imposed on the results
 by the input from the Monte Carlo and the uncertainty
 in the final result. In practice, different methods and dif-
 ferent training for Bayesian unfolding are compared for
 determination of the systematic uncertainties. For mea-
 surements where models describe the data well or where
 the resolution leads to minimal bin-to-bin smearing, bin-
 by-bin corrections are often preferred, both because of
 the potential bias and because of the difficulty of unfold-
 ing.

In order to confirm whether a particular algorithm
 used in unfolding is valid, it is necessary to perform clo-
 sure tests, demonstrations that the method leads to the
 correct value when applied to a Monte Carlo model. The
 most simple tests are to convolute the Monte Carlo truth
 distribution with the response matrix to form a simulated
 detector distribution. This distribution can then be un-
 folded and compared to the original truth distribution.
 For this test, one should use roughly the same statisti-
 cal precision as will be available in the data given how
 strongly the unfolding procedure is driven by statistics.
 However, this does not test the validity of the response
 matrix, or of the choice of spectral shape for the input
 distribution, or of the effect of combinatorial jets that
 will appear in the measured data. A more rigorous clo-
 sure test can be done by embedding the detector level
 jets into minimally biased data, and performing the back-
 ground and unfolding procedures on the embedded data
 to compare with the truth distribution.

Another approach is to “fold” the reference to take
 detector effects into account. For example, the initial
 measurements of the dijet asymmetry did not correct for
 the effect of background or detector resolution in Pb+Pb
 but instead embedded $p+p$ jets in a Pb+Pb background
 in order to smear the $p+p$ by an equivalent amount (Aad
et al., 2010; Chatrchyan *et al.*, 2011b). This may lead
 to a better comparison between data and a particular
 theory, but since the response matrix is generally not
 made available outside of the collaboration, it can only be
 done by experimentalists at the time of the publication.
 However, this would be an important cross-check for any
 model as it removes the mathematical uncertainty due to
 the ill posed inverse problem.

1592 H. Comparing different types of measurements

1593 The ultimate goal of measurements of jets in heavy ion 1642
 1594 collisions is not to learn about jets but to learn about 1643
 1595 the QGP. Measurements of jets in e^+e^- and $p+p$ colli- 1644
 1596 sions are already complicated and the addition of a large 1645
 1597 combinatorial background in heavy ion collisions imposes 1646
 1598 greater experimental challenges. Suppressing and sub- 1647
 1599 tracting the background imposes biases on the resultant 1648
 1600 jet collections. Additionally, selection criteria applied 1649
 1601 to the collection of jet candidates in order to remove 1650
 1602 the combinatorial contribution will also impose a bias. 1651
 1603 The exact bias imposed by these assumptions cannot be 1652
 1604 known without a complete understanding of the QGP, 1653
 1605 which is what we are trying to gain by studying jets. Oc- 1654
 1606 casionally various methods are claimed to be “unbiased”, 1655
 1607 but is unclear what this means precisely since every mea- 1656
 1608 surement is biased towards a subset of the population of 1657
 1609 jets created in heavy ion collisions. Any particular mea- 1658
 1610 surement may have several types of bias. We discuss a 1659
 1611 few types of bias below.

1612 *Survivor bias* As jets interact with the medium and lose 1663
 1613 energy to the medium, they may begin to look more like 1664
 1614 the medium. There are fluctuations in how much energy 1665
 1615 each individual parton will lose in the medium, and se- 1666
 1616 lecting jets which look like jets in a vacuum may skew 1667
 1617 our measurements towards partons which have lost less 1668
 1618 energy in the medium.

1619 *Fragmentation bias* Many measurement techniques select 1673
 1620 jets which have hard fragments, which may lead to a 1674
 1621 survivor bias since interactions with the medium are ex- 1675
 1622 pected to soften the fragmentation function. Some mea- 1676
 1623 surements may preferentially select jets which fragment 1677
 1624 into a particular particle, such as a neutral pion or a 1678
 1625 proton. This in turn can bias the jet population to- 1679
 1626 wards quark or gluon jets. If fragmentation is modified 1680
 1627 in the medium, it could also bias the population towards 1681
 1628 jets which either have or have not interacted with the 1682
 1629 medium.

1630 *Quark bias* Even in e^+e^- collisions, quark and gluon 1683
 1631 jets have different structures on average, with gluon 1684
 1632 jets fragmenting into more, softer particles at larger 1685
 1633 radii (Abreu *et al.*, 1996; Akers *et al.*, 1995). A 1686
 1634 bias may also be imposed by the jet-finding algorithm. 1687
 1635 OPAL found that gluon jets reconstructed with the k_T 1688
 1636 jet finding algorithm generally contained more parti- 1689
 1637 cles than those reconstructed with the cone algorithm 1690
 1638 in (Abe *et al.*, 1992) and that gluon jets contain more 1691
 1639 baryons (Ackerstaff *et al.*, 1999). 1692

The measurement techniques described above gener-
 ally focus on higher momentum jets which fragment
 into harder constituents and have narrower cone radii.
 This surely induces a bias towards quark jets. Since
 gluon jets are expected to outnumber quark jets signifi-
 cantly (Pumplin *et al.*, 2002), this may not be quantita-
 tively significant overall, depending on the measurement
 and the collision energy. In some measurements, sur-
 vivor bias is used as a tool. For instance measurements of
 hadron-jet correlations select a less modified jet by iden-
 tifying a hard hadron and then look for its partner jet on
 the away-side (Adam *et al.*, 2015c). Correlations requir-
 ing a trigger on both the near and away sides select jets
 biased to be near the surface of the medium (Agakishiev
et al., 2011). These biases are inherently unavoidable
 and they must be understood in order to properly inter-
 pret data. However, once they are well understood, the
 biases can be engineered to purposefully select particu-
 lar populations of jets, for instance to select jets biased
 towards the surface in order to increase the probability
 that the away side jet has traversed the maximum possi-
 ble medium.

As our experience with the v_n modulated background
 in dihadron correlations shows, the issue is not merely
 which measurements are most sensitive to the properties
 of the medium but the possibility that our current under-
 standing of the background may be incomplete. However,
 the potential error introduced varies widely by the mea-
 surement – single particle spectra, dihadron correlations,
 and reconstructed jets all have completely different biases
 and assumptions about the background. Our certainty in
 the interpretation of the results is therefore enhanced if
 the same conclusions can be drawn from measurements
 of multiple observables. We therefore discuss a variety of
 different measurements in Section III and demonstrate
 that they all lead to the same conclusions – partons lose
 energy in the medium and their constituents are broad-
 ened and softened in the process.

1678 III. OVERVIEW OF EXPERIMENTAL RESULTS

1679 RHIC and the LHC have provided a wealth of data
 1680 which enhance our understanding of the properties of
 1681 the QGP. This section of the article reviews experimen-
 1682 tal results available at of the time of publication, and
 is organized according to the physics addressed by the
 measurement rather than according to observable to fo-
 cus on the implications of the measurements. Therefore
 the same observable may appear in multiple subsections.
 The questions that jet studies attempt to answer to un-
 derstand the QGP are: Are there cold nuclear matter ef-
 fects which must be taken into consideration in order to
 interpret results in heavy ion collisions? Do partons lose
 energy in the medium and how much? How do partons
 fragment in the medium? Is fragmentation the same as

1693 in vacuum or is it modified? Where does the lost energy
 1694 go and how does it influence the medium? Finally, in
 1695 the next section we will discuss how well these questions
 1696 have been answered and the questions that remain.

1697 A. Cold nuclear matter effects

1698 Cold nuclear matter effects refer to observed differences
 1699 between $p+p$ and $p+A$ or $d+A$ collisions where a hot
 1700 medium is not expected, but the presence of a nucleus
 1701 in the initial state could influence the production of the
 1702 final observable. These effects may result from coherent
 1703 multiple scattering within the nucleus (Qiu and Vitev,
 1704 2006), gluon shadowing (Gelis *et al.*, 2010), or partonic
 1705 energy loss within the nucleus (Bertocchi and Treleani,
 1706 1977; Vitev, 2007; Wang and Guo, 2001). While such
 1707 effects are interesting in their own right, if present, they
 1708 would need to be taken into account in order to interpret
 1709 heavy ion collisions correctly. Studies of open heavy fla-
 1710 vor at forward rapidities through spectra (Adare *et al.*,
 1711 2012a) and correlations (Adare *et al.*, 2014b) of leptons
 1712 from heavy flavor decays indicate that heavy flavor is
 1713 suppressed in cold nuclear matter. The J/ψ is also sup-
 1714 pressed at forward rapidities (Adare *et al.*, 2013d). Re-
 1715 cent studies have also indicated that there may be col-
 1716 lective effects for light hadrons in $p+A$ collisions (Aad
 1717 *et al.*, 2014d; Adam *et al.*, 2016h; Khachatryan *et al.*,
 1718 2015a) and even high multiplicity $p+p$ events (Aad *et al.*,
 1719 2016b; Khachatryan *et al.*, 2017b). Studies of jet produc-
 1720 tion in $p+A$ or $d+A$ collisions are necessary to quantify
 1721 the cold nuclear matter effects and decouple which effects
 1722 observed in $A+A$ data come from interactions with the
 1723 medium.

1725 Measurements of inclusive hadron R_{dAu} at $\sqrt{s_{NN}} =$
 1726 200 GeV (Abelev *et al.*, 2010b; Adler *et al.*, 2007b) and
 1727 R_{pPb} at $\sqrt{s_{NN}} = 5.02$ TeV (ATL, 2016; Aad *et al.*,
 1728 2016c; Abelev *et al.*, 2013e; Khachatryan *et al.*, 2015b,
 1729 2017a) are consistent with one within the systematic un-
 1730 certainties of these measurements, indicating that the
 1731 large hadron suppression observed in $A+A$ collisions can
 1732 not be due to cold nuclear matter effects. This is shown in
 1733 Figure 9. We note here that the CMS results shown here
 1734 were updated with a $p+p$ reference measured at $\sqrt{s_{NN}}$
 1735 = 5.02 TeV (Khachatryan *et al.*, 2017a), which is also
 1736 consistent with an R_{pPb} of one.

1737 2. Reconstructed jets

1738 Measurements of reconstructed jets in $d+Au$ collisions
 1739 at $\sqrt{s_{NN}} = 200$ GeV and $p+Pb$ collisions at 5.02 TeV in-
 1740 dicate that the minimum bias R_{dAu} (Adare *et al.*, 2016b)
 1741 and R_{pPb} (Aad *et al.*, 2015a; Adam *et al.*, 2016c), re-
 1742 spectively, are also consistent with one. Figure 10 shows
 1743 R_{pPb} measured by the CMS experiment and compared

1. Inclusive charged hadrons

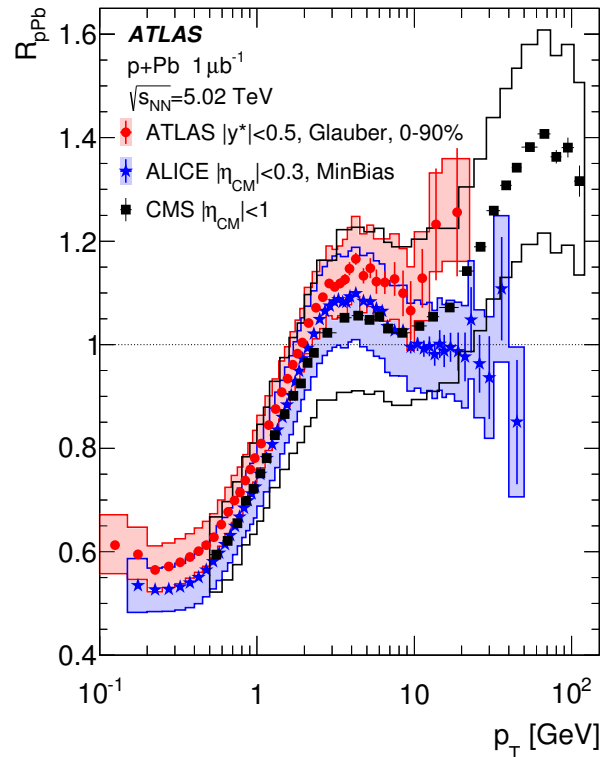


FIG. 9 Figure from ATLAS (Aad *et al.*, 2016c). The nuclear modification factor of charged hadrons in $p+Pb$ collisions at $\sqrt{s_{NN}} = 5.02$ TeV measured by the ALICE (Abelev *et al.*, 2013e), ATLAS (Aad *et al.*, 2016c), and CMS (Khachatryan *et al.*, 2015b) experiments. The data in this figure used an extrapolation of $p+p$ data from $\sqrt{s_{NN}} = 2.76$ and 7 TeV as there was not a $p+p$ reference at the same energy available at this time. This shows that R_{pPb} is consistent with one within uncertainties for high p_T hadrons.

with NLO calculations including cold nuclear matter effects. The theoretical predictions and the experimental measurements in Figure 10 show that cold nuclear matter effects are small for jets for all p_T and pseudorapidity measured at the LHC. A centrality dependence at midrapidity in 200 GeV $d+Au$ and 5.02 TeV $p+Pb$ collisions which cannot be fully explained by the biases in the centrality determination as studied in (Aad *et al.*, 2016a; Adare *et al.*, 2014a) is observed. It has been proposed that the forward multiplicities used to determine centrality are anti-correlated with hard processes at midrapidity (Armesto *et al.*, 2015; Bzdak *et al.*, 2016) or that the rare high- x parton configurations of the proton which produce high-energy jets have a smaller cross-section for inelastic interactions with nucleons in the nucleus (Alvioli *et al.*, 2016, 2014; Alvioli and Strikman, 2013; Coleman-Smith and Muller, 2014). The latter suggests that high p_T jets may be used to select proton configurations with

1762 varying sizes due to quantum fluctuations. While this 1810
 1763 is interesting in its own right and there may be initial 1811
 1764 state effects, there are currently no indications of large 1812
 1765 partonic energy loss in small systems, thus scaling the 1813
 1766 production in $p+p$ with the number of binary nucleon- 1814
 1767 nucleon collisions as a reference appears to valid for com- 1815
 1768 parison to larger systems. 1816

1769 3. Dihadron correlations

1770 Detailed studies of the jet structure in $d+Au$ and com- 1821
 1771 parisons to both PYTHIA and $p+p$ collisions using di- 1822
 1772 hadron correlations at $\sqrt{s_{NN}} = 200$ GeV found no evi- 1823
 1773 dence for modification of the jet structure at midrapid- 1824
 1774 ity in cold nuclear matter (Adler *et al.*, 2006d). Stud- 1825
 1775 ies of correlations between particles at forward rapidities 1826
 1776 ($1.4 < \eta < 2.0$ and $-2.0 < \eta < -1.4$) in order to search 1827
 1777 for fragmentation effects at low x also found no evidence 1828
 1778 for modified jets in cold nuclear matter (Adler *et al.*, 1829
 1779 2006a). However, jet-like correlations with particles at 1830
 1780 higher rapidities ($3.0 < \eta < 3.8$) indicated modifications 1831
 1781 of the correlation functions in $d+Au$ collisions at $\sqrt{s_{NN}}$ 1832
 1782 $= 200$ GeV (Adare *et al.*, 2011d). This indicates that nu- 1833
 1783 clear effects may have a strong dependence on x and that 1834
 1784 studies of cold nuclear matter effects for each observable 1835
 1785 are important in order to demonstrate the validity of the 1836
 1786 baseline for studies in hot nuclear matter. While there is 1837
 1787 little evidence for effects at midrapidity, observables at 1838
 1788 forward rapidities may be influenced by effects already 1839
 1789 present in cold nuclear matter. Searches for acoplanarity 1840
 1790 in jets in $p+Pb$ collisions observed no difference between 1841
 1791 jets in $p+Pb$ and $p+p$ collisions (Adam *et al.*, 2015b). 1842

1792 4. Summary of cold nuclear matter effects for jets

1793 Based on current evidence from $p+Pb$ and $d+Au$ colli- 1846
 1794 sions, $p+p$ collisions are an appropriate reference for jets, 1847
 1795 however, since numerous cold nuclear matter effects have 1848
 1796 been documented, each observable should be measured in 1849
 1797 cold nuclear matter in order to properly interpret data 1850
 1798 in hot nuclear matter. We therefore conclude that, based 1851
 1799 on the current evidence, $p+Pb$ and $d+Au$ collisions are 1852
 1800 appropriate reference systems for hard processes in $A+A$ 1853
 1801 collisions, although caution is needed, particularly at 1854
 1802 large rapidities and high multiplicities, and future studies 1855
 1803 in small systems may lead to different conclusions. 1856

1804 B. Partonic energy loss in the medium

1805 Electroweak probes such as direct photons, which do 1861
 1806 not interact via the strong force, are expected to es- 1862
 1807 cape the QGP unscathed while probes which interact 1863
 1808 strongly lose energy in the medium and are suppressed at 1864
 1809 high momenta. Figure 11 shows a compilation of results 1865

from PHENIX demonstrating that colored probes (high-
 p_T final state hadrons) are suppressed while electroweak
 probes (direct photons) are not at RHIC energies. Figure 12 shows a similar compilation of results from the LHC, demonstrating that this is also true at higher energies. This observed suppression in charged hadron spectra was the first indication of jet quenching in heavy ion collisions. The lowest value of the nuclear modification factor R_{AA} for light hadrons is about 0.2 in collisions at $\sqrt{s_{NN}} = 200$ GeV (Adams *et al.*, 2003b; Adler *et al.*, 2003b; Back *et al.*, 2004) and about 0.1 in Pb+Pb collisions at LHC for $\sqrt{s_{NN}} = 2.76$ TeV and $\sqrt{s_{NN}} = 5.02$ TeV (CMS, 2016a; Aamodt *et al.*, 2011b; Chatrchyan *et al.*, 2012e). The R_{AA} of the charged hadron spectra appears to reach unity at $p_T \approx 100$ GeV/c (CMS, 2016a). This is expected from all QCD-inspired energy loss models that at some point R_{AA} must reach one, because at leading order the differential cross section for interactions with the medium is proportional to $1/Q^2$ (Levai *et al.*, 2002). Studies of R_{CP} as a function of collision energy indicate that suppression sets in somewhere between $\sqrt{s_{NN}} = 27$ and 39 GeV (Adamczyk *et al.*, 2017a). At intermediate p_T the shape of R_{AA} with p_T is mass dependent with heavier particles approaching the light particle suppression level at higher momenta (Agakishiev *et al.*, 2012a). However, even hadrons containing heavy quarks are suppressed at levels similar to light hadrons (Abelev *et al.*, 2012b).

QCD-motivated models are generally able to describe inclusive single particle R_{AA} qualitatively, however, for each model the details of the calculations make it difficult to compare results between models directly and extract quantitative information about the properties of the medium from such comparisons (Adare *et al.*, 2008b). The JET collaboration was formed explicitly to make such comparisons between models and data and their extensive studies determined that for a 10 GeV/c hadron the jet transport coefficient is $\hat{q} = 1.2 \pm 0.3$ GeV² in Au+Au collisions at $\sqrt{s_{NN}} = 200$ GeV and $\hat{q} = 1.9 \pm 0.7$ GeV² in Pb+Pb collisions at $\sqrt{s_{NN}} = 2.76$ TeV (Burke *et al.*, 2014).

These detailed comparisons between data and energy loss models are one of the most important results in heavy ion physics and are one of the few results that directly constrain the properties of the medium. We emphasize that these constraints came from a careful comparison of a straightforward observable to various models. While we discuss measurements of more complicated observables later, this highlights the importance of both precision measurements of straightforward observables and careful, systematic comparisons of data to theory. Similar approaches are likely needed to further constrain the properties of the medium.

It is remarkable that the R_{AA} values for hadrons at RHIC and the LHC are so similar since one would expect energy loss to increase with increased energy density

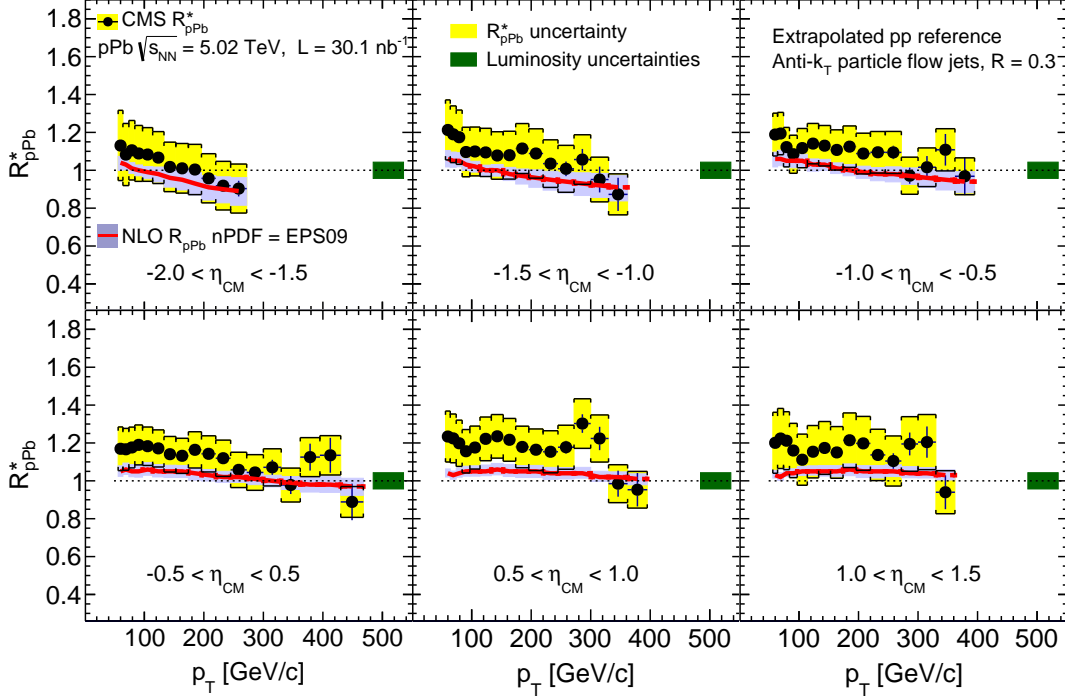


FIG. 10 Figure from CMS (Khachatryan *et al.*, 2016b). The nuclear modification factor of jets in $p+Pb$ collisions measured by the CMS experiment in various rapidity bins. This shows that cold nuclear matter effects are small for jets.

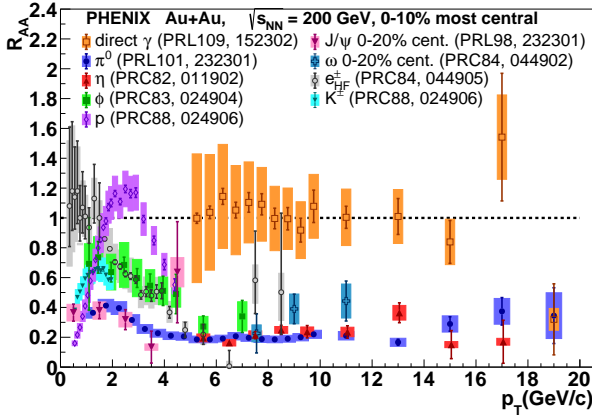


FIG. 11 R_{AA} from PHENIX for direct photons (Afanasyev *et al.*, 2012), π^0 (Adare *et al.*, 2008c), η (Adare *et al.*, 2010c), ϕ (Adare *et al.*, 2016c), p (Adare *et al.*, 2013e), J/ψ (Adare *et al.*, 2007a), ω (Adare *et al.*, 2011c), e^\pm from heavy flavor decays (Adare *et al.*, 2011a), and K^\pm (Adare *et al.*, 2013e). This demonstrates that colored probes (high- p_T final state hadrons) are suppressed while electroweak probes (direct photons) are not at RHIC.

1866 which should result in a lower R_{AA} at the LHC with its 1888
 1867 higher collision energies. However, the hadrons in a par-1889
 1868 ticular p_T range are not totally quenched but rather ap-1890

1869 pear at a lower p_T , so it is useful to study the shift of the
 1870 hadron p_T spectrum in $A+A$ collisions to $p+p$ collisions
 1871 rather than the ratio of yields. Note that the spectral
 1872 shape also depends on the collisional energy. Spectra gener-
 1873 ally follow a power law trend described by $\frac{dN}{dp_T} \propto p_T^{-n}$
 1874 at high momenta. The spectra of hadrons is steeper in
 1875 200 GeV than in 2.76 TeV collisions ($n \approx 8$ and $n \approx 6.0$
 1876 repectively for the p_T range 7-20 GeV/c) (Adare *et al.*,
 1877 2012b, 2013c). Therefore, for R_{AA} , greater energy loss
 1878 at the LHC could be counteracted by the flatter spectral
 1879 shape. To address this, another quantity, the fractional
 1880 momentum loss, (S_{loss}) has also been measured to bet-
 1881 ter probe a change in the fractional energy loss of partons
 1882 $\Delta E/E$ as a function of collision energy. This quantity is
 1883 defined as

$$S_{loss} \equiv \frac{\delta p_T}{p_T} = \frac{p_T^{pp} - p_T^{AA}}{p_T^{pp}} \sim \left\langle \frac{\Delta E}{E} \right\rangle, \quad (11)$$

1884 where p_T^{AA} is the p_T of the $A+A$ measurement. p_T^{pp} is de-
 1885 termined by first scaling p_T spectrum measured in $p+p$
 1886 collisions by the nuclear overlap function, T_{AA} of the cor-
 1887 responding $A+A$ centrality class and then determining
 the p_T at which the yield of the scaled spectrum matches
 the yield measured in $A+A$ at the p_T^{AA} point of interest.
 This procedure is illustrated pictorially in Figure 13.

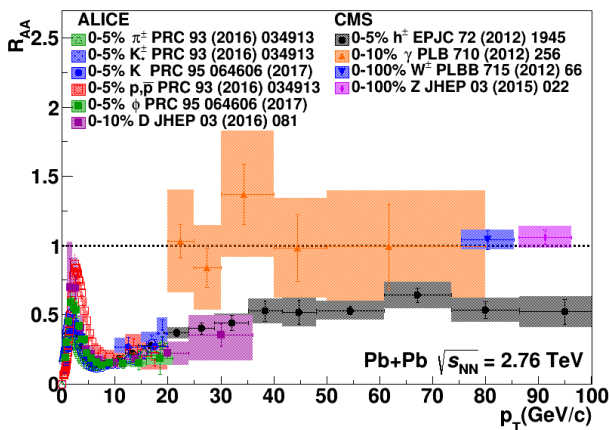


FIG. 12 R_{AA} from ALICE for identified π^\pm , K^\pm , and p (Adam *et al.*, 2016e) and D mesons (Adam *et al.*, 2016k) and CMS for charged hadrons (h^\pm) (Chatrchyan *et al.*, 2012e), direct photons (Chatrchyan *et al.*, 2012b), W bosons (Chatrchyan *et al.*, 2012f), and Z bosons (Chatrchyan *et al.*, 2011c). The W and Z bosons are shown at their rest mass and identified through their leptonic decay channel. This demonstrates that colored probes (high- p_T final state hadrons) are suppressed while electroweak probes (direct photons, W, Z) are not at the LHC.

Indeed a greater fractional momentum loss was observed for the most central 2.76 TeV Pb+Pb collisions compared to the 200 GeV Au+Au collisions (Adare *et al.*, 2016d). The analysis found that S_{loss} scales with energy density related quantities such as multiplicity ($dN_{ch}/d\eta$), as shown in Figure 13, and $dE_T/dy/A_T$ where A_T is the transverse area of the system. The latter quantity can be written in terms of Bjorken energy density, ϵ_{B_j} and the equilibrium time, τ_0 such that $dE_T/dy/A_T = \epsilon_{B_j}\tau_0$ and has been shown to scale with $dN_{ch}/d\eta$ (Adare *et al.*, 2016e). On the other hand, S_{loss} does not scale with system size variables such as N_{part} . Assuming that S_{loss} is a reasonable proxy for the mean fractional energy loss of the partons the scaling observations implies that fractional energy loss of partons scales with the energy density of the medium for these collision energies.

1. Jet R_{AA}

Measurements of hadronic observables blur essential physics due to the complexity of the theoretical description of hadronization and the sensitivity to non-perturbative effects. In principle, measurements of reconstructed jets are expected to be less sensitive to these effects. Next to leading order calculations demonstrate the sensitivity of R_{AA} measurements to the properties of the medium-induced gluon radiation (Vitev *et al.*, 2008). These measurements can differentiate between competing models of parton energy loss mechanisms, re-

ducing the large systematic uncertainties introduced by different theoretical formalisms (Majumder, 2007b). Figure 14 shows the reconstructed anti- k_T jet R_{AA} from ALICE (Adam *et al.*, 2015d) with $R = 0.2$ for $|\eta| < 0.5$, ATLAS (Aad *et al.*, 2015b) with $R = 0.4$ for $|\eta| < 2.1$, and CMS (Khachatryan *et al.*, 2017c,c) with $R = 0.2$, 0.3, and 0.4 for $|\eta| < 2.0$. At lower momenta, the ALICE data are consistent with the CMS data for all radii, while the ATLAS R_{AA} is higher than that of ALICE. At higher momenta, all measurements of jets from all three experiments agree within the experimental uncertainties of the jet measurements.

A jet is defined by the parameters of the jet finding algorithm and selection criteria such as those that are used to identify background jets due to fluctuations in heavy ion events. When making comparisons of jet observables between different experiments and to theoretical predictions, not only jet definitions but also the effects of selection criteria need to be considered carefully. While the difference between the pseudorapidity coverage is unlikely to lead to the difference between the ATLAS and ALICE results given the relatively flat distribution at mid-rapidity, the resolution parameter R as well as the different selection criteria could cause a difference as observed at low transverse momenta. The ATLAS approach to the combinatorial background, which favors jets with hard constituents, may bias the jet sample to unmodified jets, particularly at low momenta where the ATLAS and ALICE measurements overlap. ATLAS and CMS jet measurements agree at high momenta where jets are expected to be less sensitive to the measurement details. We therefore interpret the difference between the jet R_{AA} measured by the different experiments not as an inconsistency, but as different measurements due to different biases. We implore the collaborations to construct jet observables using the same approaches to background subtraction and suppression of the combinatorial background so that the measurements could be compared directly. Ultimately the overall consistency of R_{AA} at high p_T , even with widely varying jet radii and inherent biases in the jet sample, indicate that more sensitive observables are required to understand jet quenching quantitatively.

Although, the observation of jet quenching through R_{AA} was a major feat, it still leaves several open questions about hard partons' interactions with the medium. *How* do jets lose energy? Through collisions with the medium, gluon bremsstrahlung, or both? Where does that energy go? Are there hot spots or does the energy seem to be distributed isotropically in the event? Few experimental observables can compete with R_{AA} for overall precision, however, more differential observables may be more sensitive to the energy loss mechanism.

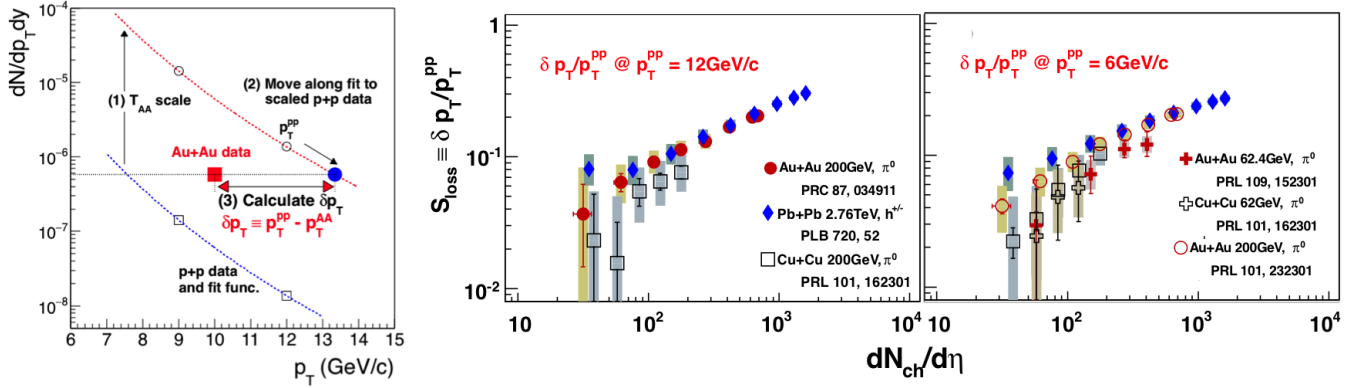


FIG. 13 Figure is a modified presentation of plots from PHENIX (Adare *et al.*, 2016d). The first plot (left) is a cartoon demonstrating how δp_T is determined. The fractional energy loss, S_{loss} measured as a function of the multiplicity, $dN_{ch}/d\eta$ is plotted for several heavy ion collision energies for hadrons with p_T^{pp} of 12 GeV (middle) and 6 GeV/c (right) where p_T^{pp} refers to the transverse momentum measured in $p+p$ collisions. The Pb+Pb data are from ALICE measured over $|\eta| < 0.8$ while all other data are from PHENIX which measures particle in the range $|\eta| < 0.35$. These results indicate that the fractional energy loss scales with the energy density of the system.

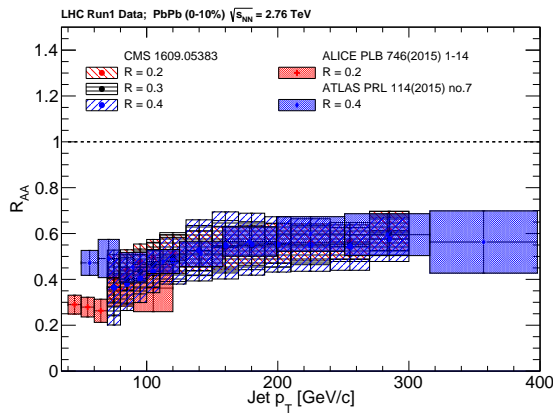


FIG. 14 Reconstructed anti- k_T jet R_{AA} from ALICE (Adam *et al.*, 2015d) with $R = 0.2$ for $|\eta| < 0.5$, ATLAS (Aad *et al.*, 2015b) with $R = 0.4$ for $|\eta| < 2.1$, and CMS (Khachatryan *et al.*, 2017c) with $R = 0.2, 0.3$ and 0.4 for $|\eta| < 2.0$. The ALICE and CMS data are consistent within uncertainties while the ATLAS data are higher. This may be due to the ATLAS technique, which could impose a survivor bias and lead to a higher jet R_{AA} at low momenta. Figure courtesy of Raghav Elayavalli Kunnawalkam.

1970 2. Dihadron correlations

1971 The precise mechanism responsible for modification
1972 of dihadron correlations cannot be determined based on
1973 these studies alone because there are many mechanisms
1974 which could lead to modification of the correlations. This
1975 includes not only energy loss and modification of jet
1976 fragmentation but also modifications of the underlying
1977 parton spectra. However, they are less ambiguous than

1978 spectra alone because the requirement of a high momen-
1979 tum trigger particle enhances the fraction of particles
1980 from jets. Figure 15 shows dihadron correlations in $p+p$,
1981 $d+Au$, and $Au+Au$ at $\sqrt{s_{NN}} = 200$ GeV, demonstrat-
1982 ing suppression of the away-side peak in central $Au+Au$
1983 collisions. The first measurements of dihadron correla-
1984 tions showed complete suppression of the away-side peak
1985 and moderate enhancement of the near-side peak (Adams
1986 *et al.*, 2003a, 2004a; Adler *et al.*, 2003a). However, as
1987 noted above, a majority of dihadron correlation studies
1988 did not take the odd v_n due to flow into account, includ-
1989 ing those in Figure 15. A subsequent measurement with
1990 similar kinematic cuts including higher order v_n shows
1991 that the away-side is not completely suppressed, as shown
in Figure 15, but rather that there is a visible but suppressed
away-side peak (Nattrass *et al.*, 2016). Studies at
higher momenta also see a visible but suppressed away-
side peak (Adams *et al.*, 2006).

The suppression is quantified by

$$I_{AA} = Y_{AA}/Y_{pp}. \quad (12)$$

1996 where Y_{AA} is the yield in $A+A$ collisions and Y_{pp} is the
1997 yield in $p+p$ collisions. The yields must be defined over
1998 finite $\Delta\phi$ and $\Delta\eta$ ranges and are usually measured for
1999 a fixed range in associated momentum, p_T^a . Similar to
2000 R_{AA} , an I_{AA} greater than one means that there are more
2001 particles in the peak in $A+A$ collisions than in $p+p$ col-
lisions and an I_{AA} less than one means that there are
fewer. Gluon bremsstrahlung or collisional energy loss
would result in more particles at low momenta and fewer
particles at high momenta, leading to an I_{AA} greater than
one at low momenta and an I_{AA} less than one at high
momenta, at least as long as the lost energy does not
reach equilibrium with the medium. Both radiative and

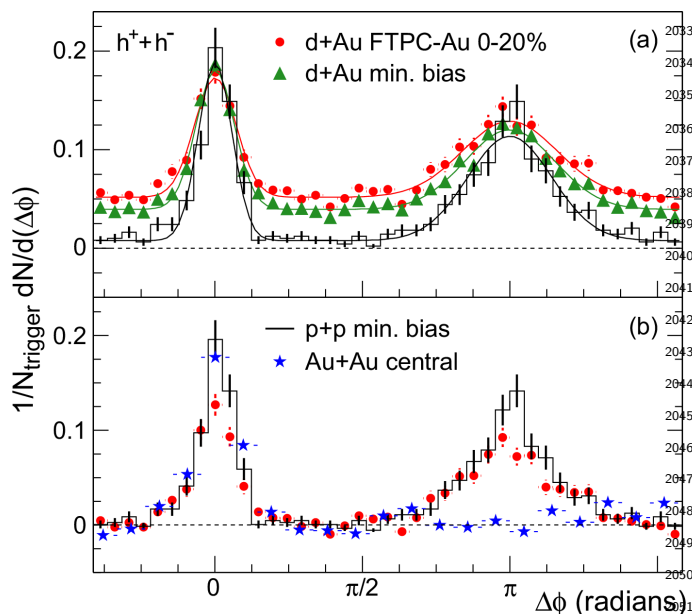


FIG. 15 Figure from STAR (Adams *et al.*, 2003a). (a) Dihadron correlations before background subtraction in $p+p$ and $d+Au$ and (b) Comparison of dihadron correlations after background subtraction in $p+p$, $d+Au$, and Au+Au at $\sqrt{s_{NN}} = 200$ GeV for associated momenta $2.0 \text{ GeV}/c < p_T^a < p_T^t$ and trigger momenta $4 < p_T^t < 6 \text{ GeV}/c$. This measurement is now understood to be quantitatively incorrect because of erroneous assumptions in the background subtraction. We now see only partial suppression on the away-side (Nattrass *et al.*, 2016).

energy loss rather than a change in the underlying jet spectra since higher energy jets are both more collimated and contain more particles.

The away-side is suppressed at high momenta at both RHIC (Abelev *et al.*, 2010a; Adams *et al.*, 2006) and the LHC (Aamodt *et al.*, 2012). A reanalysis of reaction plane dependent dihadron correlations from STAR (Agakishiev *et al.*, 2010, 2014) at low momenta using a new background method which takes odd v_n into account (Sharma *et al.*, 2016) observed suppression on the away-side but no broadening, even though broadening was observed on the near-side at the same momenta (Nattrass *et al.*, 2016). This may indicate that the away-side width is less sensitive because the width is broadened by the decorrelation between the near- and away-side jet axes rather than indicating that these effects are not present. Reaction plane dependent studies can constrain the path length dependence of energy loss because, as shown in Figure 2, partons traveling in the reaction plane (in-plane) traverse less medium than those traveling perpendicular to the reaction plane (out-of-plane). The I_{AA} is highest for low momentum particles and is at a minimum for trigger particles at intermediate angles relative to the reaction plane rather than in-plane or out-of-plane. This likely indicates an interplay between the effects of surface bias and partonic energy loss.

Energy loss models are generally able to describe I_{AA} qualitatively, however, there has been no systematic attempt to compare data to models, as was done for R_{AA} . Simultaneous comparisons of R_{AA} and I_{AA} are expected to be highly sensitive to the jet transport coefficient \hat{q} (Jia *et al.*, 2011; Zhang *et al.*, 2007). Such a theoretical comparison is partially compounded by the wide range of kinematic cuts used in experimental measurements and the fact that most measurements neglected the odd v_n in the background subtraction.

3. Dijet imbalance

The first evidence of jet quenching in reconstructed jets at the LHC was observed by measuring the dijet asymmetry, A_J . This observable measures the energy or momentum imbalance between the leading and sub-leading or opposing jet in each event. Due to kinematic and detector effects, the energy of dijets will not be perfectly balanced, even in $p+p$ collisions. Therefore to interpret this measurement in heavy ion collisions, data from $A+A$ collisions must be compared to the distributions in $p+p$ collisions. Figure 16 shows the dijet asymmetry measurement from the ATLAS experiment where $A_J = \frac{E_{T1} - E_{T2}}{E_{T1} + E_{T2}}$ (Aad *et al.*, 2010). The left panel on the top row shows the A_J distribution for peripheral Pb+Pb collisions and demonstrates that it is similar to that from $p+p$ collisions. However, dijets in central Pb+Pb collisions are more likely to have a higher A_J value than dijets in $p+p$ collisions, con-

2009 collisional energy loss would lead to broader correlations.
 2010 Partonic energy loss before fragmentation would lead to a
 2011 suppression on the away-side but no modification on the
 2012 near-side and no broadening because the near-side jet is
 2013 biased towards the surface of the medium. Changes in
 2014 the parton spectra can also impact I_{AA} because harder
 2015 partons hadronize into more particles and higher energy
 2016 jets are more collimated.

2017 No differences between $d+Au$ and $p+p$ collisions are
 2018 observed on either the near- or away-side at midrapidity
 2019 (Adler *et al.*, 2006a,d), indicating that any modifica-
 2020 tions observed are due to hot nuclear matter effects.
 2021 The near-side yields at midrapidity in $A+A$, $d+Au$, and
 2022 $p+p$ collisions are within error at RHIC (Abelev *et al.*,
 2023 2010a; Adams *et al.*, 2006; Adare *et al.*, 2008a), even at
 2024 low momenta (Abelev *et al.*, 2009b; Agakishiev *et al.*,
 2025 2012c), indicating that the near-side jet is not substan-
 2026 tially modified, although the data are also consistent
 2027 with a slight enhancement (Nattrass *et al.*, 2016). A
 2028 slight enhancement of the near-side is observed at the
 2029 LHC (Aamodt *et al.*, 2012) and a slight broadening is
 2030 observed at RHIC (Adare *et al.*, 2008a; Agakishiev *et al.*,
 2031 2012c; Nattrass *et al.*, 2016). The combination of broad-
 2032 ening and a slight enhancement favors moderate partonic

sistent with expectations from energy loss. The bottom panel shows that these jets retain a similar angular correlation with the leading jet, even as they lose energy. The CMS measurement of $A_J = \frac{p_{T1}-p_{T2}}{p_{T1}+p_{T2}}$ (Chatrchyan *et al.*, 2011b) shows similar trends. The structure in the distribution of A_J is partially due to the 100 GeV lower limit on the leading jet and the 25 GeV lower limit on the subleading jet and partially due to detector effects and background in the heavy ion collision. These measurements are not corrected for detector effects or distortions in the observed jet energies due to fluctuations in the background. Instead the jets from $p+p$ collisions are embedded in a heavy ion event in order to take the effects of the background into account.

Recently ATLAS has measured A_J , and unfolded the distribution in order to take background and detector effects into account (ATL, 2015b), with similar conclusions. For jets above 200 GeV, the asymmetry is observed to be consistent with those observed in $p+p$, indicating that sufficiently high momentum jets are unmodified. This is consistent with observation that the R_{AA} is consistent with one for hadrons at $p_T \approx 100$ GeV/ c (CMS, 2016a), indicating that very high momentum jets are not modified.

Energy and momentum must be conserved, so the balance should be restored if jets can be reconstructed such a way that the particles carrying the lost energy are included. For jets reconstructed with low momentum constituents, the background due to combinatorial jets is non-negligible, but requiring the jet to be matched to a jet constructed with higher momentum jet constituents, as well as a higher momentum jet will suppress the combinatorial jet background. STAR measurements of A_J using a high momentum constituent selection ($p_T > 2$ GeV/ c) observed the same energy imbalance seen by ATLAS and CMS. However, the energy balance was recovered by matching these jets reconstructed with high p_T constituents, to jets reconstructed with low momentum constituents ($p_T > 150$ MeV/ c) and then constructing A_J from the jets with the low momentum constituents (Adamczyk *et al.*, 2017b).

4. γ -hadron, γ -jet and Z -jet correlations

At leading order, direct photons are produced via Compton scattering, $q+g \rightarrow q+\gamma$, and quark-antiquark annihilation, as shown in the left two and right two Feynman diagrams in Figure 17, respectively. Due to the dearth of anti-quarks and abundance of gluons in the proton, Compton scattering is the dominant production mechanism for direct photons in $p+p$ and $A+A$ collisions. Therefore jets recoiling from a direct photon at midrapidity are predominantly quark jets. In the center of mass frame at leading order, the photon and recoil quark are produced heading precisely 180° away from each other in the transverse plane with the same mo-

mentum. At higher order, fragmentation photons and gluon emission impact the correlation such that the momentum is not entirely balanced and the back-to-back positions are smeared, even in $p+p$ collisions. Since photons do not lose energy in the QGP, the photon will escape the medium unscathed and the energy of the opposing quark can be determined from the energy of the photon. This channel is called the ‘‘Golden Channel’’ for jet tomography of the QGP because it is possible to calculate experimental observables with less sensitivity to hadronization and other non-perturbative effects than dihadron correlations and measurements of reconstructed jets. Additionally, direct photon analyses remove some of the ambiguity with respect to differences between quarks and gluons since the outgoing parton opposing the direct photon is predominantly a quark.

Correlations of direct photons with hadrons can be used to calculate I_{AA} , as for dihadron correlations. Studies of γ -h at RHIC led to similar conclusions to those reached by dihadron correlations, as shown in Figure 18, demonstrating suppression of the away-side jet (Abelev *et al.*, 2010c; Adamczyk *et al.*, 2016; Adare *et al.*, 2009, 2010b). In addition, γ -h correlations can measure the fragmentation function of the away-side jet assuming the jet energy is the photon energy. This is discussed in Section III.C.2. It should be noted that nonzero photon v_2 and v_3 have been observed (Adare *et al.*, 2012c, 2016a), leading to a correlated background. The physical origin of this v_2 is unclear, since photons do not interact with the medium, so it is also unclear if v_3 and higher order v_n impact the background. Measurements at high momenta are robust because the background is small and the photon v_2 appears to decrease with p_T . In (Adare *et al.*, 2013b), the systematic uncertainty due to v_3 was estimated and included in the total systematic uncertainty. Since the direct photon-hadron correlations are extracted by subtracting photon-hadron correlations from decays (primarily from $\pi^0 \rightarrow \gamma\gamma$) from inclusive photon-hadron correlations, the impact of the v_n in the final direct photon-hadron correlations is reduced as compared to dihadron and jet-hadron correlations.

Direct photons can also be correlated with a reconstructed jet. In principle, this is a direct measurement of partonic energy loss. Figure 19(a) shows measurements of the energy imbalance between a photon with energy $E > 60$ GeV and a jet at least $\frac{7}{8}\pi$ away in azimuth with at least $E_{jet} > 30$ GeV. Even in $p+p$ collisions, the jet energy does not exactly balance the photon energy because of next-to-leading order effects and because some of the quark’s energy may extend outside of the jet cone. The lower limit on the energy of the reconstructed jet is necessary in order to suppress background from combinatorial jets, but it also leads to a lower limit on the fraction of the photon energy observed. Figure 19(a) demonstrates that the quark loses energy in Pb+Pb collisions. Figure 19(b) shows the average fraction of isolated photons

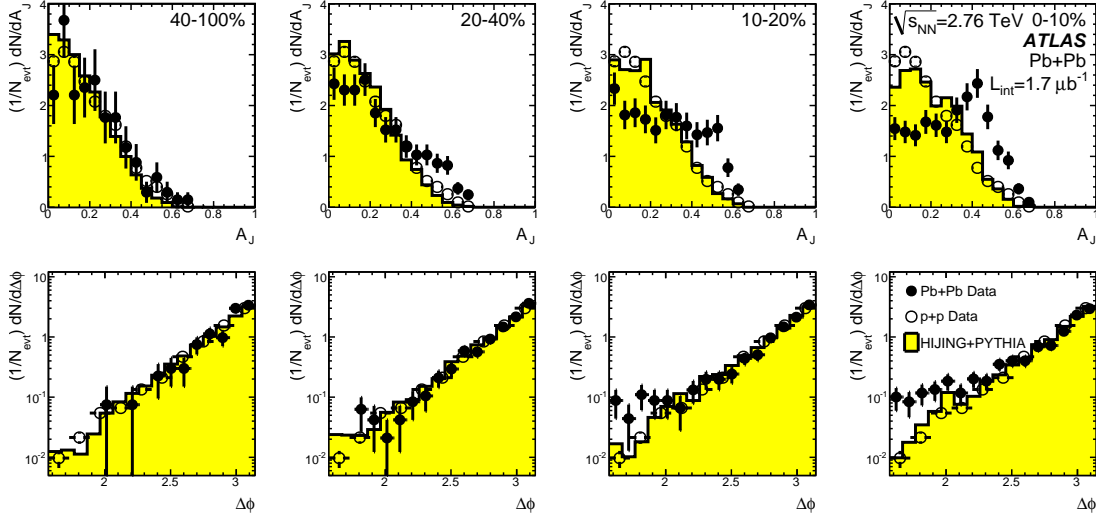


FIG. 16 Figure from ATLAS (Aad *et al.*, 2010). The top row shows comparisons of $A_J = (E_{T1} - E_{T2})/(E_{T1} + E_{T2})$ from $p+p$ and Pb+Pb collisions at $\sqrt{s_{NN}} = 2.76$ TeV with leading jets above $p_T > 100$ GeV and subleading jets above 25 GeV. The bottom row shows the angular distribution of the jet pairs. This shows that the momenta of jets in jet pairs is not balanced in central A+A collisions, indicating energy loss.



FIG. 17 Figure from PHENIX (Adare *et al.*, 2010b). The left two Feynman diagrams show direct photon production through Compton scattering and the right two diagrams show direct photon production through quark-antiquark annihilation. These are the leading order processes which contribute to the production of a gamma and a jet approximately 180° apart.

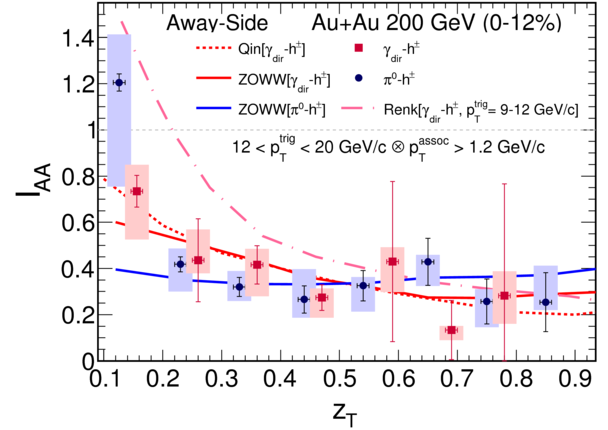


FIG. 18 Figure from STAR (Adamczyk *et al.*, 2016). The away-side I_{AA} for direct photon-hadron correlations (red squares) and π^0 -hadron correlations (blue circles) plotted as a function of $z_T = p_{T,h}/p_{T,trig}$ as measured by STAR in central 200 GeV Au+Au collisions. This shows the suppression of hadrons 180° away from a direct photon. The data are consistent with theory calculations which show the greatest suppression at high z_T and less suppression at low z_T . The curves are theory calculations from Qin (Qin *et al.*, 2009), Renk (Renk, 2009) and ZOWW (Chen *et al.*, 2010; Zhang *et al.*, 2009).

2195 matched to a jet, $R_{J\gamma}$. In $p+p$ collisions nearly 70% of
 2196 all photons are matched to a jet, but in central Pb+Pb
 2197 collisions only about half of all photons are matched to a
 2198 jet. These measurements provide unambiguous evidence
 2199 for partonic energy loss. However, the kinematic cuts
 2200 required to suppress the background leave some ambigu-
 2201 ity regarding the amount of energy that was lost. Some
 2202 of the energy could simply be swept outside of the jet
 2203 cone. The preliminary results of an analysis with higher
 2204 statistics for the $p+p$ data and the addition of $p+Pb$
 2205 collisions also shows no significant modification, confirm-
 2206 ing that the Pb+Pb imbalance does not originate from cold
 2207 nuclear matter effects (Collaboration, 2013b).

2208 By construction, measurements of the process $q+g \rightarrow$
 2209 $q+\gamma$ can only measure interactions of quarks with the
 2210 medium. Since there are more gluons in the initial state
 2211 and quarks and gluons may interact with the medium
 2212 in different ways, studies of direct photons alone cannot
 2213 give a full picture of partonic energy loss.

2214 With the large statistics data collected during the

2015 Pb+Pb running of the LHC at 5 TeV, another
 “Golden Probe” for jet tomography of the QGP, the co-
 incidences of a Z^0 and a jet, became experimentally ac-
 cessible (Neufeld *et al.*, 2011; Wang and Huang, 1997).
 While this channel has served as an essential calibrator

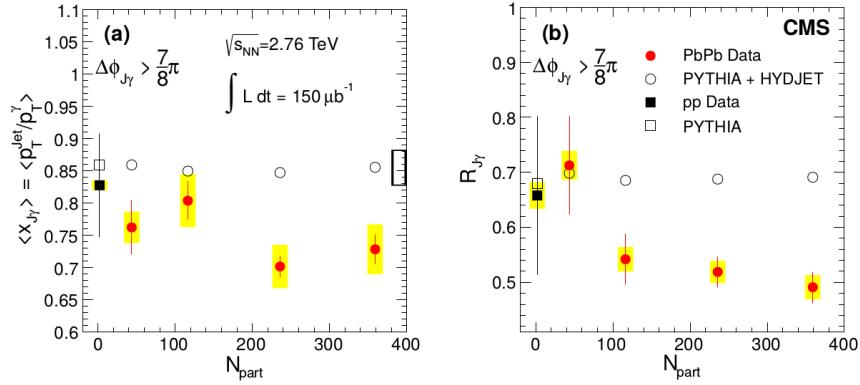


FIG. 19 Figure from CMS (Chatrchyan *et al.*, 2013b) for isolated photons with $p_T > 60$ GeV/c and associated jets with $p_T > 30$ GeV/c. (a) Average ratio of jet transverse momentum to photon transverse momentum, $\langle x_{J\gamma} \rangle$, as a function of the number of participating nucleons N_{part} . (b) Average fraction of isolated photons with an associated jet above 30 GeV/c, $R_{J\gamma}$, as a function of N_{part} . This demonstrates that the quark jet 180° away from a direct photon loses energy, with the energy loss increasing with increasing centrality.

2220 of jet energy in TeV $p+p$ collisions, in heavy ion collisions
 2221 it can be used to calibrate in-medium parton energy
 2222 loss as the Z^0 carries no color charge and is expected to
 2223 escape the medium unattenuated like the photon. How-
 2224 ever, photon measurements at higher momentum are lim-
 2225 ited due to the large background from decay photons in
 2226 experimental measurements. Recent measurements of Z
 2227 boson tagged jets in Pb+Pb collisions at $\sqrt{s_{\text{NN}}} = 5.02$
 2228 TeV (Sirunyan *et al.*, 2017c) show that angular correla-
 2229 tions between Z bosons and jets are mostly preserved in
 2230 central Pb+Pb collisions. However, the transverse mo-
 2231 mentum of the jet associated with that Z boson appears
 2232 to be shifted to lower values with respect to the observa-
 2233 tions in $p+p$ collisions, as expected from jet quenching.

2234 5. Hadron-jet correlations

2235 Correlations between a hard hadron and a recon-
 2236 structed jet were measured to overcome the downside of
 2237 an explicit bias imposed by the background suppression
 2238 techniques described in Section II.E. Similar to dihadron
 2239 correlations, a reconstructed hadron is selected and the
 2240 yield of jets reconstructed within $|\pi - \Delta\phi| < 0.6$ rela-
 2241 tive to that hadron is measured in (Adam *et al.*, 2015c).
 2242 For sufficiently hard hadrons, a large fraction of the jets
 2243 correlated with those hadrons would be jets that origi-
 2244 nated from a hard process, however, for low momentum
 2245 hadrons, the yield will be dominated by combinatorial
 2246 jets. The yield of combinatorial jets should be indepen-
 2247 dent of the hadron momentum, so the difference between
 2248 the yields, Δ_{recoil} , is calculated to subtract the back-
 2249 ground from the ensemble of jet candidates. This differ-
 2250 ence in yields is then compared to the same measurement
 2251 in $p+p$ collisions.

2252 Since the requirement of a hard hadron is opposite the

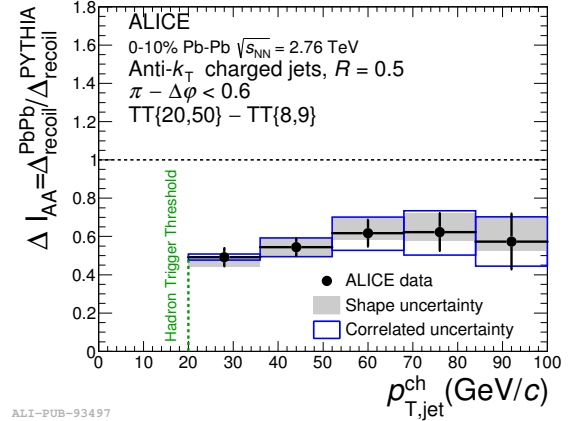


FIG. 20 Figure from ALICE (Adam *et al.*, 2015c). $\Delta I_{AA} = \Delta_{recoil}^{PbPb} / \Delta_{recoil}^{PYTHIA}$ where Δ_{recoil} is the difference between the number of jets within $\pi - \Delta\phi < 0.6$ of a hadron with $20 < p_T < 50$ GeV/c and a hadron with $8 < p_T < 9$ GeV/c. The green line indicates the momentum of the higher momentum hadron, an approximate lower threshold on the jet momentum. This demonstrates the suppression of a jet 180° away from a hard hadron.

jet being studied, no fragmentation bias is imposed on the reconstructed jet. Therefore, this measurement may be more sensitive to modified jets than observables that require selection criteria on the jet candidates themselves. Figure 20 shows the ratio of Δ_{recoil} in Pb+Pb collisions to that in $p+p$ collisions, $\Delta I_{AA} = \Delta_{recoil}^{PbPb} / \Delta_{recoil}^{PYTHIA}$. PYTHIA is used as a reference rather than data due to limited statistics available in the data at the same collision energy. PYTHIA agrees with the data from $p+p$ collisions at $\sqrt{s} = 7$ TeV. These data demonstrate that there is substantial jet suppression, consistent with the

2264 results discussed above.

2265 Measurements of hadron-jet correlations by 2318
 2266 STAR (Adamczyk *et al.*, 2017c) used a novel mixed 2319
 2267 event technique for background subtraction in order to 2320
 2268 extend the measurement to low momenta. The condi- 2321
 2269 tional yield correlated with a high momentum hadron 2322
 2270 was clearly suppressed in central Au+Au collisions 2323
 2271 relative to that observed in peripheral collisions, though 2324
 2272 substantially less so at the lowest momenta. A benefit 2325
 2273 of this method is that, in principle, the conditional yield 2326
 2274 of jets correlated with a hard hadron can be calculated 2327
 2275 with perturbative QCD.

2276 6. Path length dependence of inclusive R_{AA} and jet v_n

2277 The azimuthal asymmetry shown in Figure 2 provides 2333
 2278 a natural variation in the path length traversed by hard 2334
 2279 partons and the orientation of the reaction plane can be 2335
 2280 reconstructed from the distribution of final state hadrons. 2336
 2281 The correlations with this reaction plane can therefore 2337
 2282 be used to investigate the path length of partonic energy 2338
 2283 loss. The reaction plane dependence of inclusive particle 2339
 2284 R_{AA} demonstrates that energy loss is path length de- 2340
 2285 pendent (Adler *et al.*, 2007a), as expected from models. 2341
 2286 The path length changes with collision centrality, system 2342
 2287 size, and angle relative to the reaction plane, however, the 2343
 2288 temperature and lifetime of the QGP also change when 2344
 2289 the centrality and system size are varied. When particle 2345
 2290 production is studied relative to the reaction plane an- 2346
 2291 gle, the properties of the medium remain the same while
 2292 only the path length is changed. Because the eccentric-
 2293 ity of the medium and therefore the path length can only 2347
 2294 be determined in a model, any attempt to determine the
 2295 absolute path length is model dependent. Attempts to 2348
 2296 constrain the path length dependence of R_{AA} were ex- 2349
 2297 plored in (Adler *et al.*, 2007a). While these studies were 2350
 2298 inconclusive, they showed that R_{AA} is constant at a fixed 2351
 2299 mean path length and that there is no suppression for a 2352
 2300 path length below $L = 2$ fm, indicating that there is ei- 2353
 2301 ther a minimum time a hard parton must interact with 2354
 2302 the medium or there must be substantial effects from 2355
 2303 surface bias. More conclusive statements would require 2356
 2304 more detailed comparisons to models. 2357

2305 At high p_T , the single particle v_n in equation 2 are 2358
 2306 dominated by jet production and a non-zero v_2 indi- 2359
 2307 cates path length dependent jet quenching. Above 10 2360
 2308 GeV/c, a non-zero v_2 is observed at RHIC (Adare *et al.*, 2361
 2309 2013a) and the LHC (Abelev *et al.*, 2013a; Chatrchyan 2362
 2310 *et al.*, 2012a) and can be explained by energy loss mod- 2363
 2311 els (Abelev *et al.*, 2013a). Above 10 GeV/c, v_3 in central 2364
 2312 collisions is consistent with zero (Abelev *et al.*, 2013a). 2365
 2313 The v_n of jets themselves can be measured directly, how- 2366
 2314 ever, only jet v_2 has been measured (Aad *et al.*, 2013a; 2367
 2315 Adam *et al.*, 2016b). Figure 21 compares jet and charged 2368
 2316 particle v_2 from ATLAS and ALICE. ALICE measure- 2369

2317 ments are of charged jets, which are only constructed
 with charged particles and not corrected for the neutral
 component, with $R = 0.2$ and $|\eta| < 0.7$ and ATLAS mea-
 surements are reconstructed jets with $R = 0.2$ and $|\eta| <$
 2.1. The v_2 observed by ALICE is higher than that ob-
 served by ATLAS, although consistent within the large
 uncertainties. The ALICE measurement is unfolded to
 correct for detector effects, but it is not corrected for
 the neutral energy contribution. Both measurements use
 methods to suppress the background which could lead to
 greater surface bias or bias towards unmodified jets. The
 ALICE measurement requires a track above 3 GeV/c in
 the jet to reduce the combinatorial background. The AT-
 LAS measurement requires the calorimeter jets used in
 the measurement to be matched to a 10 GeV track jet or
 to contain a 9 GeV calorimeter cluster. Because of the
 higher momentum requirement the ATLAS measurement
 has a greater bias than the ALICE sample of jets.

These measurements provide some constraints on the
 path length dependence, however, this is not the only re-
 levant effect. Theoretical calculations indicate that both
 event-by-event initial condition fluctuations and jet-by-
 jet energy loss fluctuations play a role in v_n at high
 p_T (Betz *et al.*, 2017; Noronha-Hostler *et al.*, 2016; Zapp,
 2014a). This is perhaps not surprising, analogous to the
 importance of fluctuations in the initial state for mea-
 surements of the v_n due to flow. However, it does indi-
 cate that much more insight into which observables are
 most sensitive to path length dependence and the role of
 fluctuations in energy loss is needed from theory.

7. Heavy quark energy loss

The jet quenching due to radiative energy loss is ex-
 pected to depend upon the species of the fragmenting
 parton (Horowitz and Gyulassy, 2008). The simplest ex-
 ample is gluon jets, which are expected to lose more en-
 ergy in the medium than quark jets due to their larger
 color factor. Similarly, the mass of the initial parton also
 plays a role and the interpretation of this effect depends
 on the theoretical treatment of parton-medium interac-
 tions. Strong coupling calculations based on AdS/CFT
 correspondence predict large mass effects at all trans-
 verse momenta and in weak-coupling calculations based
 on pQCD mass effects may arise from the “dead-cone” ef-
 fect (Dokshitzer and Kharzeev, 2001), the suppression of
 gluon emission at small angles relative to a heavy quark,
 but may be limited to a small range of heavy-quark trans-
 verse momenta comparable to the heavy-quark mass.
 However, the relevance of the dead-cone effect in heavy
 ion collisions is debated (Aurenche and Zakharov, 2009).

Searches for a decreased suppression of heavy flavor
 using single particles are still inconclusive due to large
 uncertainties, although they indicate that heavy quarks
 may indeed lose less energy in the medium. As shown

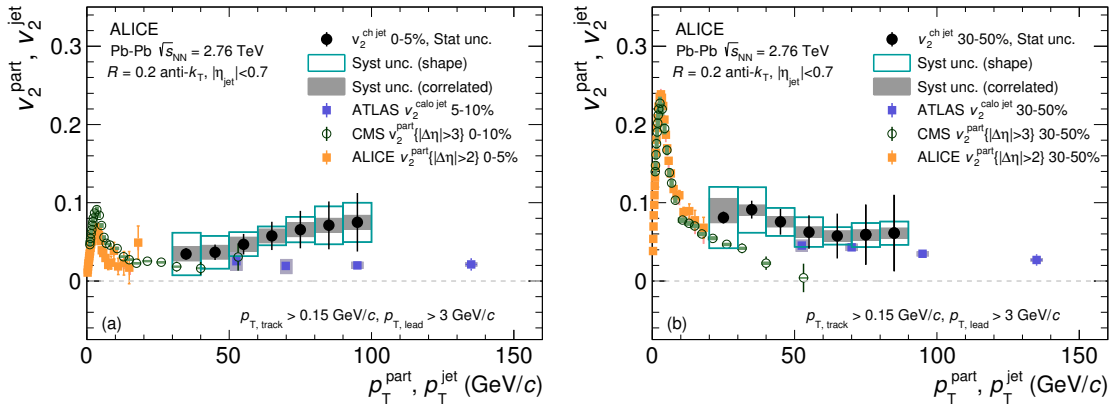


FIG. 21 Figure from ALICE (Adam *et al.*, 2016b). Jet v_2 from charged jets by ALICE (Adam *et al.*, 2016b) and calorimeter jets by ATLAS (Aad *et al.*, 2013a) compared to the charged hadron v_2 for 5–10% (left) and 30–50% collisions (Abelev *et al.*, 2013a; Chatrchyan *et al.*, 2012a). This demonstrates that partonic energy loss is path length dependent.

2370 in Figure 11, the R_{AA} of single electrons from decays of
 2371 heavy flavor hadrons is within uncertainties of that of
 2372 hadrons containing only light quarks. Measurements of
 2373 single leptons are somewhat ambiguous because of the
 2374 difference between the momentum of the heavy meson
 2375 and the decay lepton. Since the mass effect is predicted
 2376 to be momentum dependent with negligible effects for
 2377 $p_T \gg m$, the decay may wash out any mass effect. The
 2378 R_{AA} of D mesons is within uncertainties of the light
 2379 quark R_{AA} (Adam *et al.*, 2015a, 2016k; Adamczyk *et al.*,
 2380 2014b). Particularly at the LHC, these results may be
 2381 somewhat ambiguous because D mesons may also be pro-
 2382 duced in the fragmentation of light quark or gluon jets.
 2383 B mesons are much less likely to be produced by frag-
 2384 mentation. Preliminary measurements of B meson R_{AA}
 2385 show less suppression than for light mesons, although
 2386 the uncertainties are large and prohibit strong conclu-
 2387 sions (CMS, 2016b).

2388 Experimentally, heavy flavor jets are primarily identi-
 2389 fied using the relative long lifetimes of hadrons containing
 2390 heavy quarks, resulting in decay products significantly
 2391 displaced from the primary vertex. A variant of the
 2392 secondary vertex mass, requiring three or more charged
 2393 tracks, is also used to extract the relative contribution
 2394 of charm and bottom quarks to various heavy flavor jet
 2395 observables. However these methods cannot discriminate
 2396 between heavy quarks from the original hard scattering,
 2397 which then interact with the medium and lose energy, and
 2398 those from a parton fragmenting into bottom or charm
 2399 quarks (Huang *et al.*, 2013). A requirement of an addi-
 2400 tional B-meson in the event could ensure a purer sam-
 2401 ple of bottom tagged jets (Huang *et al.*, 2015), however,
 2402 this is not currently experimentally accessible due to the
 2403 limited statistics. Figure 22 shows a compilation of all
 2404 current measurements of heavy flavor jets at LHC (Cha-
 2405 trchyan *et al.*, 2014a; Khachatryan *et al.*, 2016d; Sirunyan
 2406 *et al.*, 2017b). The R_{AA} of bottom quark tagged jets is

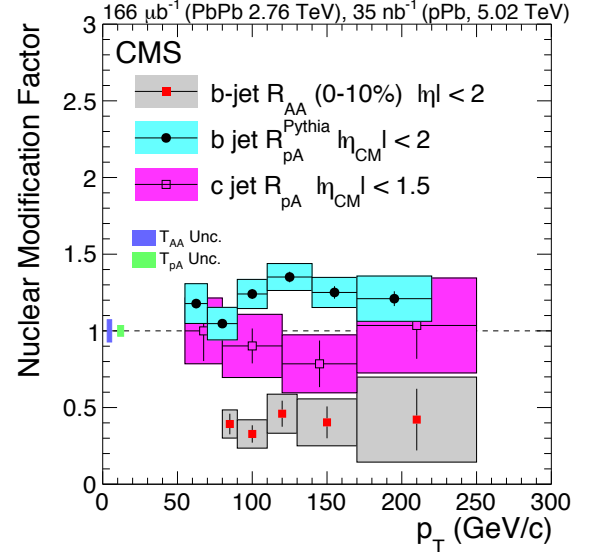


FIG. 22 The R_{AA} and R_{pPb} of heavy flavor associated jets measured by the CMS Collaboration (Chatrchyan *et al.*, 2014a; Khachatryan *et al.*, 2016d; Sirunyan *et al.*, 2017b). This shows that b quarks lose energy in the medium. Figure courtesy of Kurt Jung.

measured utilizing the Pb+Pb and $p+p$ data collected at $\sqrt{s_{\text{NN}}} = 2.76$ TeV. Bottom tagged jet measurements in $p+Pb$ collisions are also performed to study cold nuclear matter effects in comparison to expectations from PYTHIA at the 5 TeV center of mass energy (Khachatryan *et al.*, 2016d). Jets which are associated with the charm quarks in $p+Pb$ collisions are also studied with a variant of the bottom tagging algorithm (Sirunyan *et al.*, 2017b). A strong suppression of R_{AA} of jets associated with bottom quarks is observed in Pb+Pb collisions while the R_{pPb} is consistent with unity. These CMS measure-

ments demonstrate that jet quenching does not have a strong dependence on parton mass and flavor, at least in the jet p_T range studied (Chatrchyan *et al.*, 2014a; Khachatryan *et al.*, 2017c). The charm jet R_{pPb} also shows consistent results with negligible cold nuclear matter effects when compared with the measurements from $p+p$ collisions.

8. Summary of experimental evidence for partonic energy loss in the medium

Partonic energy loss in the medium is demonstrated by numerous measurements of jet observables. To date, the most precise quantitative constraints on the properties of the medium come from comparisons of R_{AA} to models by the JET collaboration (Burke *et al.*, 2014). The interpretation of R_{AA} as partonic energy loss is confirmed by measurements of dihadron, gamma-hadron, jet-hadron, hadron-jet, and jet-jet correlations. The assumption about the background contribution and the biases of these measurements vary widely, so the fact that they all lead to a coherent physical interpretation strengthens the conclusion that they are due to partonic energy loss in the medium. This energy loss scales with the energy density of the system rather than the system size.

Reaction plane dependent inclusive particle R_{AA} , inclusive particle v_2 , and jet v_2 indicate that this energy loss is path length dependent, perhaps requiring a parton to traverse a minimum of around 2 fm of QGP to lose energy. Comparison of jet v_n to models indicates that jet-by-jet fluctuations in partonic energy loss impacts reaction plane dependent measurements significantly, however, this is not yet fully understood theoretically.

Measurements of heavy quark energy loss are consistent with expectations from models, however, they are also consistent with the energy loss observed for gluons and light quarks. Studies of heavy quark energy loss will improve substantially with the slated increases in luminosity and detector upgrades. The STAR heavy flavor tracker has already enabled higher precision measurements of heavy flavor at RHIC and one of the core goals of the proposed detector upgrade, sPHENIX, is precision measurements of heavy flavor jets. Run 3 at the LHC will enable higher precision measurements of heavy flavor, including studies of heavy flavor jets in the lower momentum region which may be more sensitive to mass effects.

The key question for the field is how to constrain the properties of the medium further. The Monte Carlo models the Jetscape collaboration is developing will include both hydrodynamics and partonic energy loss and the Jetscape collaboration plans Bayesian analyses similar to (Bernhard *et al.*, 2016; Novak *et al.*, 2014) incorporating jet observables. These models will also enable

the exact same analysis techniques and background subtraction methods to be applied to data and theoretical calculations. We propose including single particle R_{AA} (including particle type dependence), jet R_{AA} (with experimental analysis techniques applied), high momentum single particle v_2 , jet v_2 , hadron-jet correlations, and I_{AA} from both γ -hadron and dihadron correlations. The analysis method for all of these observables should be replicable in Monte Carlo. We omit A_J because a majority of these measurements are not corrected for detector effects. Bayesian analyses comparing theoretical calculations to data may be the best avenue for constraining the properties of the medium using measurements of jets. This is likely to improve our understanding of which observables are most useful for constraining models.

C. Influence of the medium on the jet

Section III.B examined the evidence that partons lose energy in the medium, but did not examine how partons interact with the medium. Understanding modifications of the jet by the medium requires a bit of a paradigm shift. As highlighted in Section II, a measurement of a jet is not a measurement of a parton but a measurement of final state hadrons generated by the fragmentation of the parton. Final state hadrons are grouped into the jet (or not) based on their spatial correlations with each other (and therefore the parton). Whether or not the lost energy retains its spatial correlation with the parent parton depends on whether or not the lost energy has had time to equilibrate in the medium. If a bremsstrahlung gluon does not reach equilibrium with the medium, when it fragments it will be correlated with the parent parton. Interactions with the medium shift energy from higher momentum final state particles to lower momentum particles and broadens the jet. Similar apparent modifications could occur if partons from the medium become correlated with the hard parton through medium interactions (Casalderrey-Solana *et al.*, 2017). Whether or not this lost energy is reconstructed as part of a jet depends on the jet finding algorithm and its parameters.

Whereas the observation that energy is lost is relatively straightforward, there are many different ways in which the jet may be modified, and we cannot be sure which mechanisms actually occur in which circumstances until we have measured observables designed to look for these effects. There are several different observables indicating that jets are indeed modified by the medium, each with different strengths and weaknesses. We distinguish between mature observables – those which have been measured and published, usually by several experiments – and new observables – those which have either only been published recently or are still preliminary. Mature observables largely focus on the average properties of jets as a function of variables which we can either mea-

sure directly or are straightforward to calculate, such as momentum and the position of particles in a jet. This includes dihadron correlations (h-h); correlations of a direct photon or Z with either a hadron or a reconstructed jet (γ -h and γ -jet); the jet shape ($\rho(r)$); the dijet asymmetry (A_J); the momentum distribution of particles in a reconstructed jet, called the fragmentation function ($D_{jet}(z)$ where $z = p_T/E_{jet}$); identification of constituents (PID) and heavy flavor jets (HF jets). Where our experimental measurements of these observables have limited precision, this is either due to the limited production cross section (heavy flavor jets and correlations with direct photons) or due to limitations in our understanding of the background (identified particles).

Our improving understanding of the parton-medium interactions has largely motivated the search for new, more differential observables. Partonic energy loss is a statistical process so ensemble measurements such as the average distribution of particles in a jet, or the average fractional energy loss, are important but can only give a partial picture of partonic energy loss. Just as fluctuations in the initial positions of nucleons must be understood to properly interpret the final state anisotropies of the medium, fluctuations play a key role in partonic interactions with the medium. The average shape and energy distribution of a jet is smooth, but each individual jet is a lumpy object. These new observables include the jet mass M_{jet} , subjettiness ($N_{subjettiness}$), LeSub, the splitting function z_g , the dispersion (p_T^D), and the girth (g). We leave the definitions of these variables to the following sections and we focus our discussion on observables which have been measured in heavy ion collisions, omitting those which have only been proposed date. In general these observables are sensitive to the properties and structure of individual jets, and they are adapted from advances in jet measurements from particle physics. Investigations of new observables are important because they will allow access to well defined pQCD observables, which increases the sensitivity of our measurements to the properties of the QGP. The goal of each new observable is to construct something that is sensitive to properties of the medium that our mature observables are not sufficiently sensitive to, or to be able to disentangle physics processes that are not directly related to the medium properties, such as the difference in fragmentation between quark and gluon jets. Most measurements of these new observables are still preliminary and we therefore avoid drawing strong conclusions from them. Our understanding of these observables is still developing, particularly our understanding of how they are impacted by analysis cuts and the approach to the approach used to remove background effects. An observable which is highly effective for, say, distinguishing between quark and gluon jets in $p+p$ collisions, may not be as effective in heavy ion collisions.

We summarize the current status of observables sensi-

tive to the medium modifications of jets in Table III. This list of observables also shows the evolution of the field. Early on, due to statistical limitations, studies focused on dihadron correlations. These measurements are straightforward experimentally, however, they are difficult to calculate theoretically because all hadron pairs contribute and the kinematics of the initial hard scattering is poorly constrained. In contrast, as discussed in Section III.B.4, when direct photons are produced in the process $q+g \rightarrow q+\gamma$, the initial kinematics of the hard scattered partons are known more precisely. In some kinematic regions, these measurements are limited by statistics, and in others they are limited by the systematic uncertainty predominantly from the subtraction of background photons from π^0 decay. Measurements of reconstructed jets are feasible over a wider kinematic region, but the kinematics of the initial hard scattering are not constrained as well. Nearly all measurements are biased towards quarks for the reasons discussed in Section II, however, it may be possible to tune the bias either using identified particles or by using new observables that select for particular fragmentation patterns.

Table III summarizes whether or not modifications, particularly broadening and softening, have been observed using each observable and which experiments have measured them. This table demonstrates that each measurement has strengths and weaknesses and that all observations contribute to our current understanding. Modifications to the jet structure have been observed for most observables, but not all. Since each observable is sensitive to different modifications, all provide useful input for differentiating between jet quenching models and understanding the effects of different types of initial and final state processes. We begin our discussion of measurements indicating modification of jets by the medium with mature observables. For each observable we revisit these issues in a discussion stating what we have learned from that observable.

1. Fragmentation functions with jets

Fragmentation functions are a measure of the distribution of final state particles resulting from a hard scattering and represent the sum of parton fragmentation functions, D_i^h , where i represents each parton type ($u, d, g, etc.$) contributing to the final distribution of hadrons, h . Typically, fragmentation functions are measured as a function of z or ξ where $z = p^h/p$ and $\xi = -\ln(z)$, where p is the momentum of parton produced by the hard scattering. Jet reconstruction can be used to determine the jet momentum, p^{jet} to approximate the parton momentum p , while the momentum of the hadrons, p^h , are measured for each hadron that is clustered into the jet by the jet reconstruction algorithm. In collider experiments, the transverse momentum, p_T , is

TABLE III Summary of measurements sensitive to fragmentation in heavy ion collisions. Preliminary measurements are denoted with a (P). New observables are separated from mature observables by a line. The first two columns after the observable describe biases inherent to the observable, while the next four columns refer to observations made from the measured results. We refer the readers to each section for details of measurements of each observable.

Observable	kinematics	q/g bias	evidence of modification	evidence of broadening	evidence of softening	measured by	Discussion
$D_{jet}(z)$	constrained	q bias	yes	insensitive	yes	CMS, ATLAS	III.C.1
γ -h	very well	q only	yes	yes	yes	STAR, PHENIX	III.C.2
γ -jet	very well	q only	yes			CMS	III.C.2
h-h	poor	unknown	yes	yes	yes	STAR, PHENIX, ALICE, CMS	III.C.3
jet-h	constrained	q bias	yes	yes	yes	ALICE(P), CMS, STAR	III.C.4
A_J	constrained	q bias	yes	insensitive	yes	STAR, ATLAS, CMS	III.C.5
$\rho(r)$	constrained	q bias	yes	yes	yes	CMS	III.C.6
identified h-h	poor	select	no			STAR, PHENIX	III.C.7
HF jets	constrained	q	yes			CMS	N/A
LeSub	constrained	unknown	no			ALICE(P)	III.C.8
p_T^D	constrained	select	yes			ALICE(P)	III.C.10
girth	constrained	select	yes			ALICE(P)	III.C.11
z_g	constrained	unknown	yes (CMS), no (STAR)			CMS, STAR(P)	III.C.12
τ_N	constrained	unknown	no			ALICE(P)	III.C.13
M_{jet}	constrained	unknown	no			ALICE	III.C.9

typically substituted for the total momentum p in the fragmentation function. It should be noted that this is not precisely the same observable as what is commonly referred to as the fragmentation function by theorists.

The fragmentation functions for jets in Pb+Pb collisions at $\sqrt{s_{NN}} = 2.76$ TeV have been measured by the ATLAS (Aad *et al.*, 2014c) and CMS (Chatrchyan *et al.*, 2012c, 2014c) Collaborations. The ratios of the fragmentation functions for several different centrality bins to the most peripheral centrality bin are shown in Figure 23. The most central collisions show a significant change in the average fragmentation function relative to peripheral collisions. At low z there is a noticeable enhancement followed by a depletion at intermediate z . This suggests that the energy loss observed for mid to high momentum hadrons is redistributed to low momentum particle production. We note that this corresponds to only a few additional particles and is a small fraction of the energy that R_{AA} , A_J and the other energy loss observables discussed in Section III.B indicate is lost. Arguably, this is the most direct observation of the softening of the fragmentation function expected from partonic energy loss in the medium. However, the definition of a fragmentation function in Equation 1 uses the momentum of the initial parton and, as discussed in Section II, a jet's momentum is not the same as the parent parton's momentum. Fragmentation functions measured with jets with large radii are approximately the same as the fragmentation functions in Equation 1, but this is not true for the jets with smaller radii measured in heavy ion collisions.

It is important to note that initial fragmentation measurements from the LHC used only dijets samples with

large momenta ($p_T > 4$ GeV/c) constituents, which indicated that there was no modification of fragmentation functions (Chatrchyan *et al.*, 2012c). With increased statistics and improved background estimation techniques these fragmentation measurements were re-measured later with inclusive jets with constituent tracks with $p_T > 1$ GeV/c utilizing the 2011 data. Figure 24 compares the measurements from CMS from two different measurements using 2010 and 2011 data. The initial 2010 analysis did not include lower momentum jet constituents due to the difficulty with background subtraction in that kinematic region and focused on leading and subleading jets. While the two measurements are consistent, the conclusion drawn from the 2010 data alone was that there was no apparent modification of the jet fragmentation functions. This highlights how critical biases are to the proper interpretation of measurements. The high momentum of these jets combined with the background subtraction and suppression techniques also means that the data in both Figure 23 and Figure 24 are likely biased towards quark jets.

2. Boson tagged fragmentation functions

As described previously, bosons can be used to tag the initial kinematics of the hard scattering. For fragmentation functions, this gives access to the initial parton momentum in the calculation of the fragmentation variable z . At the top Au+Au collision energy at RHIC, $\sqrt{s_{NN}} = 200$ GeV, there have been no direct measurements of fragmentation functions from reconstructed jets

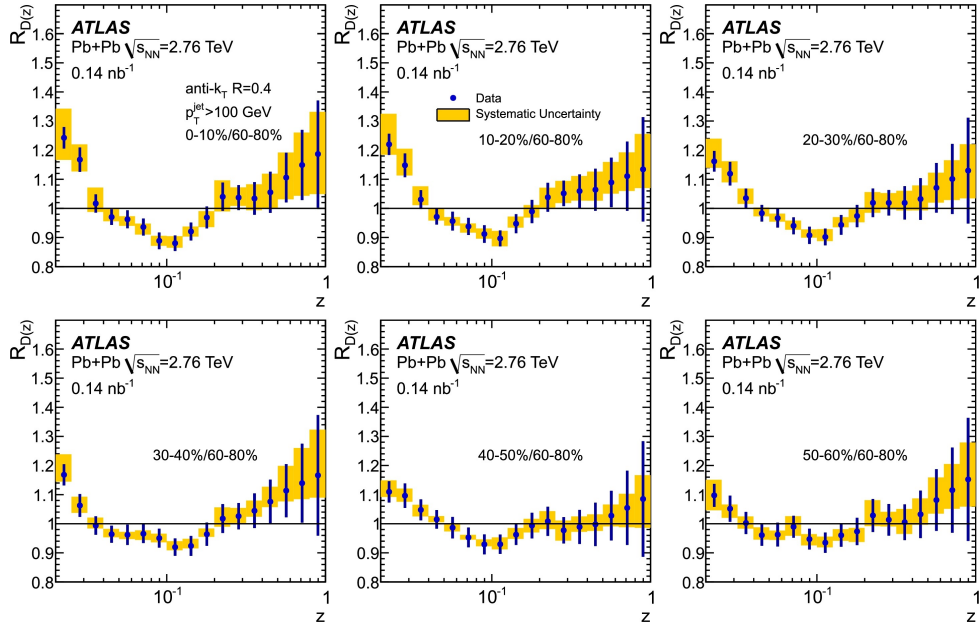


FIG. 23 Figure from ATLAS (Aad *et al.*, 2014c). Ratio of fragmentation functions from reconstructed jets measured by ATLAS for jets in Pb+Pb collisions at various centralities to those in 60-80% central collisions at $\sqrt{s_{NN}} = 2.76$ TeV. This shows that fragmentation functions are modified in $A+A$ collisions, with an enhancement at low momenta (low z) and a depletion at intermediate momenta (intermediate z), with the modification increasing from more peripheral to more central collisions.

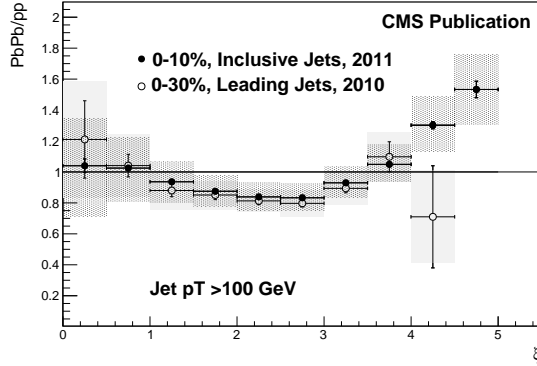


FIG. 24 Comparison of CMS measurements of fragmentation functions in Pb+Pb over pp from reconstructed jets for jets in Pb+Pb collisions at $\sqrt{s_{NN}} = 2.76$ TeV from 2010 and 2011 data (Chatrchyan *et al.*, 2012c, 2014c). Even though the two measurements are consistent, the 2010 data in isolation indicate that fragmentation is not modified while the 2011 data, which extend to lower momenta and use a less biased jet sample, clearly show modification at low momenta (high ξ). This highlights the difficulty in drawing conclusions from a single measurement, particularly when neglecting possible biases.

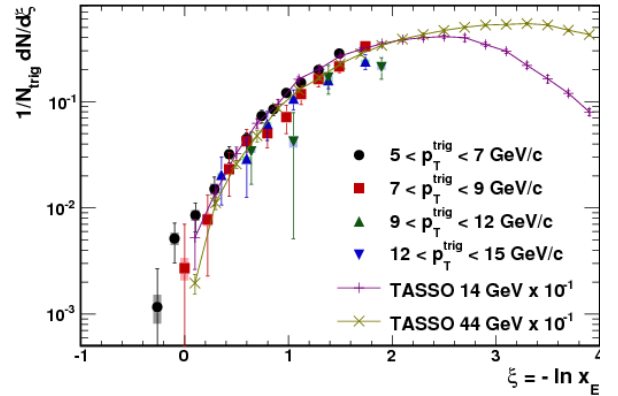


FIG. 25 Figure from PHENIX (Adare *et al.*, 2010b). $\xi = -\ln(x_E)$ distributions where $x_E = -|p_T^a/p_T^t| \cos(\Delta\phi) \approx z$ for isolated direct photon-hadron correlations for several photon p_T ranges from $p+p$ collisions at $\sqrt{s} = 200$ GeV compared to TASSO measurements in e^+e^- collisions at $\sqrt{s} = 14$ and 44 GeV. This demonstrates that direct photon measurements can be used reliably to extract quark fragmentation functions in $p+p$ collisions and that fragmentation functions are the same in e^+e^- and $p+p$ collisions.

2694 so far, however, γ -hadron correlations have been mea- 2698
 2695 sured both in $p+p$ and Au+Au collisions. The fragmen- 2699
 2696 tation function was measured in $p+p$ collisions at RHIC 2700
 2697 as a function of $x_E = -|p_T^a/p_T^t| \cos(\Delta\phi) \approx z$ (Adare *et al.*, 2701

2010b) and is shown in Figure 25. The $p+p$ results agree well with the TASSO measurements of the quark fragmentation function in electron-positron collisions, which is consistent with the production of a quark jet oppo-

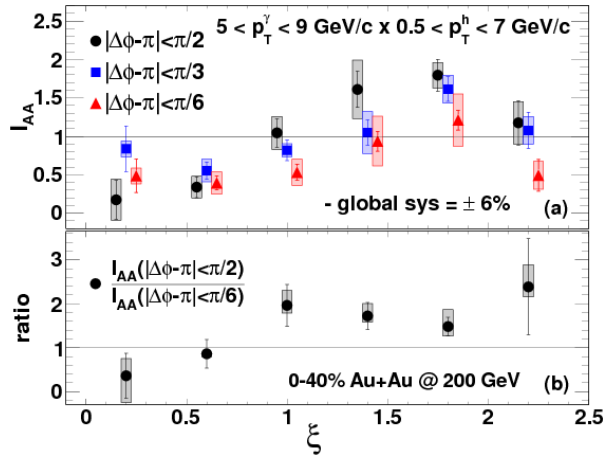


FIG. 26 Figure from PHENIX (Adare *et al.*, 2013b). The top panel shows I_{AA} for the away-side as a function of $\xi = \log(\frac{1}{z}) = \log(\frac{p_{jet}^{jet}}{p_{had}})$. The points are shifted for clarity. The bottom panel shows the ratio of the I_{AA} for $|\Delta\phi - \pi| < \pi/2$ to $|\Delta\phi - \pi| < \pi/6$. This demonstrates the enhancement at low momentum combined with a suppression at high momentum, a shift consistent with expectations from energy loss models. The change is largest for wide angles from the direct photon.

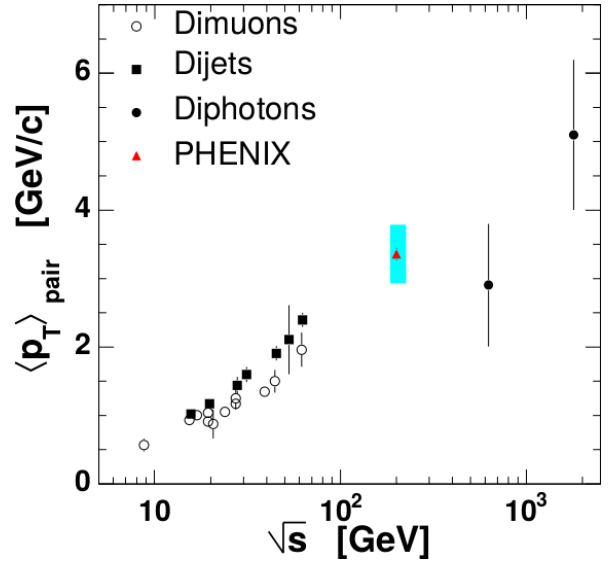


FIG. 27 Figure from PHENIX (Adler *et al.*, 2006c). Compilation of $\langle p_T \rangle_{pair} = \sqrt{2}k_T$ measurements where k_T is the acoplanarity momentum vector. Dihadron correlation measurements in $p+p$ collisions from PHENIX are consistent with the trend from dimuon, dijet and diphoton measurements at other collision energies. Dimuon and dijet measurements are from fixed target experiments and the diphoton measurements are from the Tevatron.

2702 site the direct photon as expected in Compton scattering.
 2703 Using the $p+p$ results as a reference, direct photon-
 2704 hadron correlations were measured in Au+Au collisions
 2705 at RHIC (Adare *et al.*, 2013b). The I_{AA} are shown in
 2706 Figure 26. A suppression is observed for $\xi < 1$ ($z > 0.4$)
 2707 while an enhancement is observed for $\xi > 1$ ($z < 0.4$).
 2708 This suggests that energy loss at high z is redistributed
 2709 to low z . Comparing these results to the results from
 2710 STAR (Abelev *et al.*, 2010c; Adamczyk *et al.*, 2016) sug-
 2711 gests that this is not a z_T dependent effect but rather
 2712 a p_T dependent effect. STAR measured direct photon-
 2713 hadron correlations for a similar z_T range but does not
 2714 observe the clear enhancement exhibited in the PHENIX
 2715 measurement. However, STAR is able to measure low
 2716 values of z_T by increasing the trigger photon p_T , while
 2717 PHENIX goes to low z_T by decreasing the associated
 2718 hadron p_T . Preliminary PHENIX results as a function of
 2719 photon p_T are consistent with the conclusion that modi-
 2720 fications of fragmentation depend on associated particle
 2721 p_T rather than z_T . Furthermore, STAR does observe an
 2722 enhancement for jet-hadron correlations with hadrons of
 2723 $p_T < 2$ GeV/c which is consistent with the PHENIX di-
 2724 rect photon-hadron observation.

2725 The direct photon-hadron correlations also suggest
 2726 that the low p_T enhancement occurs at wide angles with
 2727 respect to the axis formed by the hard scattered partons.
 2728 Figure 26 shows the yield measured by PHENIX for dif-
 2729 ferent $\Delta\phi$ windows on the away-side. The enhancement
 2730 is most significant for the widest window, $|\Delta\phi - \pi| < \pi/2$.

2731 3. Dihadron correlations

2732 Measurements of dihadron correlations are sensitive to
 2733 modifications in fragmentation, although the interpreta-
 2734 tion is complicated because the initial kinematics of the
 2735 hard scattering are poorly constrained. Differences ob-
 2736 served in the correlations can either be due to medium
 2737 interactions or due to changes in the parton spectrum.
 2738 At high p_T , there are no indications of modification of
 2739 the near- or away-side at midrapidity in $d+Au$ colli-
 2740 sions (Adler *et al.*, 2006a,d) so any effects observed in
 2741 $A+A$ are hot nuclear matter effects and either $d+Au$ or
 2742 $p+p$ can be used as a reference for $A+A$ collisions.

2743 The near-side peak can be used to study the angu-
 2744 lar distribution of momentum and particles around the
 2745 triggered jet. The away-side peak is wider than the near-
 2746 side due to the resolution of the triggered jet peak axis
 2747 and the effect of the acoplanarity momentum vector, k_T .
 2748 Dihadron correlations have been measured in $p+p$ colli-
 2749 sions to determine the intrinsic k_T . Measurements of
 2750 $\langle p_T \rangle_{pair} = \sqrt{2}k_T$ as a function of \sqrt{s} are shown in Fig-
 2751 ure 27.

The effect of the nucleus on k_T has been studied in
 $d+Au$ collisions at 200 GeV (Adler *et al.*, 2006d) and
 in $p+Pb$ collisions at 5.02 TeV (Adam *et al.*, 2015b) via
 dihadron correlations and reconstructed jets respectively.
 The dihadron measurements in $d+Au$ are consistent with
 the PHENIX $p+p$ measurements shown in Figure 27,

while the p +Pb dijet results agree with PYTHIA expectations. Since no broadening has been observed in p +Pb or d +Au collisions, any broadening of the away-side jet peak in A + A collisions would be the result of modifications from the QGP. Assuming this is purely from radiative energy loss, the transport coefficient \hat{q} can be extracted directly from a measurement of k_T according to $\hat{q} \propto \langle k_T^2 \rangle$ (Tannenbaum, 2017).

Figure 28 shows the widths in $\Delta\phi$ and $\Delta\eta$ on the near-side as a function of p_T^t , p_T^a , and the average number of participant nucleons, $\langle N_{\text{part}} \rangle$ for d +Au, Cu+Cu, and Au+Au collisions at $\sqrt{s_{\text{NN}}} = 62.4$ and 200 GeV (Agakishiev *et al.*, 2012c). The near-side is broader in both $\Delta\phi$ and $\Delta\eta$ in central collisions. This broadening does not have a strong dependence on the angle of the trigger particle relative to the reaction plane (Nattrass *et al.*, 2016). One interpretation of this is that the jet-by-jet fluctuations in partonic energy loss are more significant than path length dependence for this observable (Zapp, 2014a). Higher energy jets have higher particle yields and are more collimated, so if changes were due to an increase in the average parton energy the yield would increase but the width would decrease. In contrast, interactions with the medium would lead to broadening and the softening of the fragmentation function which would lead to more particles. The near-side yields are not observed to be modified (Agakishiev *et al.*, 2012c), although I_{AA} at RHIC (Nattrass *et al.*, 2016) is also consistent with the slight enhancement seen at the LHC (Aamodt *et al.*, 2012). This indicates that the increase in width is most likely due to medium interactions rather than changes in the parton spectra.

Recent studies of the away-side do not indicate a measurable broadening (Nattrass *et al.*, 2016), at least for the low momenta in this study ($4 < p_T^t < 6$ GeV/ c , 1.5 GeV/ $c > p_T^a$). This is in contrast to earlier studies which neglected odd v_n in the background subtraction, indicating dramatic shape changes. These earlier studies are discussed in greater detail in Section III.D.3 because the modifications observed were generally interpreted as an impact of the medium on the jet. We note that broadening is observed on the away-side for jet-hadron correlations, as discussed below. The current apparent lack of broadening in dihadron correlations may indicate that this is not the most sensitive observable because of the decorrelation between the trigger on the near-side and the angle of the away-side jet. It may also be a kinematic effect because modifications are extremely sensitive to momentum. The away-side I_{AA} decreases with increasing p_T^a , indicating a softening of the fragmentation function of surviving jets (Nattrass *et al.*, 2016).

A large collection of experimental measurements in e^+e^- collisions show that jets initiated by gluons exhibit differences with respect to jets from light-flavor quarks (Abreu *et al.*, 1996; Acton *et al.*, 1993; Akers *et al.*, 1995; Barate *et al.*, 1998; Buskulic *et al.*, 1996).

First, the charged particle multiplicity is higher in gluon jets than in light-quark jets. Second, the fragmentation functions of gluon jets are considerably softer than that of quark jets. Finally, gluon jets appeared to be less collimated than quark jets. These differences have already been exploited to differentiate between gluon and quark jets in p + p collisions (Collaboration, 2013a). The simplest and most studied variable used experimentally is the multiplicity, the total number of constituents of reconstructed jet. Since gluon hadronization produces jets which are ‘wider’ than jets induced by quark hadronization, jet shapes could be studied with jet width variables to distinguish quark and gluon jets.

Since there are significant differences in baryon and meson production in A + A collisions compared to p + p collisions, such differences may exist for jets. Furthermore, energy loss is different for quark and gluon jets, so species-dependent energy loss may mean that there are differences between jets with different types of leading hadrons. These differences may be observed through comparisons of jets with leading baryons and mesons or light and strange hadrons. The OPAL collaboration measured the ratio of K_0^S production in e^+e^- collisions in gluon jets to that in quark jets to be $1.10 \pm 0.02 \pm 0.02$ and the ratio of Λ production in gluon jets to that in quark jets to be $1.41 \pm 0.04 \pm 0.04$ (Ackerstaff *et al.*, 1999), meaning that jets containing a Λ or a proton are somewhat more likely to arise from gluon jets than jets which do not contain a baryon. This difference is small, however, a large difference in the interactions between quark and gluon jets in heavy ion collisions may be observable.

Measurements of dihadron correlations with identified leading triggers may be sensitive to these effects. Studies of identified strange trigger particles found a somewhat higher yield in jets with a leading K_0^S than those with a leading unidentified charged hadron or Λ at the same momentum (Abelev *et al.*, 2016). This was also observed in d +Au collisions, indicating that the more massive leading Λ simply takes a larger fraction of the jet energy. The slight centrality dependence indicates there may be medium effects, however, these could arise from differences in quark and gluon jets or from strange and non-strange jets. Ultimately these data are inconclusive due to their low precision. Dihadron correlations with identified pion and non-pion triggers (Adamczyk *et al.*, 2015) shown in Figure 29 observed a higher yield in jets with a leading pion than those with a leading kaon or proton. This difference was larger in Au+Au collisions than in d +Au collisions, which (Adamczyk *et al.*, 2015) proposes may be impacted to fewer baryon trigger particles coming from jets due to recombination. Both of these results could be impacted by several effects – differences in quark and gluon jets in the vacuum, differences in energy loss in the medium for quark and gluon jets, and modified fragmentation in the medium. Since both stud-

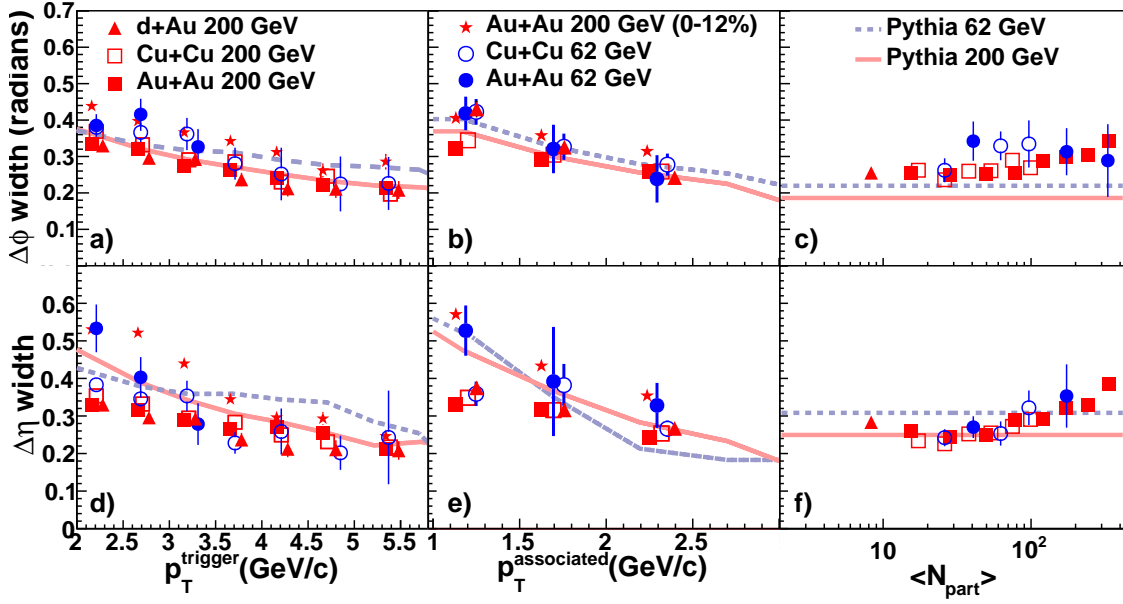


FIG. 28 Figure from STAR (Agakishiev *et al.*, 2012c). Dependence of the Gaussian widths in $\Delta\phi$ and $\Delta\eta$ on p_T^{trigger} for $1.5 \text{ GeV}/c < p_T^{\text{a}} < p_T^{\text{t}}$, p_T^{t} for $3 < p_T^{\text{t}} < 6 \text{ GeV}/c$, and $\langle N_{\text{part}} \rangle$ for $3 < p_T^{\text{t}} < 6 \text{ GeV}/c$ and $1.5 \text{ GeV}/c < p_T^{\text{a}} < p_T^{\text{t}}$ for 0-95% d+Au, 0-60% Cu+Cu at $\sqrt{s_{\text{NN}}} = 62.4 \text{ GeV}$ and $\sqrt{s_{\text{NN}}} = 200 \text{ GeV}$, 0-80% Au+Au at $\sqrt{s_{\text{NN}}} = 62.4 \text{ GeV}$, and 0-12% and 40-80% Au+Au at $\sqrt{s_{\text{NN}}} = 200 \text{ GeV}$. This demonstrates that the correlation is broadened in central Au+Au collisions.

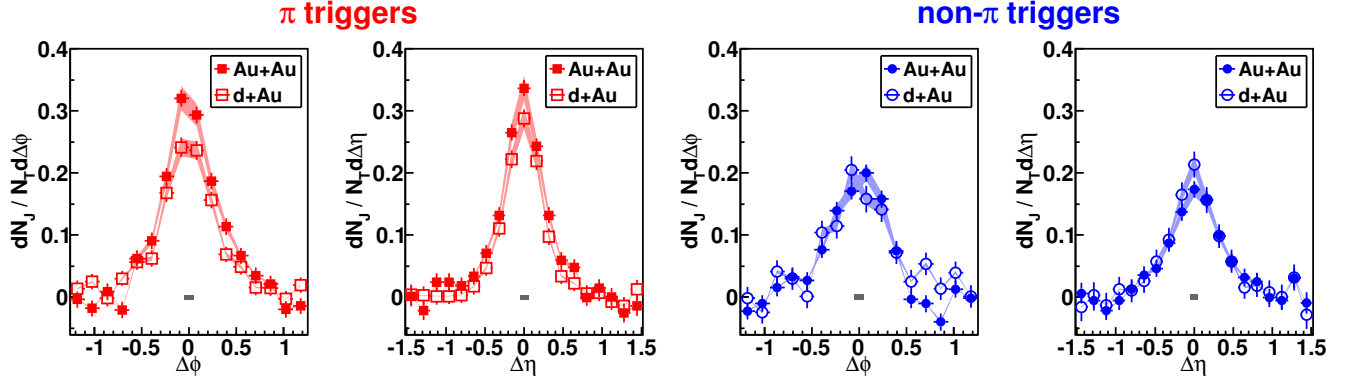


FIG. 29 Figure from STAR (Adamczyk *et al.*, 2015). The $\Delta\phi$ and $\Delta\eta$ projections of the correlation for $|\Delta\eta| < 0.78$ and $|\Delta\phi| < \pi/4$, respectively, for pion triggers (left two panels) and non-pion triggers (right two panels). Filled symbols show data from the 0-10% most central Au+Au collisions at $\sqrt{s_{\text{NN}}} = 200 \text{ GeV}$. Open symbols show data from minimum bias d+Au data at $\sqrt{s_{\text{NN}}} = 200 \text{ GeV}$. This figure shows that the yield is higher for pion trigger particles than non-pion trigger particles, which are mostly kaons and protons, and that there is a higher yield for pion trigger particles in central Au+Au collisions than in d+Au collisions. This may be an indication of differences in partonic energy loss for quarks and gluons in the medium.

2870 ies observe differences, at least some of these effects are 2877
 2871 present in the data, however, the data cannot distinguish 2878
 2872 which effects are present.

2873 4. Jet-hadron correlations

2874 Measurements of jet-hadron correlations are sensitive 2884
 2875 to the broadening and softening of the fragmentation 2885
 2876 function, but have the advantage over dihadron correla- 2886

tions that the jet will be more closely correlated with the
 kinematics of its parent parton than a high p_T hadron.
 2879 Figure 30 shows jet-hadron correlations measured by
 2880 CMS (Khachatryan *et al.*, 2016a) as a function of $\Delta\eta$
 2881 from the trigger jet. Not shown here are the results as
 2882 a function of $\Delta\phi$ from the trigger jet, however the con-
 2883 clusions were quantitatively the same. The jets in this
 sample had a resolution parameter of $R = 0.3$ and a lead-
 ing jet $p_T > 120 \text{ GeV}/c$ in order to reduce the effect of the
 background on the trigger jet sample. The background

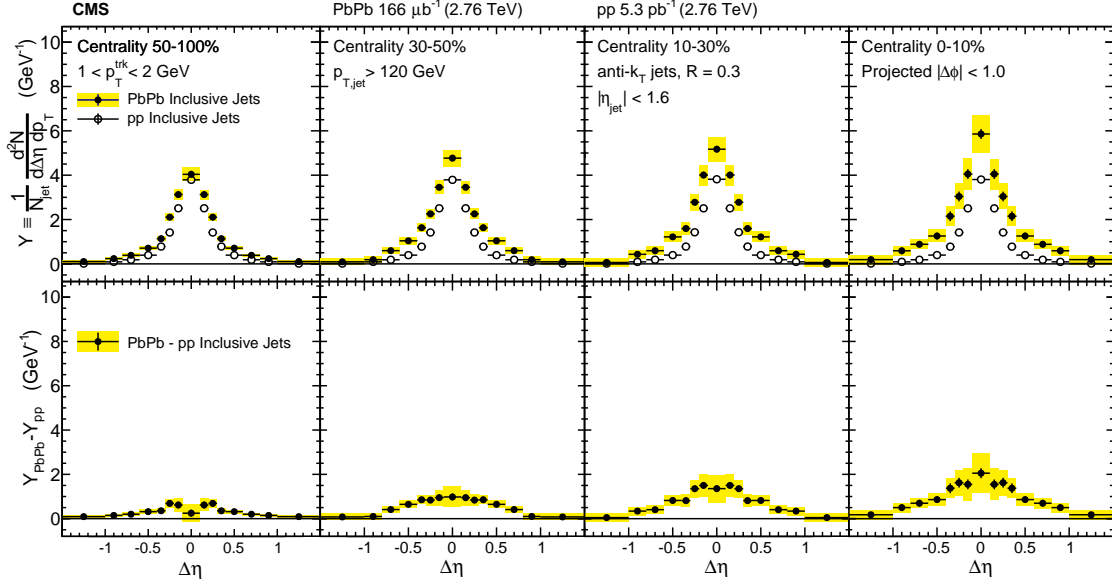


FIG. 30 Figure from CMS (Khachatryan *et al.*, 2016a). Symmetrized $\Delta\eta$ distributions correlated with Pb+Pb and $p+p$ inclusive jets with $p_T > 120$ GeV are shown in the top panels for tracks with $1 < p_T < 2$ GeV. The difference between per-jet yields in Pb+Pb and $p+p$ collisions is shown in the bottom panels. These measurements indicate that the jet is broadened and softened, as expected from energy loss models.

removal for the jets reconstructed in Pb+Pb was done via the HF/Voronoi method, which is described in (CMS, 2013), a slightly different method than described in Section II. The effect of the combinatorial background on the distribution of associated tracks was removed by a sideband method, in which the background is approximated by the measured two dimensional correlations in the range $1.5 < |\Delta\eta| < 3.0$. Jets in Pb+Pb are observed to be broader, with the greatest increase in the width for low momentum associated particles. This is consistent with expectations from partonic energy loss. These studies found that the subleading jet was broadened even more than the leading jet, indicating a bias towards selecting less modified jets as the leading jet.

Jet hadron correlations have also been studied at RHIC energies, where the width and yield of the away-side peak, rather than the associated particle correlations themselves, can be seen in Figure 31. This figure shows the away-side widths and

$$D_{AA} = Y_{Au+Au} \langle p_T^{assoc} \rangle_{Au+Au} - Y_{p+p} \langle p_T^{assoc} \rangle_{p+p} \quad (13)$$

where Y_{Au+Au} and Y_{p+p} are the number of particles the away-side from (Adamczyk *et al.*, 2014a) for two different ranges of jet p_T . The width in $p+p$ is consistent with that in Au+Au within uncertainties, although the uncertainties are large due to the large uncertainties in the v_n . The D_{AA} shows that momentum is redistributed within the jet, with suppression ($D_{AA} < 0$) for $p_T < 2$ GeV/c associated particles and enhancement ($D_{AA} > 0$) for > 2 GeV/c. This indicates that the suppression at

high momenta was balanced by the enhancement at low momenta, which means that this change in the jet structure likely comes from modification of the jet rather than modifications of the jet spectrum. This enhancement at low p_T is at the same associated momentum for both jet energies, which may indicate that the enhancement is not dependent on the energy of the jet but the momentum of the constituents.

5. Dijets

The LHC A_J measurements shown in Figure 16 show a significant energy imbalance for dijets due to medium effects in central collisions (Aad *et al.*, 2010; Chatrchyan *et al.*, 2011b) while RHIC A_J measurements suggest that energy imbalance observed for jet cones of $R=0.2$ can be recovered within a jet cone of $R=0.4$ for measurable dijet events (Adamczyk *et al.*, 2017b). The STAR measurements demonstrate that the energy imbalance is recovered when including low p_T constituents (Adamczyk *et al.*, 2017b), also indicating a softening of the fragmentation function. Comparing these two results is complicated since they have very different surface biases, both due to the experimental techniques and the different collision energies. In order to interpret such comparisons and draw definitive conclusions a robust Monte Carlo generator is required because the differences in these observables are not analytically calculable. To develop a better picture of the transverse structure of the jets, it

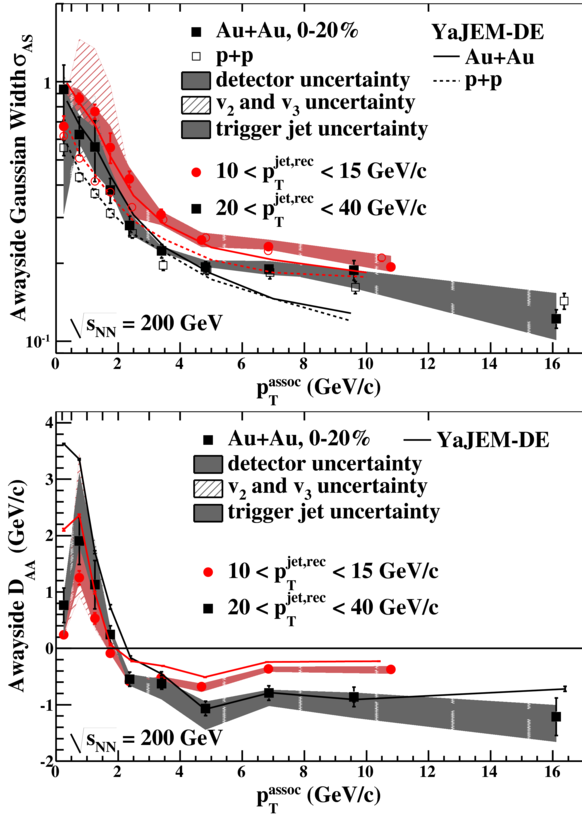


FIG. 31 Figure from STAR (Adamczyk *et al.*, 2014a). Gaussian widths of the away-side peaks (σ_{AS}) for $p+p$ collisions (open squares) and central Au+Au collisions (solid squares) (upper) and away-side momentum difference D_{AA} as defined in Equation 13 (lower) are both plotted as a function of p_T^a . The widths (note the log scale on the y-axis) show no evidence of broadening in Au+Au relative to $p+p$ due to the large uncertainties in the Au+Au measurement. However, D_{AA} shows the suppression of high momentum particles associated with the jet is balanced by the enhancement of lower momentum associated particles. The point at which enhancement transitions to suppression appears to occur at the same associated particle's momentum and does not depend on the jet momentum. Data are for $\sqrt{s_{NN}} = 200$ GeV collisions and YaJEM-DE model calculations are from (Renk, 2013b).

is best to measure observables specifically designed to probe the transverse direction.

The effect on dijets along the direction transverse to the jet axis was studied by measuring the angular difference between the reconstructed jet axis of the leading and sub-leading jets (Aad *et al.*, 2010; Chatrchyan *et al.*, 2011b). These results are shown in Figure 16 and little change to the angular deflection of the sub-leading jet in central Pb+Pb collisions compared to $p+p$ collisions is observed. It is important to point out that the tails in the $p+p$ distribution may be due to 3-jet events while those pairs in Pb+Pb events are the results of dijets undergoing energy loss.

6. Jet Shapes

Another observable that is related to the structure of the jet is the called the jet shape. This observable is constructed with the idea that the high energy jets we are interested in are roughly conical. First a jet finding algorithm is run to determine the axis of the jet, and then the sum of the transverse momentum of the tracks in concentric rings about the jet axis are summed together (and divided by the total transverse jet momentum). The differential jet shape observable $\rho(r)$ is thus the radial distribution of the transverse momentum:

$$\rho(r) = \frac{1}{\delta r} \frac{1}{N_{jet}} \sum_{jets} \frac{\sum_{tracks \in [r_a, r_b]} p_T^{track}}{p_T^{jet}} \quad (14)$$

where the jet cone is divided rings of width δr which have an inner radius r_a and an outer radius r_b .

The differential and integrated jet shape measurements measured by CMS are shown in Figure 32. For this CMS study, inclusive jets with $p_T > 100$ GeV/c, resolution parameter $R = 0.3$ and constituent tracks with $p_T > 1$ GeV/c were used. The effect of the background on the signal jets was removed through the iterative subtraction technique described in Section II. The associated tracks were not explicitly required to be the constituent tracks, however given that the momentum selection criteria is the same and the conical nature of jets at this energy, they will essentially be the same. The effect of the background on the distribution of the associated particles was removed via an η reflection method, where the analysis was repeated for an $R = 0.3$ cone with the opposite sign η but same ϕ . This preserves the flow effects in a model independent way in the determination of the background. The differential jet shapes in the most central Pb+Pb collisions are broadened in comparison to measurements done in $p+p$ collisions at the same center of mass energy (Chatrchyan *et al.*, 2013a). As shown in other measurements, the effect is centrality dependent. These measurements demonstrate that there is an enhancement in the modification with increasing angle from the jet axis, indicating a broadening of the jet profile and a depletion near $r \approx 0.2$.

7. Particle composition

Theory predicts higher production of baryons and strange particles in jets fragmenting in the medium relative to jets fragmenting in the vacuum (Sapeta and Wiedemann, 2008). The only published study searching for modified particle composition in jets in heavy ion collisions is the Λ/K_S^0 ratio in the near-side jet-like correlation of dihadron correlations in Cu+Cu collisions at $\sqrt{s_{NN}} = 200$ GeV by STAR (Abelev *et al.*, 2016) shown in Figure 33. This measurement indicated that particle

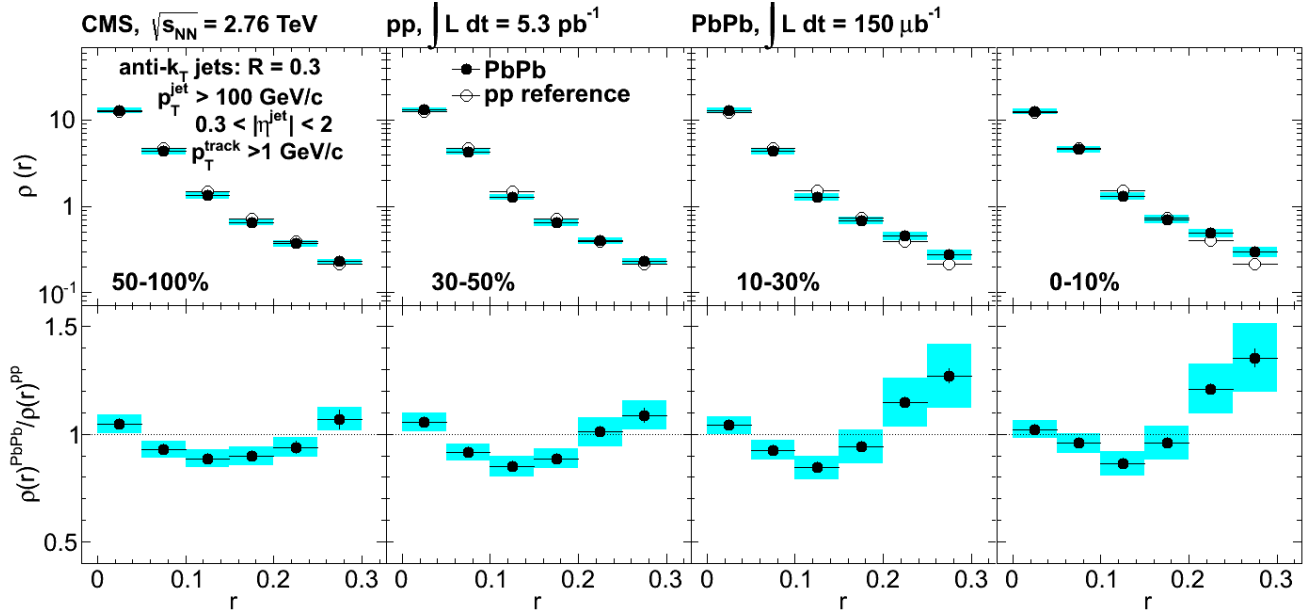


FIG. 32 Figure from CMS (Chatrchyan *et al.*, 2013a). Differential jet shapes in Pb+Pb and $p+p$ collisions for four Pb+Pb centralities. Each spectrum is normalized so that its integral is unity. This shows that there are more particles in jets in central collisions and these modifications are primarily at large angles relative to the jet axis, as expected from partonic energy loss.

2988 ratios in the near-side jet-like correlation are compara- 3014
 2989 ble to the inclusive particle ratios in $p+p$ collisions. At
 2990 high momenta, the inclusive particle ratios in $p+p$ colli-
 2991 sions are expected to be dominated by jet fragmentation
 2992 and therefore are a good proxy for direct observation of
 2993 the particle ratios in reconstructed jets. PYTHIA stud-
 2994 ies show that the inclusive particle ratios in $p+p$ colli-
 2995 sions are approximately the same as the particle ratios
 2996 in dihadron correlations with similar kinematic cuts; 3015
 2997 differences are well below the uncertainties on the exper- 3016
 2998 imental measurements. The consistency between the 3017
 2999 Λ/K_S^0 ratio in the jet-like correlation in Cu+Cu collisions 3018
 3000 and the inclusive ratio in $p+p$ collisions is therefore in- 3019
 3001 terpreted as evidence that the particle ratios in jets are 3020
 3002 the same in $A+A$ collisions and $p+p$ collisions, that at 3021
 3003 least the particle ratios are not modified. In contrast, the 3022
 3004 inclusive Λ/K_S^0 reaches a maximum near 1.6 (Agakishiev 3023
 3005 *et al.*, 2012b), a few times that in $p+p$ collisions. Prelim- 3024
 3006 inary measurements from both the STAR dihadron correla- 3025
 3007 tions (Suarez, 2012) and ALICE collaborations from 3026
 3008 both dihadron correlations (Veldhoen, 2013) and recon- 3027
 3009 structed jets (Kucera, 2016; Zimmermann, 2015) support 3028
 3010 this conclusion. However, experimental uncertainties are 3029
 3011 large and for studies in dihadron correlations, results are 3030
 3012 not available for the away-side and the near-side is known 3031
 3013 to be surface biased.

8. LeSub

One of the new observables constructed in order to attempt to create well defined QCD observables is LeSub, defined as:

$$\text{LeSub} = p_T^{\text{lead,track}} - p_T^{\text{sublead,track}} \quad (15)$$

LeSub characterizes the hardest splitting, so it should be insensitive to background, however, it is not collinear safe and therefore cannot be calculated reliably in pQCD. It agrees well with PYTHIA simulations of $p+p$ collisions and is relatively insensitive to the PYTHIA tune (Cunqueiro, 2016), which is not surprising as the hardest splittings in PYTHIA do not depend on the tune. LeSub calculated in PYTHIA agrees well with the data from Pb+Pb collisions for $R = 0.2$ charged jets. This indicates that the hardest splittings are likely unaffected by the medium. Modifications may depend on the jet momentum, as the ALICE results are for relatively low momentum jets at the LHC. The ALICE measurement is also for relatively small jets, which preferentially selects more collimated fragmentation patterns, but it indicates that observables that depend on the first splittings are insensitive to the medium.

9. Jet Mass

In a hard scattering the partons are produced off-shell, and the amount they are off-shell is the virtuality (Ma-

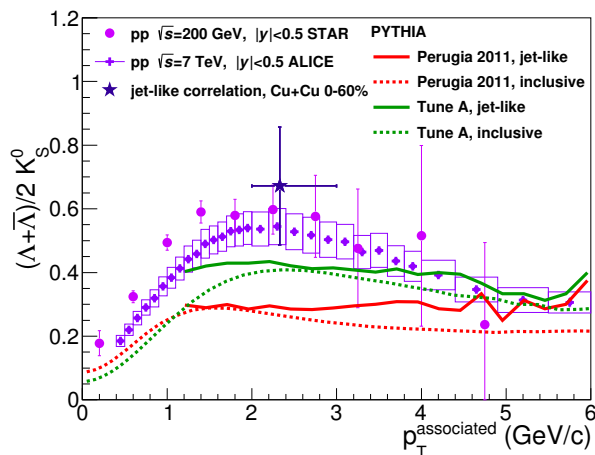


FIG. 33 Figure from STAR (Abelev *et al.*, 2016). Λ/K_S^0 ratio measured in jet-like correlations in 0-60% Cu+Cu collisions at $\sqrt{s_{NN}} = 200$ GeV for $3 < p_T^{\text{trigger}} < 6$ GeV/c and $2 < p_T^{\text{associated}} < 3$ GeV/c along with this ratio obtained from inclusive p_T spectra in $p+p$ collisions. Data are compared to calculations from PYTHIA (Sjostrand *et al.*, 2006) using the Perugia 2011 tunes (Skands, 2010) and Tune A (Field and Group, 2005). This shows that, within the large uncertainties, there is no indication that the particle composition of jets is modified in $A+A$ collisions, where Λ/K_S^0 reaches a maximum of 1.6 (Agakishiev *et al.*, 2012b).

3035 junder and Putschke, 2016). When a jet showers in vacu-
 3036 uum, at each splitting the virtuality is reduced and mo-
 3037 mentum is produced transverse to the original scattered
 3038 parton's direction, until the partons are on-shell and thus
 3039 hadronize. For a vacuum jet, if the four vectors of all of
 3040 the daughters from the original parton are combined, the
 3041 mass calculated from the combination of the daughters
 3042 would be precisely equal to the virtuality. The virtual-
 3043 ity of hard scattered parton is important as it is directly
 3044 related to how broad the jet itself is, as it is directly re-
 3045 lated to how much momentum transverse to the jet axis
 3046 the daughters can have.

3047 The mass of a jet might serve as a way to better char-
 3048 acterize the state of the initial parton. It is important to
 3049 construct observables where the only difference between
 3050 $p+p$ collisions compared to heavy ion collisions is due to
 3051 the effects of jet quenching, and not the result of biases
 3052 in the jet selection. Jet mass may make a much closer
 3053 comparison between heavy ion and $p+p$ observables by
 3054 selecting more similar populations of parent partons than
 3055 could be achieved by selecting differentially in transverse
 3056 momentum alone. Secondly, the measured jet mass itself
 3057 could be affected by in-medium interactions as the vir-
 3058 tuality of the jet can increase for a given splitting due to
 3059 the medium interaction, unlike in the vacuum case.

3060 Figure 34 shows the ALICE (Acharya *et al.*, 2017) jet
 3061 mass measurement of charged jets for most central colli-
 3062 sions. No difference is observed between PYTHIA Peru-

3063 gia 2011 tune (Skands, 2010) and data from Pb+Pb col-
 3064 lisions in all jet p_T bins indicating no apparent modifica-
 3065 tion within uncertainties. In addition to PYTHIA, these
 3066 distributions were compared to three different quenching
 3067 models, JEWEL (Zapp, 2014a) with recoil on, JEWEL
 3068 with recoil off, and Q-PYTHIA (Armento *et al.*, 2009).
 3069 Both Q-PYTHIA and JEWEL with the recoil on pro-
 3070 duced jets with a larger mass distribution than in the
 3071 data, whereas JEWEL with the recoil off gives a slightly
 3072 lower value than the data. This implies that jet mass
 3073 as a distribution in these energy and momentum ranges
 3074 is rather insensitive to medium effects, as JEWEL and
 3075 Q-PYTHIA both incorporate medium effects whereas
 3076 PYTHIA describes vacuum jets. The agreement between
 3077 PYTHIA and data could also indicate that the jets se-
 3078 lected in this analysis were biased towards those that
 3079 fragmented in a vacuum-like manner. More differential
 3080 measurements of jet mass are needed to determine the
 3081 usefulness of jet mass variable.

3082 10. Dispersion

3083 Since quark jets have harder fragmentation functions,
 3084 they are more likely to produce jets with hard con-
 3085 stituents that carry a significant fraction of the jet energy.
 3086 This can be studied with $p_T^D = \sqrt{\sum_i p_{T,i}^2} / \sum_i p_{T,i}$. This
 3087 observable was initially developed in order to distinguish
 3088 between quark and gluon jets with quark jets yielding a
 3089 larger mean p_T^D (Collaboration, 2013a). The ALICE ex-
 3090 periment has measured p_T^D in Pb+Pb collisions, shown
 3091 in Figure 35. The data from Pb+Pb collisions for $R =$
 3092 0.2 charged jets with transverse momentum between 40
 3093 and 60 GeV is compared to data from PYTHIA with the
 3094 Perugia 11 tune. In Pb+Pb collisions, the mean p_T^D was
 3095 found to be larger compared to the PYTHIA reference,
 3096 which had been validated by comparisons with $p+p$ data.
 3097 This may indicate either a selection bias towards quark
 3098 jets or harder fragmenting jets.

3099 11. Girth

The jet girth is another new observable describing the
 shape of a jet. The jet girth, g , is the p_T weighted width
 of the jet

$$g = \sum_i \frac{p_T^i}{p_T^{\text{jet}}} |r_i|, \quad (16)$$

where r_i is the angular distance between particle i and
 the jet axis. If jets are broadened by the medium, we
 would expect that g would be increased, and the con-
 verse would be that if jets were collimated than g would
 be reduced. While the distributions overlap, the gluon
 jets are broader and have a higher average g than quark

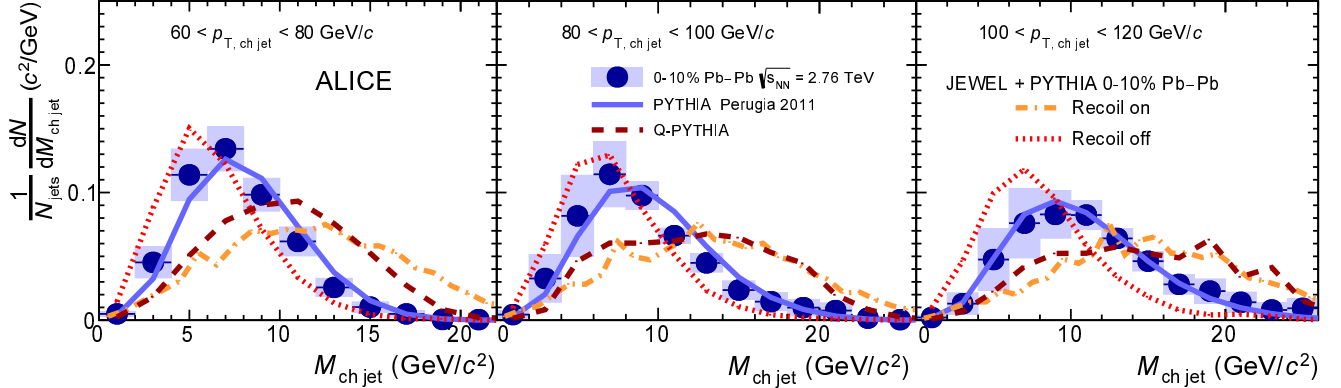


FIG. 34 Figure from ALICE (Acharya *et al.*, 2017). Fully-corrected jet mass distribution for anti- k_T jets with $R=0.4$ in the 10% most central Pb+Pb collisions compared to PYTHIA (Sjostrand *et al.*, 2006) with the Perugia 2011 tune (Skands, 2010) and predictions from the jet quenching event generators JEWEL (Zapp, 2014a) and Q-PYTHIA (Armesto *et al.*, 2009). No difference is observed between PYTHIA and the data. This shows that there is no modification of the jet mass within uncertainties.

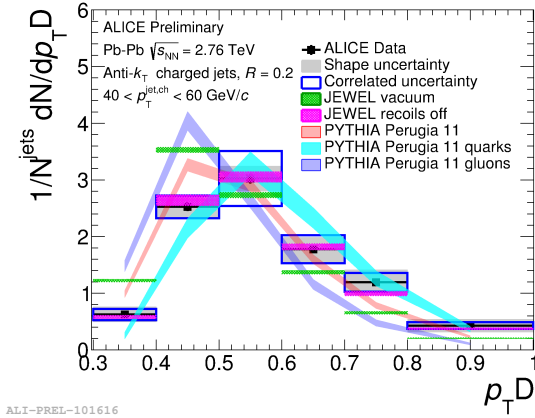


FIG. 35 Figure from ALICE (Cunqueiro, 2016). Unfolded p_T^D shape distribution in Pb+Pb collisions for $R=0.2$ charged jets with momenta between 40 and 60 GeV/c compared to PYTHIA simulations, to JEWEL calculations, and to q/g PYTHIA templates. This shows that the dispersion is larger in Pb+Pb collisions than in $p+p$ collisions. This may indicate either modifications or a quark bias.

3117 Figure 36. JEWEL includes partonic energy loss and
 3118 predicts little modification of the girth in heavy ion colli-
 3119 sions. PYTHIA calculations include inclusive jets, quark
 3120 jets, and gluon jets. The data are closest to PYTHIA
 3121 predictions for quark jets. This may be due to bias to-
 3122 wards quarks in surviving jets in Pb+Pb collisions.

3123 One of the unanswered questions regarding jets in
 3124 heavy ion collisions is whether jets start to fragment
 3125 while they are in the medium, or whether they simply
 3126 lose energy to the medium and then fragment similar to
 3127 fragmentation in vacuum after reaching the surface. If
 3128 the latter is true, jet quenching would be described as
 3129 a shift in parton p_T followed by vacuum fragmentation,
 3130 which would mean that jets shapes in Pb+Pb collisions
 3131 would be consistent with jet shapes in $p+p$ collisions. If g
 3132 is shifted, this would favor fragmentation in the medium
 3133 and if it is not, it would favor vacuum fragmentation.
 3134 These observations are qualitatively consistent with the
 3135 measurements of p_T^D discussed in Section III.C.6 and the
 3136 jet shape discussed in Section III.C.6.

3137 12. Grooming

3106 jets. The ALICE experiment has shown that distribu- 3138
 3107 tions of g in $p+p$ collisions agree well with PYTHIA dis- 3139
 3108 tributions, indicating that it is a reasonable probe and 3140
 3109 that PYTHIA can be used as a reference. In Pb+Pb col- 3141
 3110 lisions, the ALICE experiment found that g is slightly 3142
 3111 shifted towards smaller values compared to the PYTHIA 3143
 3112 reference for $R = 0.2$ charged jets (Cunqueiro, 2016), 3144
 3113 although the significance of this shift is unclear. This in- 3145
 3114 dicates that the core may appear to be more collimated 3146
 3115 in Pb+Pb collisions than $p+p$ collisions. Measurements 3147
 3116 are compared to JEWEL and PYTHIA calculations in 3148

Jet grooming algorithms (Butterworth *et al.*, 2008; Dasgupta *et al.*, 2013; Ellis *et al.*, 2010; Krohn *et al.*, 2010) attempt to remove soft radiation from the leading partonic components of the jet, isolating the larger scale structure. The motivation for algorithms such as jet grooming was to develop observables which can be calculated with perturbative QCD, and which are relatively insensitive to the details of the soft background. This allows us to determine whether the medium affects the jet formation process from the hard process through hadronization, or whether the parton loses energy to the

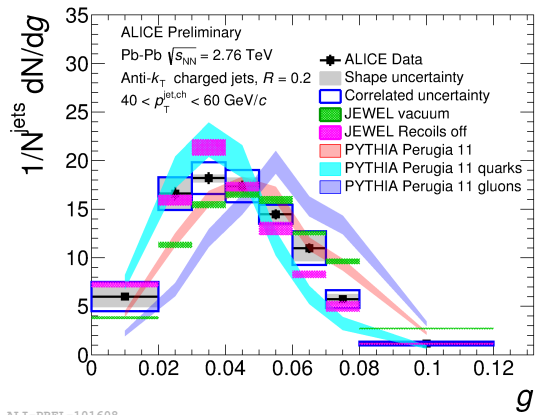


FIG. 36 Figure from ALICE (Cunquero, 2016). The girth g for $R=0.2$ charged jets in Pb+Pb collisions with jet p_T^{ch} between 40 and 60 GeV/c compared to a PYTHIA simulations, to JEWEL calculations, and to q/g PYTHIA templates. This shows that jets are somewhat more collimated in Pb+Pb collisions than in $p+p$ collisions. This may indicate a quark bias in surviving jets in Pb+Pb collisions.

medium with fragmentation only affected at much later stages. It is important to realize that the answers to these questions will depend on the jet energy and momentum, so there will not be a single definitive answer. Jet grooming allows separation of effects of the length scale from effects of the hardness of the interaction. Essentially this will allow us to see whether we are scattering off of point-like particles in the medium or scattering off of something with structure. However, to properly apply this class of algorithms to the data, a precision detector is needed.

The jet grooming algorithm takes the constituents of a jet, and recursively declusters the jet's branching history and discards the resulting subjets until the transverse momenta, $p_{T,1}, p_{T,2}$, of the current pair fulfills the soft drop condition (Larkoski *et al.*, 2014):

$$\frac{\min(p_{T,1}, p_{T,2})}{p_{T,1} + p_{T,2}} > z_{cut} \theta^\beta \quad (17)$$

where θ is an additional measure of the relative angular distance between the two sub-jets and z_{cut} and θ^β are parameters which can select how strict the soft drop condition is. For the heavy-ion analyses conducted so far, β has been set to zero and z_{cut} has been set to 0.1.

A measurement of the first splitting of a parton in heavy ion collisions is performed by the CMS collaboration in Pb+Pb collisions at $\sqrt{s_{NN}} = 5$ TeV. The splitting function is defined as $z_g = p_{T2}/(p_{T1} + p_{T2})$ with p_{T2} indicating the transverse momentum of the least energetic subjet and p_{T1} the transverse momentum of the most energetic subjet, applied to those jets that passed the soft drop condition outlined above. Figure 37 shows the ratio of z_g in Pb+Pb to that in $p+p$ from CMS for several cen-

trality intervals for jets within the transverse momentum range of 160–180 GeV/c (Sirunyan *et al.*, 2017a). While the measured z_g distribution in peripheral Pb+Pb collisions is in agreement with the expected $p+p$ measurement within uncertainties, a difference becomes apparent in the more central collisions. This observation indicates that the splitting into two branches becomes increasingly more unbalanced for more central collisions for the jets within the transverse momentum range of 160–180 GeV/c. A similar preliminary measurement by STAR observes no modification in z_g (Kauder, 2017). The apparent modifications seen by CMS were proposed to be due to a restriction to subjets with a minimum separation between the two hardest subjets $R_{12} > 0.1$ (Milhano, 2017). This indicates that there may be modifications of z_g limited to certain classes of jets but not observed globally. This dependence of modifications on jets may be a result of interactions with the medium (Milhano *et al.*, 2017). While grooming and measurements of the jet substructure are promising, we emphasize the need for a greater understanding of the impact of the large combinatorial background and the bias of kinematic cuts on z_g .

13. Subjettiness

The observable τ_N is a measure of how many hard cores there are in a jet. This was initially developed to tag jets from Higgs decays in high energy $p+p$ collisions. A jet from a single parton usually has one hard core, but a hard splitting or a bremsstrahlung gluon would lead to an additional hard core within the jet. An increase in the fraction of jets with two hard cores could therefore be evidence of gluon bremsstrahlung.

The jet is clustered into N subjets, and the following calculation is performed over each track in the jet:

$$\tau_N = \frac{\sum_{i=1}^M (p_T^i \min(\Delta R_{1,i}, \Delta R_{2,i}, \dots, \Delta R_{N,i}))}{R_0 \sum_{i=1}^N p_T^i} \quad (18)$$

where $\Delta R_{N,i}$ is the distance in $\eta-\phi$ between the i th track and the axis of the N th subjet and the original jet has resolution parameter R_0 . In the case that all particles are aligned exactly with one of the subjets' axes, τ_N will equal zero. In the case where there are more than N hard cores, a substantial fraction of tracks will be far from the nearest subjet axis, however, all tracks must have $\min(\Delta R_{1,i}, \Delta R_{2,i}, \dots, \Delta R_{N,i}) \leq R_0$ because they are contained within the original jet. The maximum value of τ_N is therefore one, the case when all jet constituents are at the maximum distance from the nearest subjet axis.

Jets that have a low value of τ_N are therefore more likely to have N or fewer well defined cores in their substructure, whereas jets with a high value are more likely to contain at least $N+1$ cores. A shift in the distribution of τ_N in a jet population towards lower values can

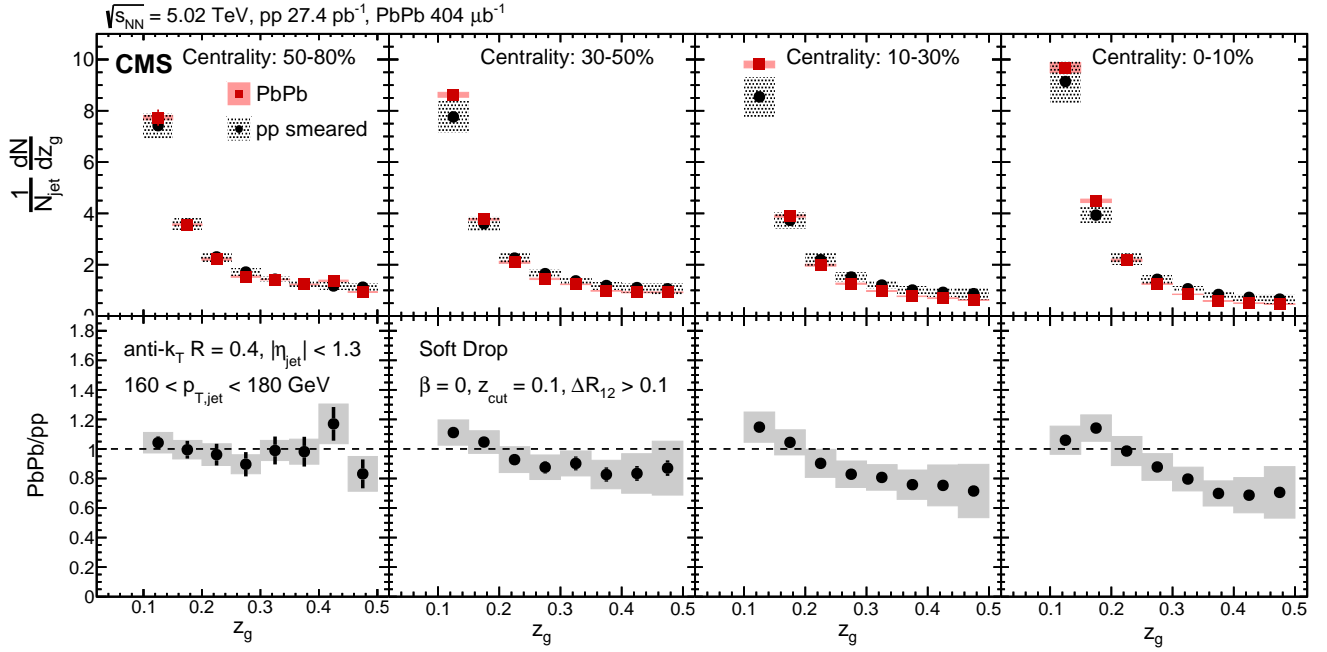


FIG. 37 Figure from CMS (Sirunyan *et al.*, 2017a). Ratio of the splitting function $z_g = p_{T2}/(p_{T1} + p_{T2})$ in Pb+Pb and $p+p$ collisions with the jet energy resolution smeared to match that in Pb+Pb for various centrality selections and $160 < p_{T,jet}^{jet} < 180$ GeV. This shows that the splitting function is modified in central Pb+Pb collisions compared to $p+p$ collisions, which may indicate either a difference in the structure of jets in the two systems or an impact of the background.

3220 indicate fewer subjects while a shift to higher τ_N can indicate
 3221 more subjects. The observable τ_2/τ_1 was constructed
 3222 by the ALICE experiment (Zardoshti, 2017). Similar to
 3223 the approach in (Adam *et al.*, 2015c; Adamczyk *et al.*,
 3224 2017c), background was subtracted using the coincidence
 3225 between a soft trigger hadron, which should have only a
 3226 weak correlation with jet production, and a high momentum
 3227 trigger hadron, and can be seen in Figure 38. A
 3228 jet where this ratio is close to zero most likely has two
 3229 hard cores. This observable is relatively insensitive to
 3230 the fluctuations in the background, as it would have to
 3231 carry a significant fraction of the jet momentum to be
 3232 modified. The ALICE result shows that the structure of
 3233 the jets was unmodified for $R = 0.4$ charged jets with 40
 3234 $\leq p_{t,jet}^{ch} < 60$ GeV/c compared to PYTHIA calculations.
 3235 This implies that medium interactions do not lead to extra
 3236 cores within the jet, at least for selection of jets in
 3237 this measurement. As for many jet observables, this ob-
 3238 servable may be difficult to interpret for low momentum
 3239 jets in a heavy ion environment.

3240 14. Summary of experimental evidence for medium 3241 modification of jets

3242 The broadening and softening of jets due to interac- 3247
 3243 tions with the medium is demonstrated clearly by several 3248
 3244 mature observables which measure the average properties 3249
 3245 of jets. This includes fragmentation functions measured 3250

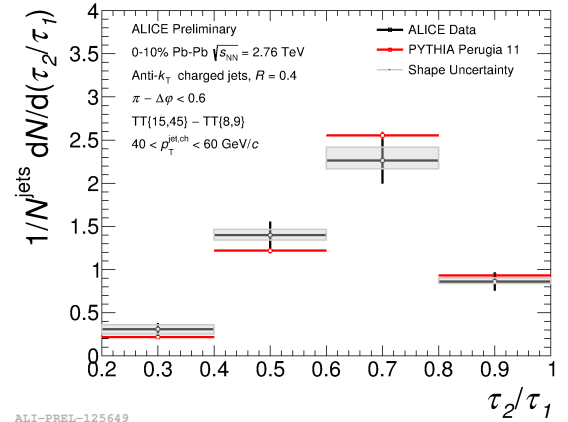


FIG. 38 Figure from (Zardoshti, 2017). τ_2/τ_1 fully corrected recoil $R=0.4$ jet shape in 0-10% Pb+Pb collisions at $40 \leq p_{t,jet}^{ch} < 60$ GeV/c. This shows that, at least for this kinematic selection, the subjettness is not modified. The trigger tracks are 8–9 GeV/c for the background dominated region and 15–45 GeV/c for the signal dominated region.

3246 with both jets and bosons, widths of dihadron correla-
 3247 tions, jet-hadron correlations, and measurements of the
 3248 jet shape. On average, no change in the particle compo-
 3249 sition of jets in heavy ion collisions as compared to $p+p$
 3250 collisions is observed. There are some indications from

dihadron correlations that quark and gluon jets do not interact with the medium in the same way. These observables generally preferentially select quark jets over gluon jets, even in $p+p$ collisions. Some of the observables have a strong survivor bias due to the kinematic cuts that are applied in order to reduce the combinatorial background.

As our understanding of partonic energy loss has improved, the community has sought more differential observables. This is motivated in part by an increased understanding of the importance of fluctuations – while the average properties of jets are smooth, individual jets are lumpy, and by a desire to construct well defined QCD observables. These new observables give us access to differential properties of jets, such as allowing distinction between quark and gluon jets, and therefore may be more sensitive to the properties of the medium. Since the exploration of these observables is in its early stages, it is unclear whether we fully understand the impact of the background or kinematic cuts applied to the analyses. It is therefore unclear in practice how much additional information these observables can provide about the medium, without applying the observables to Monte Carlo events with different jet quenching models. We encourage cautious optimism and more detailed studies of these observables.

For future studies to maximize our understanding of the medium by the Jetscape collaboration using a Bayesian analysis, we propose first to produce comparisons between dihadron correlations, jet-hadron correlations, and γ -hadron correlations to insure that the models have properly accounted for the path length dependence, initial state effects and the basics of fragmentation and hadronization. We do not list R_{AA} here as it is likely that this observable will be used to tune some aspects of the model, as it has been used in the past. For the most promising jet quenching models, we would propose that these studies would be followed by comparisons of observables that depend more heavily on the details of the fragmentation, but are still based on the average distribution such as jet shapes, fragmentation functions, and particle composition. Finally, it would be useful to see the comparison of z_g to models. We urge that initial investigations of the latter happen early so that the background effect can be quantified.

We note that the same analysis techniques and selection criteria must be used for analyses of the experiment and of the models in order for the comparisons to be valid. This is particularly true for studies using reconstructed jets where experimental criteria to remove the effects of the background can bias the sample of jets used in construction of the observables. We omit A_J from consideration because nearly any reasonable model gives a reasonable value, thus it is not particularly differential. We also omit heavy flavor jets because current data do not give much insight into modifications of fragmentation, and it is not clear whether it will be possible exper-

imentally to measure jets with a low enough p_T that the mass difference between heavy and light quarks is relevant. Inclusion of new observables into these studies may increase the precision with which medium properties can be constrained, but it is critical to replicate the exact analysis techniques.

In order to compare experimental data, or to compare experimental data with theory, not only is it necessary for the analyses to be conducted the same way as it is stated above, but they should be on the same footing. Thus comparing unfolded results to uncorrected results is not useful. In general, we urge extreme caution in interpreting uncorrected results, especially for observables created with reconstructed jets. Since it is unclear how much the process of unfolding may bias the results, an important check would be to compare the raw results with the folded theory. However, this requires complete documentation of the raw results and the response matrix on the experimental side, and requires a complete treatment of the initial state, background, and hadronization on the theory side. This comparison, which we could think of as something like a closure test, would still require that the same jet finding algorithms with the same kinematic selections are applied to the model.

D. Influence of the jet on the medium

The preceding sections have demonstrated that hard partons lose energy to the medium, most likely through gluon bremsstrahlung and collisional energy loss. Often an emitted gluon will remain correlated with the parent parton so that the fragments of both partons are spatially correlated over relatively short ranges ($R = \sqrt{\Delta\phi^2 + \Delta\eta^2} \lesssim 0.5$). Hadrons produced from the gluon may fall inside or outside the jet cone of the parent parton, depending on the jet resolution parameter. Whether or not this energy is then reconstructed experimentally as part of the jet depends on the resolution parameter and the reconstruction algorithm. For sufficiently large resolution parameters, the “lost” energy will still fall within the jet cone, so that the total energy clustered into the jet would remain the same. “Jet quenching” is then manifested as a softening and broadening of the structure of the jet. The evidence for these effects was discussed in the previous section.

If, however, a parton loses energy and that energy interacts with or becomes equilibrated in the medium, it may no longer have short range spatial correlations with the parent parton. This energy would then be distributed at distances far from the jet cone. Alternately, the energy may have very different spatial correlations with the parent parton so that it no longer looks like a jet formed in a vacuum, and a jet finding algorithm may no longer group that energy with the jet that contains most of the energy of its parent parton. Evidence for these effects is

difficult to find, both because of the large and fluctuating background contribution from the underlying event, and because it is unclear how this energy would be different from the underlying event. We discuss both the existing evidence that there may be some energy which reaches equilibrium with the medium, and the ridge and the Mach cone, which are now understood to be features of the medium rather than indications of interactions of hard partons with the medium. We also discuss searches for direct evidence of Molière scattering off of partons in the medium.

1. Evidence for out-of-cone radiation

The dijet asymmetry measurements demonstrate momentum imbalance for dijets in central heavy ion collisions, implying energy loss, but do not describe where that energy goes. To investigate this, CMS looked at the distribution of momentum parallel to the axis of a high momentum leading jet in three regions (Chatrchyan *et al.*, 2011b), shown schematically in Figure 39. The jet reconstruction used in this analysis was an iterative cone algorithm with a modification to subtract the soft underlying event on an event-by-event basis, the details of which can be found in (Kodolova *et al.*, 2007). Each jet was selected with a radius $R = 0.5$ around a seed of minimum transverse energy of 1 GeV. Since energy can be deposited outside $R > 0.5$ even in the absence of medium effects and medium effects are expected to broaden the jet, the momenta of all particles within in a slightly larger region, $R < 0.8$, were summed, regardless of whether or not the particles were jet constituents or subtracted as background. This region is called in-cone and the region $R > 0.8$ is called out-of-cone.

CMS investigated these different regions of the events with a measurement of the projection of the p_T of reconstructed charged tracks onto the leading jet axis. For each event, this projection was calculated as

$$\mathcal{P}_T^{\parallel} = \sum_i -p_T^i \cos(\phi_i - \phi_{\text{Leading Jet}}), \quad (19)$$

where the sum is over all tracks with $p_T > 0.5$ GeV/c. These results were then averaged over events to obtain $\langle \mathcal{P}_T^{\parallel} \rangle$. This momentum imbalance in-cone and out-of-cone as a function of A_J , shown as black points in Figure 40. The momentum parallel to the jet axis in-cone is large, but should be balanced by the partner jet 180° away in the absence of medium effects. A large A_J indicates substantial energy loss for the away-side jet, while a small A_J indicates little interaction with the medium. This shows that the total momentum in the event is indeed balanced. For small A_J , the $\langle \mathcal{P}_T^{\parallel} \rangle$ in the in-cone and out-of-cone regions is within zero as expected for balanced jets. For large A_J , the momentum in-cone is non-zero, balanced by the momentum out-of-cone. These events

were compared to PYTHIA+HYDJET simulations in order to understand which effects were simply due to the presence of a fluctuating background and which were due to jet quenching effects. In both the central Pb+Pb data and the Monte Carlo, an imbalance in jet A_J also indicated an imbalance in the p_T of particles within the cone of $R = 0.8$ about either the leading or subleading jet axes. To investigate further, CMS added up the momentum contained by particles in different momentum regions. The imbalance in the direction of the leading jet is dominated by particles with $p_T > 8$ GeV/c, but is partially balanced in the subleading direction by particles with momenta below 8 GeV/c. The distributions look very similar in both the data and the Monte Carlo for the in-cone particle distribution. The out-of-cone distributions indicated a slightly different story. For both the data and the Monte Carlo, the missing momentum was balanced by additional, lower momentum particles, in the subleading jet direction. The difference is that in the Pb+Pb data, the balance was achieved by very low momentum particles, between 0.5 and 1 GeV/c. In the Monte Carlo, the balance was achieved by higher momentum particles, mainly above 4 GeV/c, which indicates a different physics mechanism. In the Monte Carlo, the results could be due to semi-hard initial- or final-state radiation, such as three jet events.

The missing transverse momentum analysis was recently extended by examining the multiplicity, angular, and p_T spectra of the particles using different techniques. As above, these results were characterized as a function of the Pb+Pb collision centrality and A_J (Khachatryan *et al.*, 2016c). This extended the results to quite some distance from the jet axes, up to a ΔR of 1.8. The angular pattern of the energy flow in Pb+Pb events was very similar to that seen in $p+p$ collisions, especially when the resolution parameter is small. This indicates that the leading jet could be getting narrower, and/or the subleading jet is getting broader due to quenching effects. For a given range in A_J , the in-cone imbalance in p_T in Pb+Pb collisions is found to be balanced by relatively low transverse momentum out-of-cone particles with $0.5 < p_T < 2$ GeV/c. This was quantitatively different than in $p+p$ collisions where most of the momentum balance comes from particles with p_T between $2 < p_T < 8$ GeV/c. This could indicate a softening of the radiation responsible for the p_T imbalance of dijets in the medium formed in Pb+Pb collisions. In addition, a larger multiplicity of associated particles is seen in Pb+Pb than in $p+p$ collisions. In every case, the difference between $p+p$ and Pb+Pb observations increased for more central Pb+Pb collisions.

However, some caution should be used in interpreting the result as these measurements make assumptions about the background, and require certain jet kinematics, which may limit how robust the conclusions are. It is unlikely that the medium would focus the leading jet

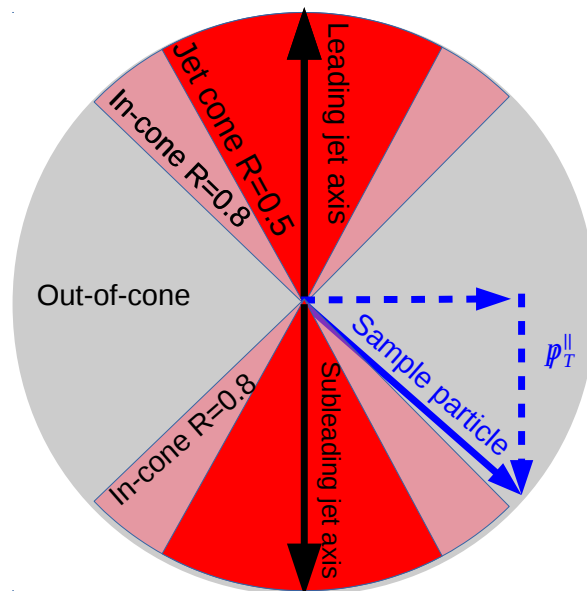


FIG. 39 Schematic diagram showing the definitions used in Figure 40.

3462 so that it would be more collimated, for instance, but
 3463 that a selection bias causes narrower jets to be selected
 3464 in Pb+Pb collisions for a given choice in R and jet kine-
 3465 matics. Additionally, as with any analysis that attempts
 3466 to disentangle the effects of the medium on the jet with
 3467 the jet on the medium, the ambiguity in what is consid-
 3468 ered part of the medium and what is considered part
 3469 of the jet can also complicate the interpretation of this
 3470 result. While the results demonstrate that there is a dif-
 3471 ference in the missing momentum in Pb+Pb and $p+p$
 3472 collisions, in order to identify the mechanism responsi-
 3473 ble, the data would need to be compared to a Monte
 3474 Carlo model that incorporates jet quenching, and pre-
 3475 serves momentum and energy conservation between the
 3476 jet and medium.

3477 2. Searches for Molière scattering

3478 The measurement of jets correlated with hard hadrons
 3479 in (Adam *et al.*, 2015c) was also used to look for broad-
 3480 ening of the correlation function between a high momen-
 3481 tum hadron and jets. Such broadening could result from
 3482 Molière scattering of hard partons off other partons in the
 3483 medium, coherent effects from the scattering of a wave
 3484 off of several scatterers. No such broadening is observed,
 3485 although the measurement is dominated by the statistical
 3486 uncertainties. Similarly, STAR observes no evidence for
 3487 Molière scattering (Adamczyk *et al.*, 2017c). We note
 3488 that this would mainly be sensitive to whether or not
 3489 the jets are deflected rather than whether or not jets are
 3490 broadened.

3491 3. The rise and fall of the Mach cone and the ridge

3492 Several theoretical models proposed that a hard par-
 3493 ton traversing the medium would lose energy similar
 3494 to the loss of energy by a supersonic object traveling
 3495 through the atmosphere (Casalderrey-Solana *et al.*, 2005;
 3496 Renk and Ruppert, 2006; Ruppert and Muller, 2005).
 3497 The energy in this wave forms a conical structure about
 3498 the object called a Mach cone. Early dihadron corre-
 3499 lations studies observed a displaced peak in the away-
 3500 side (Adare *et al.*, 2007b, 2008d; Adler *et al.*, 2006b; Ag-
 3501 garwal *et al.*, 2010). Three-particle correlation studies
 3502 observed that this feature was consistent with expecta-
 3503 tions from a Mach cone (Abelev *et al.*, 2009a). Studies
 3504 indicated that its spectrum was softer than that of the
 3505 jet-like correlation on the near-side (Adare *et al.*, 2008d)
 3506 and its composition similar to the bulk (Afanasiev *et al.*,
 3507 2008), as might be expected from a shock wave from
 3508 a parton moving faster than the speed of light in the
 3509 medium. Curiously, the Mach cone was present only at
 3510 low momenta (Adare *et al.*, 2008a; Aggarwal *et al.*, 2010),
 3511 whereas some theoretical predictions indicated that a
 3512 true Mach cone would be more significant at higher mo-
 3513 menta (Betz *et al.*, 2009).

3514 At the same time, studies of the near-side indicated
 3515 that there was a feature correlated with the trigger par-
 3516 ticle in azimuth but not in pseudorapidity (Abelev *et al.*,
 3517 2009b; Alver *et al.*, 2010), dubbed the ridge. The ridge
 3518 was also observed to be softer than the jet-like correla-
 3519 tion (Abelev *et al.*, 2009b) and to have a particle compo-
 3520 sition similar to the bulk (Bielcikova, 2008; Suarez, 2012).
 3521 Several of the proposed mechanisms for the production of

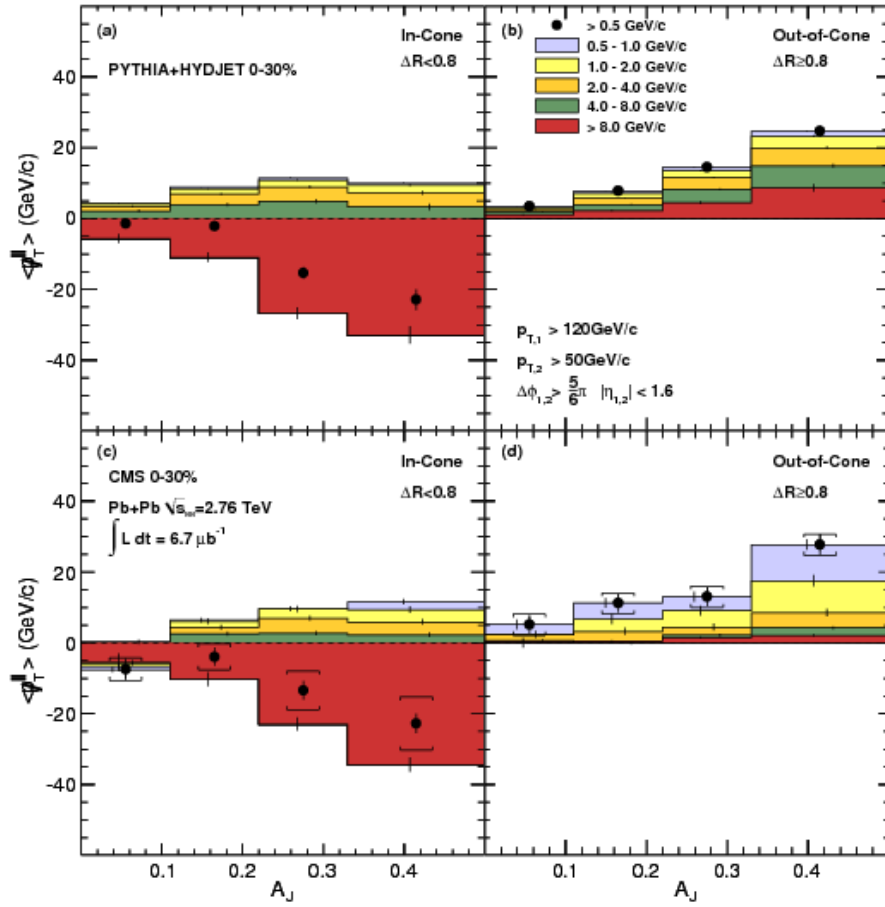


FIG. 40 Figure from CMS (Chatrchyan *et al.*, 2011b). Average missing transverse momentum for tracks with $p_T > 0.5$ GeV/c, projected onto the leading jet axis is shown in solid circles. The average missing p_T values are shown as a function of dijet asymmetry A_J for 0–30% centrality, inside a cone of $\Delta R < 0.8$ of one of the leading or subleading jet cones on the left, and outside ($\Delta R > 0.8$) the leading and subleading jet cones on the right. The solid circles, vertical bars and brackets represent the statistical and systematic uncertainties, respectively. For the individual p_T ranges, the statistical uncertainties are shown as vertical bars. This shows that missing momentum is found outside of the jet cone, indicating that the lost energy may have equilibrated with the medium.

3522 the ridge involved interactions between the hard parton
 3523 and the medium, including collisional energy loss (Wong,
 3524 2007, 2008) and recombination of the hard parton with a
 3525 parton in the medium (Chiu and Hwa, 2009; Chiu *et al.*,
 3526 2008; Hwa and Yang, 2009).

3527 However, the observation of odd v_n in heavy ion col-
 3528 lisions (Aamodt *et al.*, 2011a; Adamczyk *et al.*, 2013;
 3529 Adare *et al.*, 2011b) indicated that the Mach cone and
 3530 the ridge may be an artifact of erroneous background sub-
 3531 traction. Since the ridge was defined as the component
 3532 correlated with the trigger in azimuth but not in pseu-
 3533 dorapidity, it is now understood to be entirely due to v_3 .
 3534 Initial dihadron correlation studies after the observation
 3535 of odd v_n are either inconclusive about the presence or
 3536 absence of shape modifications on the away-side (Adare
 3537 *et al.*, 2013b) or indicate that the shape modification per-

3538 sists (Agakishiev *et al.*, 2014). A reanalysis of STAR
 3539 dihadron correlations (Agakishiev *et al.*, 2010, 2014) us-
 3540 ing a new method for background subtraction (Sharma
 3541 *et al.*, 2016) found that the Mach cone structure is not
 3542 present (Nattrass *et al.*, 2016). This new analysis in-
 3543 dicates that jets are broadened and softened (Nattrass
 3544 *et al.*, 2016), as observed in studies of reconstructed
 3545 jets (Aad *et al.*, 2014c; Chatrchyan *et al.*, 2014c).

3546 While the ridge is currently understood to be due to v_3
 3547 in heavy ion collisions, a similar structure has also been
 3548 observed in high multiplicity $p+p$ collisions (Aaboud
 3549 *et al.*, 2017; Khachatryan *et al.*, 2010). There are some
 3550 hypotheses that this might indicate that a medium is
 3551 formed in violent $p+p$ collisions (Khachatryan *et al.*,
 3552 2017b), although there are other hypotheses such as pro-
 3553 duction due to gluon saturation (Ozonder, 2016) or string

percolation (Andrs *et al.*, 2016). Whatever the production mechanism for the ridge in $p+p$ collisions, there is currently no evidence that it is related to or correlated with jet production in either $p+p$ or heavy ion collisions.

4. Summary of experimental evidence for modification of the medium by jets

Measurements of the impact of jets on the medium are difficult because of the large combinatorial background. The background may distort reconstructed jets and requiring the presence of a jet may bias the event selection. Because the energy contained within the background is large compared to the energy of the jet, even slight deviations of the background from the assumptions of the structure of the background used to subtract its effect could skew results. A confirmation of the CMS result indicating that the lost energy is at least partially equilibrated with the medium will require more detailed theoretical studies, preferably using Monte Carlo models so that the analysis techniques can be applied to data. The misidentification of the ridge and the Mach cone as arising due to partonic interactions with the medium highlights the perils of an incomplete understanding of the background.

E. Summary of experimental results

Section III.A reviews studies of cold nuclear matter effects, indicating that currently it does not appear that there are substantial cold nuclear matter effects modifying jets at mid-rapidity and that therefore effects observed thus far on jets in A+A collisions are primarily due to interactions of the hard parton with the medium. We note, however, that our understanding of cold nuclear matter effects is evolving rapidly and recommend that each observable is measured in both cold and hot nuclear matter in order to disentangle effects from hot and cold nuclear matter. Section III.B shows that there is ample evidence for partonic energy loss in the QGP. Nearly every measurement demonstrates that high momentum hadrons are suppressed relative to expectations from $p+p$ and $p+Pb$ collisions in the absence of quenching. Section III.C reviews the evidence that these partonic interactions with the medium result in more lower momentum particles and particles at larger angles relative to the parent parton, as expected from both gluon bremsstrahlung and collisional energy loss. Table III summarizes physics observations, selection biases and ability to constrain the initial kinematics of the measured observables. Section III.D discusses the evidence that at least some of this energy may be fully equilibrated with the medium and no longer distinguishable from the background.

For future studies to maximize our understanding of

the medium, most observables can be incorporated into a Bayesian analysis. We encourage exploration of comparisons of new observables to describe the jet structure. However, we caution that many observables are sensitive to kinematic selections and analysis techniques so that a replication of these techniques is required for the measurements to be comparable to theory.

IV. DISCUSSION AND THE PATH FORWARD

In the last several years, we have seen a dramatic increase in the number of experimentally accessible jet observables for heavy-ion collisions. During the early days of RHIC, measurements were primarily limited to R_{AA} and dihadron correlations, and reconstructed jets were measured only relatively recently. Since the start of the LHC, measurements of reconstructed jets have become routine, fragmentation functions have been measured directly, and the field is investigating and developing more sophisticated observables in order to quantify partonic energy loss and its effects on the QGP. The constraint of \hat{q} , the energy loss squared per fm of medium traversed, using R_{AA} measurements by the JET collaboration is remarkable. However, studies of jets in heavy ion collisions largely remain phenomenological and observational. This is probably the correct approach at this point in the development of the field, but a quantitative understanding of partonic energy loss in the QGP requires a concerted effort by both theorists and experimentalists to both make measurements which can be compared to models and use those measurements to constrain or exclude those models.

Below we lay out several of the steps we think are necessary to reach this quantitative understanding of partonic energy loss. We think that it is critical to quantitatively understand the impact of measurement techniques on jet observables in order to make meaningful comparisons to theory. We encourage the developments in new observables but urge caution – new observables may not have as many benefits as they first appear to when their biases and sensitivities to the medium are better understood. Many experimental and theoretical developments pave the way towards a better quantitative understanding of partonic energy loss. However, we think that the field will not fully benefit from these without discussions targeted at a better understanding of and consistency between theory and experiment and evaluating the full suite of observables considering all their biases. One of the dangers we face is that many observables are created by experimentalists, which often yields observables that are easy to measure such as A_J , but that are not particularly differential with respect to constraining jet quenching models.

A. Understand bias

As we discussed in Section II, all jet measurements in heavy ion collisions are biased towards a particular subset of the population of jets produced in these collisions. The existence of such biases is transparent for many measurements, such as surface bias in measurements of dihadron correlations at RHIC. However, for other observables such as those relating to reconstructed jets, these biases are not always adequately discussed in the interpretation of the results. As the comparison between ALICE, ATLAS, and CMS jet R_{AA} at low jet momenta shows, requiring a hard jet core in order to suppress background and reduce combinatorial jets leads to a strong bias which cannot be ignored. The main biases that pertain to jets in heavy ion collisions are: fragmentation, collision geometry, kinematic and parton species bias. The fragmentation bias can be simply illustrated by the jet R_{AA} measurement. Requiring a particular value of the resolution parameter, a particular constituent cut, or even the particular trigger detector used by the experiment selects a particular shower structure for the jet. The geometry bias is commonly discussed as a surface bias, since the effect of the medium increases with the path length causing more hard partons come from the surface of the QGP. The kinematic bias is somewhat related to the fragmentation bias as the fragmentation depends on the kinematics of the parton, but the energy loss in the medium means that jets of given kinematics do not come from the same selection of initial parton kinematics in vacuum and in heavy ion collisions. The parton species bias results as the gluons couple more strongly with the medium, and thus are expected to be more modified. This can be summarized by stating that nearly every technique favors measurement of more quark jets over gluon jets, is biased towards high z fragments, and is biased towards jets which have lost less energy in the medium.

While some measurements may claim to be bias free because they deal with the background effects in a manner which makes comparisons with theoretical models more straightforward, they still contain biases, usually towards jets which interacted less with the medium and therefore have lost less energy. For example, for the hadron-jet coincidence measurements, it is correct to state that the away side jet does not have a fragmentation bias since the hadron trigger is not part of its shower. However, this does not mean that this measurement is completely unbiased since the trigger hadron may select jets that have traveled through less medium or interacted less with the medium. In addition, the very act of using a jet finding algorithm introduces a bias (particularly toward quark jets) that is challenging to calculate. Given the large combinatorial background, such biases are most likely unavoidable.

We propose that these biases should be treated as tools through jet geometry engineering rather than a handicap.

These experimental biases should also be made transparent to the theory community. Frequently the techniques which impose these biases are buried in the experimental method section, with no or little mention of the impact of these biases on the results in the discussion. Theorists should not neglect the discussion of the experimental techniques, and experimentalists should make a greater effort to highlight potential impacts of the techniques to suppress and subtract the background on the measurement.

B. Make quantitative comparisons to theory

With the explosion of experimentally accessible observables, much of the focus has been on making as many measurements as possible with less consideration of whether such observables are calculable, or capable of distinguishing between different energy loss models. Even without direct comparisons to theory, these studies have been fruitful because they contribute to a phenomenological understanding of the impact of the medium on jets and vice versa. While we still feel that such exploratory studies are valuable, the long term goal of the field is to measure the properties of the QGP quantitatively, making theoretical comparisons essential. Some of the dearth of comparisons between measurements and models is due to the relative simplicity of the models and their inability to include hadronization.

The field requires another systematic attempt to constrain the properties of the medium from jet measurements. The Jetscape collaboration has formed in order to incorporate theoretical calculations of partonic energy loss into Monte Carlo simulations, which can then be used to directly calculate observables using the same techniques used for the measurements. This will then be followed up by a Bayesian analysis similar to previous work (Bernhard *et al.*, 2016; Novak *et al.*, 2014) but incorporating measurements of jets. This is essential, both to improve our theoretical understanding and to provide Monte Carlo models which can be used for more reliable experimental corrections. In our opinion, it should be possible to incorporate most observables into these measurements. However, we urge careful consideration of all experimental techniques and kinematic selections in order to ensure an accurate comparison between data and theory. The experimental collaborations should cooperate with the Jetscape collaboration to ensure that response matrices detailing the performance of the detectors for different observables are available.

C. More differential measurements

The choices of what to measure, how to measure it and how to both define and treat the background are

key to our quantitative understanding of the medium. There have been substantial improvements in the ability to measure jets in heavy ion collisions in recent years, such as the available kinematic reach due to accelerator and detector technology improvements. Additionally, our quantitative understanding of the effect of the background in many observables has also significantly improved. Given the continuous improvement in technology and analysis techniques, it is vital that the some of the better understood observables such as R_{AA} and I_{AA} are repeated with higher precision. Theoretical models should be able to simultaneously predict these precisely measured jet observables with different spectral shapes and path length dependencies. While this is necessary it is not sufficient to validate a theoretical model. Given that these will also depend on the collision energy, comparisons between RHIC and the LHC would be valuable, but again only when all biases are carefully considered. Now that the era of high statistics and precision detectors is here, the field is currently exploring several new observables to attempt to identify the best observables to constrain the properties of the medium. Older observables, such as R_{AA} , were built with the mindset that the final state jet reflects the kinematics of its parent parton, and the change in these kinematics due to interactions with the medium would be reflected in the change in the jet distributions. One of the lessons learned is that the majority of the modification of the fragmentation occurs at a relatively low p_T compared to the momentum of the jet. However, jet finding algorithms were specifically designed in order to not be sensitive to the details of the soft physics, which means that the very thing we are trying to measure and quantify is obscured by jet finder. The new observables are based on the structure of the jet, rather than on its kinematics alone. Specifically, they recognize that a hard parton could split into two hard daughters. If this splitting occurs in the medium, not only can the splitting itself be modified by the presence of the medium, but each of the daughters could lose energy to the medium independently. This would be actually be rather difficult to see in an ensemble structure measurement such as the jet fragmentation function, which yields a very symmetric picture of a jet about its axis, and so requires the specific structures within the jet to be quantified. While these new observables hold a lot of promise in terms of our understanding, caution must also be used in interpreting them until precisely how the background removal process or the detector effects will play a role in these measurements is carefully studied.

The investigations into these different observables are very important, since we have likely not identified the observables most sensitive to the properties of the medium. We cannot forget that we want to quantify the temperature dependence of the jet transport coefficients, as well as determine the size of the medium objects the jets are scattering off of. While these are global and fundamen-

tal descriptors of a medium, the fact that the process by which we make these measures is statistical means that the development of quantitative Monte Carlo simulations is key. Not only will they allow calculations of jet quenching models to be compared with the same initial states, hadronization schemes, etc, but they also could make the calculations of even more complicated observables feasible.

However, the sensitivity of simple observables should not be underestimated as with every set of new observables there are new mistakes to be made, and we can be reasonably sure that we understand the biases inherent in these simple observables. While it is not likely that comparison between R_{AA} and theories will constrain the properties of the medium substantially better than the JET collaboration's calculation of \hat{q} , calculations of γ -hadron, dihadron, and jet hadron correlations are feasible with the development of realistic Monte Carlo models. The relative simplicity of these observables makes them promising for subsequent attempts to constrain \hat{q} and other transport coefficients, especially since we now have a fairly precise quantitative experimental understanding of the background. This may be a good initial focus for systematic comparisons between theory and experiment. Interpreting a complicated result with a simple model that misses a lot of physics is a misuse of that model, and can lead to incorrect assumptions.

We caution against overconfidence, and encourage scrutiny and skepticism of measurement techniques and all observables. For each observable, an attempt needs to be made to quantify its biases, and determine which dominate. Observables should be measured in the same kinematic region and, if possible, with the same resolution parameters in order to ensure consistency between experiments. If initial studies of a particular observable reveal that it is either not particularly sensitive to the properties of the medium, or that it is too sensitive to experimental technique, we should stop measuring that observable. We urge caution when using complicated background subtraction and suppression techniques, which may be difficult to reproduce in models and requires Monte Carlo simulations that accurately model both the hard process that has produced the jet and the soft background. Given that the response of the detector to the background is different from experiment to experiment, complicated subtraction processes may make direct comparisons across experiments and energies difficult.

We also caution against the overuse and blind use of unfolding. Unfolding is a powerful technique which is undoubtedly necessary for many measurements. It also has the potential to impose biases by shifting measurements towards the Monte Carlo used to calculate the response matrix, and obfuscating the impact of detector effects and analysis techniques. When unfolding is necessary, it should be done carefully in order to make sure all effects are understood and that the result is robust. Since most

effects are included in the response matrix rather than corrected for separately, it can be difficult to understand the impact of different effects, such as track reconstruction efficiency and energy resolution. Unfolding is not necessarily superior to careful studies of detector effects and corrections, and attempts to minimize their impact on the observables chosen. Given the relative simplicity of folding a result, for all observables we should perform a theory-experiment closure test where the theoretical results are folded and compared to the raw data. Since the robustness of a particular measurement depends on the unfolding corrections, the details of the unfolding method should be also transparent to both experimental and theoretical communities.

Of course making more differential measurements is aided by better detectors. The LHC detectors use advanced detector technology, and are designed for jet measurements. However, the current RHIC detectors were not optimized for jet measurements, which has limited the types of jet observables at these lower energies. Precise measurements of jets over a wide range of energies is necessary to truly understand partonic energy loss. The proposed sPHENIX detector will greatly aid these measurements by utilizing some of the advanced detector technology that has been developed since the design of the original RHIC experiments (Adare *et al.*, 2015). The high rate and hermetic detector will improve the results by reducing detector uncertainties and increasing the kinematic reach so that a true comparison between RHIC and LHC can be made. In particular, upgrades at both RHIC and LHC will make precise measurements of heavy-flavor tagged jets and boson-tagged jets, which constrain the initial kinematics of the hard scattering, possible.

D. An agreement on the treatment of background in heavy ion collisions

The issues we listed above are complicated and require substantive, ongoing discussions between theorists and experimentalists. A start in this direction can be found in the Lisbon Accord where the community agreed to use Rivet (Buckley *et al.*, 2013), a C++ library which provides a framework and tools for calculating observables at particle level developed for particle physics. Rivet allowed event generator models and experimental observables to be validated. Agreeing on a framework that all physicists can use is an important first step, however it is not sufficient. It would not prevent a comparison of two observables with different jet selection criteria, or a comparison of a theoretical model with a different treatment or definition of the background than a similar experimental observable. The problems we face are similar to those faced by the particle physics community as they learned how to study and utilize jets, to make

them one of the best tools we have for understanding the Standard Model. An agreement on the treatment of the background in heavy ion collisions experimentally and theoretically is required as it is part of the definition of the observable. Theorists and experimentalists need to understand each other's techniques and find common ground, to define observables that experimentalists can measure and theorists can calculate. We need to recognize that observables based on pQCD calculations are needed if we are to work towards a text-book formulation of jet quenching, and what we learn about QCD from studying the strongly coupled QGP. However, observables that are impossible to measure are not useful, nor is it useful to measure observables that are impossible to calculate or are insensitive to the properties of the medium. We propose a targeted workshop to address these issues in heavy ion collisions with the goal of an agreement similar to the Snowmass Accord. Ideally we would agree on a series of jet algorithms, including selection criteria, that all experiments can measure, and a background strategy that can be employed both in experiment and theory.

V. ACKNOWLEDGEMENTS

We thank Will Witt for productive discussions about unfolding. We thank Redmer Bertens, Jana Bielčikova, Leticia Cunqueiro Mendez, Kate Jones, Kolja Kauder, Abhijit Majumder, Jaki Noronha-Hostler, Thomas Papenbrock, Dennis Perepelitsa, Jörn Putschke, Soren Sorensen, Peter Steinberg, and Giorgio Torrieri for useful advice on the manuscript and useful discussions. We thank Raghav Elayavalli Kunnawalkam, Boris Hippolyte, Kurt Jung, Igor Lokhtin, Thomas Ullrich, and the experimental collaborations for permission to reproduce their figures for this work. This material is based upon work supported by the Division of Nuclear Physics of the U.S. Department of Energy under Grant No. DE-FG02-96ER40982 and by the National Science Foundation under Grant Nos. 1352081 and 1614474.

REFERENCES

- (2009), "Particle-Flow Event Reconstruction in CMS and Performance for Jets, Taus, and MET," .
- (2013), .
- (2015a), *Jet energy scale and its uncertainty for jets reconstructed using the ATLAS heavy ion jet algorithm*, Tech. Rep. ATLAS-CONF-2015-016 (CERN, Geneva).
- (2015b), "Measurement of dijet p_T correlations in Pb+Pb and pp collisions at $\sqrt{s_{NN}} = 2.76$ TeV with the ATLAS detector," ATLAS-CONF-2015-052.
- (2016), "Measurement of charged particle spectra in pp collisions and nuclear modification factor R_{pPb} at $\sqrt{s_{NN}} = 5.02$ TeV with the ATLAS detector at the LHC," ATLAS-CONF-2016-108.

- (2016a), “Measurement of the charged particle nuclear modification factor in PbPb collisions at $\sqrt{s_{NN}} = 5.02$ TeV,” CMS-PAS-HIN-15-015.
- (2016b), “Study of B^+ meson production in pp and PbPb collisions at $\sqrt{s_{NN}} = 5.02$ TeV using exclusive hadronic decays,” CMS-PAS-HIN-16-011.
- Aaboud, M., *et al.* (ATLAS) (2017), Phys. Rev. **C96** (2), 024908, arXiv:1609.06213 [nucl-ex].
- Aad, G., *et al.* (ATLAS) (2008), JINST **3**, S08003.
- Aad, G., *et al.* (ATLAS) (2010), Phys.Rev.Lett. **105**, 252303.
- Aad, G., *et al.* (ATLAS) (2012), Phys. Lett. **B710**, 363.
- Aad, G., *et al.* (ATLAS) (2013a), Phys.Rev.Lett. **111** (15), 152301.
- Aad, G., *et al.* (ATLAS) (2013b), Phys.Lett. **B719**, 220.
- Aad, G., *et al.* (ATLAS) (2014a), Phys. Rev. **C90** (2), 024905.
- Aad, G., *et al.* (ATLAS) (2014b), Eur. Phys. J. **C74** (11), 3157.
- Aad, G., *et al.* (ATLAS) (2014c), Phys.Lett. **B739**, 320.
- Aad, G., *et al.* (ATLAS) (2014d), Phys. Rev. **C90** (4), 044906.
- Aad, G., *et al.* (ATLAS) (2015a), Phys. Lett. **B748**, 392.
- Aad, G., *et al.* (ATLAS) (2015b), Phys.Rev.Lett. **114** (7), 072302.
- Aad, G., *et al.* (ATLAS) (2016a), Phys. Lett. **B756**, 10.
- Aad, G., *et al.* (ATLAS) (2016b), Phys. Rev. Lett. **116** (17), 172301.
- Aad, G., *et al.* (ATLAS) (2016c), .
- Aamodt, K., *et al.* (ALICE) (2008), JINST **3**, S08002.
- Aamodt, K., *et al.* (ALICE) (2010), Phys. Rev. Lett. **105**, 252301.
- Aamodt, K., *et al.* (ALICE) (2011a), Phys. Rev. Lett. **107**, 032301.
- Aamodt, K., *et al.* (ALICE) (2011b), Phys.Lett. **B696**, 30.
- Aamodt, K., *et al.* (ALICE) (2012), Phys.Rev.Lett. **108**, 092301.
- Abe, F., *et al.* (CDF) (1992), Phys. Rev. **D45**, 1448.
- Abelev, B., *et al.* (STAR) (2009a), Phys.Rev.Lett. **102**, 052302.
- Abelev, B., *et al.* (STAR) (2009b), Phys.Rev. **C80**, 064912.
- Abelev, B., *et al.* (STAR) (2010a), Phys.Lett. **B683**, 123.
- Abelev, B., *et al.* (ALICE) (2012a), JHEP **1203**, 053.
- Abelev, B., *et al.* (ALICE) (2012b), JHEP **09**, 112.
- Abelev, B., *et al.* (ALICE) (2013a), Phys.Lett. **B719**, 18.
- Abelev, B., *et al.* (ALICE) (2013b), Phys. Rev. **C88**, 044910.
- Abelev, B., *et al.* (ALICE) (2013c), Phys. Rev. **C88** (4), 044909, arXiv:1301.4361 [nucl-ex].
- Abelev, B., *et al.* (ALICE) (2013d), Phys.Lett. **B722**, 262.
- Abelev, B., *et al.* (ALICE) (2013e), Phys. Rev. Lett. **110** (8), 082302.
- Abelev, B., *et al.* (ALICE Collaboration) (2014a), JHEP **1403**, 013.
- Abelev, B., *et al.* (STAR) (2016), Phys. Rev. **C94** (1), 014910.
- Abelev, B. B., *et al.* (ALICE) (2013f), Phys. Rev. Lett. **111**, 222301.
- Abelev, B. B., *et al.* (ALICE) (2013g), Phys. Lett. **B727**, 371.
- Abelev, B. B., *et al.* (ALICE) (2014b), Phys. Lett. **B728**, 216, [Erratum: Phys. Lett. **B734**, 409(2014)].
- Abelev, B. I., *et al.* (STAR) (2006), Phys. Rev. Lett. **97**, 152301.
- Abelev, B. I., *et al.* (STAR) (2008), Phys. Rev. **C77**, 044908.
- Abelev, B. I., *et al.* (STAR) (2009c), Phys. Rev. Lett. **103**, 251601.
- Abelev, B. I., *et al.* (STAR) (2010b), Phys. Rev. **C81**, 064904.
- Abelev, B. I., *et al.* (STAR) (2010c), Phys. Rev. **C82**, 034909.
- Abreu, P., *et al.* (DELPHI) (1996), Z. Phys. **C70**, 179.
- Acharya, S., *et al.* (ALICE) (2017), arXiv:1702.00804 [nucl-ex].
- Ackermann, K. H., *et al.* (STAR) (2003), Nucl. Instrum. Meth. **A499**, 624.
- Ackerstaff, K., *et al.* (OPAL) (1999), Eur. Phys. J. **C8**, 241.
- Acton, P. D., *et al.* (OPAL) (1993), Z. Phys. **C58**, 387.
- Adam, J., *et al.* (ALICE) (2015a), JHEP **11**, 205.
- Adam, J., *et al.* (ALICE) (2015b), Phys. Lett. **B746**, 385.
- Adam, J., *et al.* (ALICE) (2015c), JHEP **09**, 170.
- Adam, J., *et al.* (ALICE) (2015d), Phys.Lett. **B746**, 1.
- Adam, J., *et al.* (ALICE) (2016a), Phys. Rev. Lett. **116** (13), 132302.
- Adam, J., *et al.* (ALICE) (2016b), Phys. Lett. **B753**, 511.
- Adam, J., *et al.* (ALICE) (2016c), Eur. Phys. J. **C76** (5), 271.
- Adam, J., *et al.* (ALICE) (2016d), Phys. Rev. Lett. **116** (22), 222302.
- Adam, J., *et al.* (ALICE) (2016e), Phys. Rev. **C93** (3), 034913.
- Adam, J., *et al.* (ALICE) (2016f), Phys. Rev. **C93** (4), 044903.
- Adam, J., *et al.* (ALICE) (2016g), Phys. Lett. **B754**, 235.
- Adam, J., *et al.* (ALICE) (2016h), Phys. Lett. **B753**, 126.
- Adam, J., *et al.* (ALICE) (2016i), Phys. Rev. **C94** (3), 034903.
- Adam, J., *et al.* (ALICE) (2016j), Phys. Rev. **C93** (2), 024917.
- Adam, J., *et al.* (ALICE) (2016k), JHEP **03**, 081.
- Adamczyk, L., *et al.* (STAR) (2013), Phys. Rev. **C88** (1), 014904.
- Adamczyk, L., *et al.* (STAR) (2014a), Phys.Rev.Lett. **112** (12), 122301.
- Adamczyk, L., *et al.* (STAR) (2014b), Phys. Rev. Lett. **113** (14), 142301.
- Adamczyk, L., *et al.* (STAR) (2015), Phys. Lett. **B751**, 233.
- Adamczyk, L., *et al.* (STAR) (2016), Phys. Lett. **B760**, 689.
- Adamczyk, L., *et al.* (STAR) (2017a), arXiv:1707.01988 [nucl-ex].
- Adamczyk, L., *et al.* (STAR) (2017b), Phys. Rev. Lett. **119** (6), 062301, 1609.03878.
- Adamczyk, L., *et al.* (STAR) (2017c), arXiv:1702.01108 [nucl-ex].
- Adamczyk, M., *et al.* (BRAHMS) (2003), Nucl. Instrum. Meth. **A499**, 437.
- Adams, J., *et al.* (STAR) (2003a), Phys. Rev. Lett. **91**, 072304.
- Adams, J., *et al.* (STAR) (2003b), Phys.Rev.Lett. **91**, 172302.
- Adams, J., *et al.* (STAR) (2004a), Phys.Rev.Lett. **93**, 252301.
- Adams, J., *et al.* (STAR) (2004b), Phys. Rev. **C70**, 054907.
- Adams, J., *et al.* (STAR) (2005a), Phys.Rev.Lett. **95**, 152301.
- Adams, J., *et al.* (STAR) (2005b), Nucl. Phys. **A757**, 102.
- Adams, J., *et al.* (STAR) (2006), Phys.Rev.Lett. **97**, 162301.
- Adare, A., *et al.* (PHENIX) (2007a), Phys. Rev. Lett. **98**, 232301.
- Adare, A., *et al.* (PHENIX) (2007b), Phys.Rev.Lett. **98**, 232302.
- Adare, A., *et al.* (PHENIX) (2008a), Phys.Rev. **C78**, 014901.
- Adare, A., *et al.* (PHENIX) (2008b), Phys.Rev. **C77**, 064907.
- Adare, A., *et al.* (PHENIX) (2008c), Phys. Rev. Lett. **101**, 232301.
- Adare, A., *et al.* (PHENIX) (2008d), Phys.Rev. **C77**, 011901.
- Adare, A., *et al.* (PHENIX) (2009), Phys.Rev. **C80**, 024908.
- Adare, A., *et al.* (PHENIX) (2010a), Phys. Rev. Lett. **104**, 132301.
- Adare, A., *et al.* (PHENIX) (2010b), Phys.Rev. **D82**, 072001.

- Adare, A., *et al.* (PHENIX) (2010c), Phys. Rev. **C82**, 011902. 4169
- Adare, A., *et al.* (PHENIX Collaboration) (2011a), Phys.Rev. 4170
C84, 044905. 4171
- Adare, A., *et al.* (PHENIX) (2011b), Phys. Rev. Lett. **107**, 4172
252301. 4173
- Adare, A., *et al.* (PHENIX) (2011c), Phys. Rev. **C84**, 044902. 4174
- Adare, A., *et al.* (PHENIX) (2011d), Phys.Rev.Lett. **107**, 4175
172301. 4176
- Adare, A., *et al.* (PHENIX) (2012a), Phys. Rev. Lett. 4177
109 (24), 242301. 4178
- Adare, A., *et al.* (PHENIX) (2012b), Phys. Rev. Lett. **109**, 4179
152301. 4180
- Adare, A., *et al.* (PHENIX) (2012c), Phys. Rev. Lett. **109**, 4181
122302. 4182
- Adare, A., *et al.* (PHENIX) (2013a), Phys. Rev. **C88** (6), 4183
064910. 4184
- Adare, A., *et al.* (PHENIX) (2013b), Phys.Rev.Lett. **111** (3), 4185
032301. 4186
- Adare, A., *et al.* (PHENIX) (2013c), Phys. Rev. **C87** (3), 4187
034911. 4188
- Adare, A., *et al.* (PHENIX) (2013d), Phys. Rev. Lett. 4189
111 (20), 202301. 4190
- Adare, A., *et al.* (PHENIX) (2013e), Phys. Rev. **C88** (2), 4191
024906. 4192
- Adare, A., *et al.* (PHENIX) (2014a), Phys. Rev. **C90** (3), 4193
034902. 4194
- Adare, A., *et al.* (PHENIX) (2014b), Phys.Rev. **C89** (3), 4195
034915. 4196
- Adare, A., *et al.* (2015), arXiv:1501.06197 [nucl-ex]. 4197
- Adare, A., *et al.* (PHENIX) (2016a), Phys. Rev. **C94** (6), 4198
064901. 4199
- Adare, A., *et al.* (PHENIX) (2016b), Phys. Rev. Lett. 4200
116 (12), 122301. 4201
- Adare, A., *et al.* (PHENIX) (2016c), Phys. Rev. **C93** (2), 4202
024904. 4203
- Adare, A., *et al.* (PHENIX) (2016d), Phys. Rev. **C93** (2), 4204
024911. 4205
- Adare, A., *et al.* (PHENIX) (2016e), Phys. Rev. **C93** (2), 4206
024901. 4207
- Adcox, K., *et al.* (PHENIX) (2003), Nucl. Instrum. Meth. 4208
A499, 469. 4209
- Adcox, K., *et al.* (PHENIX) (2004), Phys. Rev. **C69**, 024904. 4210
- Adcox, K., *et al.* (PHENIX) (2005), Nucl. Phys. **A757**, 184. 4211
- Adler, C., *et al.* (STAR) (2001), Phys. Rev. Lett. **87**, 182301. 4212
- Adler, C., *et al.* (STAR) (2003a), Phys.Rev.Lett. **90**, 082302. 4213
- Adler, S., *et al.* (PHENIX) (2003b), Phys.Rev.Lett. **91**, 4214
072301. 4215
- Adler, S., *et al.* (PHENIX) (2006a), Phys.Rev.Lett. **96**, 4216
222301. 4217
- Adler, S., *et al.* (PHENIX) (2006b), Phys.Rev.Lett. **97**, 4218
052301. 4219
- Adler, S., *et al.* (PHENIX) (2006c), Phys.Rev. **D74**, 072002. 4220
- Adler, S., *et al.* (PHENIX) (2006d), Phys.Rev. **C73**, 054903. 4221
- Adler, S., *et al.* (PHENIX) (2007a), Phys.Rev. **C76**, 034904. 4222
- Adler, S. S., *et al.* (PHENIX) (2003c), Phys. Rev. Lett. **91**, 4223
182301. 4224
- Adler, S. S., *et al.* (PHENIX) (2004), Phys. Rev. **C69**, 034909. 4225
- Adler, S. S., *et al.* (PHENIX) (2005), Phys. Rev. **C71**, 034908, 4226
[Erratum: Phys. Rev.C71,049901(2005)]. 4227
- Adler, S. S., *et al.* (PHENIX) (2007b), Phys. Rev. Lett. **98**, 4228
172302. 4229
- Adye, T. (2011), in *Proceedings, PHYSTAT 2011 Workshop* 4230
on Statistical Issues Related to Discovery Claims in Search 4231
Experiments and Unfolding, CERN, Geneva, Switzerland 4232
17-20 January 2011, CERN (CERN, Geneva) pp. 313–318.
- Afanasiev, S., *et al.* (PHENIX) (2008), Phys.Rev.Lett. **101**,
082301. 4171
- Afanasiev, S., *et al.* (PHENIX) (2012), Phys. Rev. Lett. **109**,
152302. 4172
- Agakishiev, G., *et al.* (STAR) (2012a), Phys. Rev. Lett. **108**,
072302. 4173
- Agakishiev, G., *et al.* (STAR) (2012b), Phys. Rev. Lett. **108**,
072301, arXiv:1107.2955 [nucl-ex]. 4174
- Agakishiev, G., *et al.* (STAR) (2012c), Phys.Rev. **C85**,
014903. 4175
- Agakishiev, H., *et al.* (STAR) (2010), arXiv:1010.0690 [nucl-
ex]. 4176
- Agakishiev, H., *et al.* (STAR) (2011), Phys.Rev. **C83**, 061901. 4177
- Agakishiev, H., *et al.* (STAR) (2014), Phys. Rev. **C89** (4),
041901. 4178
- Aggarwal, M., *et al.* (STAR) (2010), Phys.Rev. **C82**, 024912. 4179
- Akers, R., *et al.* (OPAL) (1995), Z. Phys. **C68**, 179. 4180
- Akiba, Y., *et al.* (2015), arXiv:1502.02730 [nucl-ex]. 4181
- Albacete, J. L., N. Armesto, J. G. Milhano, C. A. Salgado,
and U. A. Wiedemann (2005), Phys. Rev. **D71**, 014003. 4182
- Alver, B., *et al.* (PHOBOS) (2007), Phys. Rev. Lett. **98**,
242302. 4183
- Alver, B., *et al.* (PHOBOS) (2010), Phys.Rev.Lett. **104**,
062301. 4184
- Alves, Jr., A. A., *et al.* (LHCb) (2008), JINST **3**, S08005. 4185
- Alvioli, M., B. A. Cole, L. Frankfurt, D. V. Perepelitsa, and
M. Strikman (2016), Phys. Rev. **C93** (1), 011902. 4186
- Alvioli, M., L. Frankfurt, V. Guzey, and M. Strikman (2014),
Phys. Rev. **C90**, 034914. 4187
- Alvioli, M., and M. Strikman (2013), Phys. Lett. **B722**, 347. 4188
- Andrs, C., A. Moscoso, and C. Pajares (2016), *Proceedings*
37th International Conference on High Energy Physics
(ICHEP 2014), Nucl. Part. Phys. Proc. **273-275**, 1513. 4189
- Aprahamian, A., *et al.* (2015), “Reaching for the horizon: The
2015 long range plan for nuclear science,”. 4190
- Armesto, N., L. Cunqueiro, and C. A. Salgado (2009), Eur.
Phys. J. **C63**, 679. 4191
- Armesto, N., D. C. Glhan, and J. G. Milhano (2015), Phys.
Lett. **B747**, 441. 4192
- Armesto, N., *et al.* (2012), Phys. Rev. **C86**, 064904. 4193
- Arnold, P. B., G. D. Moore, and L. G. Yaffe (2002), JHEP
06, 030. 4194
- Arsene, I., *et al.* (BRAHMS) (2005a), Phys. Rev. **C72**,
014908. 4195
- Arsene, I., *et al.* (BRAHMS) (2005b), Nucl. Phys. **A757**, 1. 4196
- Arsene, I. G., *et al.* (BRAHMS) (2010), Phys. Lett. **B684**,
22. 4197
- Aurenche, P., and B. G. Zakharov (2009), JETP Lett. **90**,
237. 4198
- Back, B., *et al.* (PHOBOS) (2004), Phys.Rev. **C70**, 061901. 4199
- Back, B. B., *et al.* (PHOBOS) (2003), Nucl. Instrum. Meth.
A499, 603. 4200
- Back, B. B., *et al.* (2005), Nucl. Phys. **A757**, 28. 4201
- Back, B. B., *et al.* (PHOBOS) (2007), Phys. Rev. **C75**,
024910. 4202
- Baier, R., Y. L. Dokshitzer, A. H. Mueller, S. Peigne, and
D. Schiff (1997), Nucl. Phys. **B483**, 291. 4203
- Baier, R., Y. L. Dokshitzer, A. H. Mueller, and D. Schiff
(1998), Phys. Rev. **C58**, 1706. 4204
- Baier, R., Y. L. Dokshitzer, S. Peigne, and D. Schiff (1995),
Phys.Lett. **B345**, 277. 4205
- Baier, R., D. Schiff, and B. G. Zakharov (2000), Ann. Rev.
Nucl. Part. Sci. **50**, 37. 4206

- 4233 Barate, R., *et al.* (ALEPH) (1998), Phys. Rept. **294**, 1. 4297
- 4234 Bazavov, A., *et al.* (HotQCD) (2014), Phys. Rev. **D90** (9), 4298
094503. 4299
- 4235 Bernhard, J. E., J. S. Moreland, S. A. Bass, J. Liu, and 4300
4236 U. Heinz (2016), Phys. Rev. **C94** (2), 024907. 4301
- 4237 Berta, P., M. Spousta, D. W. Miller, and R. Leitner (2014), 4302
4238 JHEP **06**, 092. 4303
- 4239 Bertocchi, L., and D. Treleani (1977), J. Phys. **G3**, 147. 4304
- 4240 Betz, B., M. Gyulassy, M. Luzum, J. Noronha, J. Noronha- 4305
4241 Hostler, I. Portillo, and C. Ratti (2017), Phys. Rev. 4306
4242 **C95** (4), 044901. 4307
- 4243 Betz, B., M. Gyulassy, J. Noronha, and G. Torrieri (2009), 4308
4244 Phys. Lett. **B675**, 340. 4309
- 4245 Bielcikova, J. (STAR) (2008), in *Proceedings, 43rd Rencontres* 4310
4246 *de Moriond on QCD and high energy interactions.* 4311
- 4247 Bielcikova, J., S. Esumi, K. Filimonov, S. Voloshin, and 4312
4248 J. Wurm (2004), Phys.Rev. **C69**, 021901. 4313
- 4249 Bjorken, J. D. (1982), “Energy Loss of Energetic Partons in 4314
4250 Quark - Gluon Plasma: Possible Extinction of High p(t) 4315
4251 Jets in Hadron - Hadron Collisions,” FERMILAB-PUB- 4316
4252 82-059-THY, FERMILAB-PUB-82-059-T. 4317
- 4253 Borghini, N., P. M. Dinh, and J.-Y. Ollitrault (2000), Phys. 4318
4254 Rev. **C62**, 034902. 4319
- 4255 Buckley, A., J. Butterworth, L. Lonnblad, D. Grellscheid, 4320
4256 H. Hoeth, J. Monk, H. Schulz, and F. Siegert (2013), Com- 4321
4257 put. Phys. Commun. **184**, 2803, arXiv:1003.0694 [hep-ph]. 4322
- 4258 Burke, K. M., *et al.* (JET) (2014), Phys.Rev. **C90** (1), 014909. 4323
- 4259 Buskalic, D., *et al.* (ALEPH) (1996), Phys. Lett. **B384**, 353. 4324
- 4260 Butterworth, J. M., A. R. Davison, M. Rubin, and G. P. 4325
4261 Salam (2008), Phys. Rev. Lett. **100**, 242001. 4326
- 4262 Buzzatti, A., and M. Gyulassy (2012), Phys. Rev. Lett. **108**, 4327
4263 022301. 4328
- 4264 Bzdak, A., V. Skokov, and S. Bathe (2016), Phys. Rev. 4329
4265 **C93** (4), 044901. 4330
- 4266 Cacciari, M., J. Rojo, G. P. Salam, and G. Soyez (2011), 4331
4267 Eur.Phys.J. **C71**, 1539. 4332
- 4268 Cacciari, M., G. P. Salam, and G. Soyez (2008a), JHEP **04**, 4333
4269 063. 4334
- 4270 Cacciari, M., G. P. Salam, and G. Soyez (2008b), JHEP 4335
4271 **0804**, 005. 4336
- 4272 Cacciari, M., G. P. Salam, and G. Soyez (2012), Eur.Phys.J. 4337
4273 **C72**, 1896. 4338
- 4274 Casalderrey-Solana, J., D. Gulhan, G. Milhano, D. Pablos, 4339
4275 and K. Rajagopal (2017), JHEP **03**, 135. 4340
- 4276 Casalderrey-Solana, J., Y. Mehtar-Tani, C. A. Salgado, and 4341
4277 K. Tywoniuk (2013), Phys. Lett. **B725**, 357. 4342
- 4278 Casalderrey-Solana, J., E. V. Shuryak, and D. Teaney 4343
4279 (2005), *Proceedings, 18th International Conference on* 4344
4280 *Ultra-Relativistic Nucleus-Nucleus Collisions (Quark* 4345
4281 *Matter 2005)*, J. Phys. Conf. Ser. **27**, 22, [Nucl. 4346
4282 Phys.A774,577(2006)]. 4347
- 4283 Chatrchyan, S., *et al.* (CMS) (2008), JINST **3**, S08004. 4348
- 4284 Chatrchyan, S., *et al.* (CMS) (2011a), JHEP **08**, 141. 4349
- 4285 Chatrchyan, S., *et al.* (CMS) (2011b), Phys. Rev. **C84**, 4350
4286 024906. 4351
- 4287 Chatrchyan, S., *et al.* (CMS) (2011c), Phys. Rev. Lett. **106**, 4352
4288 212301. 4353
- 4289 Chatrchyan, S., *et al.* (CMS) (2012a), Phys. Rev. Lett. **109**, 4354
4290 022301. 4355
- 4291 Chatrchyan, S., *et al.* (CMS) (2012b), Phys. Lett. **B710**, 256. 4356
- 4292 Chatrchyan, S., *et al.* (CMS) (2012c), JHEP **1210**, 087. 4357
- 4293 Chatrchyan, S., *et al.* (CMS) (2012d), Phys. Rev. Lett. **109**, 4358
4294 152303. 4359
- 4295 Chatrchyan, S., *et al.* (CMS) (2012e), Eur.Phys.J. **C72**, 1945. 4360
- 4296 Chatrchyan, S., *et al.* (CMS) (2012f), Phys. Lett. **B715**, 66. 4361
- 4297 Chatrchyan, S., *et al.* (CMS) (2012g), JHEP **05**, 063. 4362
- 4298 Chatrchyan, S., *et al.* (CMS Collaboration) (2013a), Phys. 4363
4299 Lett. B **730** (arXiv:1310.0878. CMS-HIN-12-002. CERN- 4364
4300 PH-EP-2013-189), 243. 31 p. 4365
- 4301 Chatrchyan, S., *et al.* (CMS) (2013b), Phys. Lett. **B718**, 773. 4366
- 4302 Chatrchyan, S., *et al.* (CMS) (2014a), Phys. Rev. 4367
4303 Lett. **113** (13), 132301, [Erratum: Phys. Rev. 4368
4304 Lett.115,no.2,029903(2015)]. 4369
- 4305 Chatrchyan, S., *et al.* (CMS) (2014b), Phys. Rev. **C89** (4), 4370
4306 044906. 4371
- 4307 Chatrchyan, S., *et al.* (CMS) (2014c), Phys.Rev. **C90** (2), 4372
4308 024908. 4373
- 4309 Chen, X.-F., C. Greiner, E. Wang, X.-N. Wang, and Z. Xu 4374
4310 (2010), Phys. Rev. **C81**, 064908. 4375
- 4311 Chiu, C. B., and R. C. Hwa (2009), Phys. Rev. C **79**, 034901. 4376
- 4312 Chiu, C. B., R. C. Hwa, and C. B. Yang (2008), Phys. Rev. 4377
4313 C **78** (4), 044903. 4378
- 4314 CMS, C. (2010), “CMS collision events: from lead ion colli- 4379
4315 sions,” CMS-PHO-EVENTS-2010-003. 4380
- 4316 Coleman-Smith, C. E., and B. Muller (2014), Phys. Rev. 4381
4317 **D89**, 025019. 4382
- 4318 Collaboration, C. (CMS) (2013a), “Performance of 4383
4319 quark/gluon discrimination in 8 TeV pp data,” CMS-PAS- 4384
4320 JME-13-002. 4385
- 4321 Collaboration, C. (CMS) (2013b), “Study of isolated pho- 4386
4322 ton+jet correlation in PbPb and pp collisions at $\sqrt{s_{NN}} =$ 4387
4323 2.76 TeV and pPb collisions at $\sqrt{s_{NN}} = 5.02$ TeV,” CMS- 4388
4324 PAS-HIN-13-006. 4389
- 4325 Collaboration”, J. (2017), “<http://jetscape.wayne.edu/>,” . 4390
- 4326 Collins, J. C., D. E. Soper, and G. F. Sterman (1985), Nucl. 4391
4327 Phys. **B261**, 104. 4392
- 4328 Cowan, G. (2002), *Advanced Statistical Techniques in Particle* 4393
4329 *Physics. Proceedings, Conference, Durham, UK, March 18-* 4394
4330 *22, 2002*, Conf. Proc. **C0203181**, 248, [,248(2002)]. 4395
- 4331 Cunqueiro, L. (ALICE) (2016), *Proceedings, 25th Interna-* 4396
4332 *tional Conference on Ultra-Relativistic Nucleus-Nucleus* 4397
4333 *Collisions (Quark Matter 2015): Kobe, Japan, September* 4398
4334 *27-October 3, 2015*, Nucl. Phys. **A956**, 593. 4399
- 4335 D’Agostini, G. (1995), Nucl. Instrum. Meth. **A362**, 487. 4400
- 4336 Das, S. J., G. Giacalone, P.-A. Monard, and J.-Y. Ollitrault 4401
4337 (2017), arXiv:1708.00081 [nucl-th]. 4402
- 4338 Dasgupta, M., A. Fregoso, S. Marzani, and G. P. Salam 4403
4339 (2013), Journal of High Energy Physics **2013** (9), 1. 4404
- 4340 Djordjevic, M., and M. Gyulassy (2004), Nucl. Phys. **A733**, 4405
4341 265. 4406
- 4342 Djordjevic, M., M. Gyulassy, and S. Wicks (2005), Phys. Rev. 4407
4343 Lett. **94**, 112301. 4408
- 4344 Djordjevic, M., and U. W. Heinz (2008), Phys. Rev. Lett. 4409
4345 **101**, 022302. 4410
- 4346 Dokshitzer, Y. L., and D. E. Kharzeev (2001), Phys. Lett. B 4411
4347 **519**, 199. 4412
- 4348 Dover, C. B., U. W. Heinz, E. Schnedermann, and J. Zimanyi 4413
4349 (1991), Phys. Rev. **C44**, 1636. 4414
- 4350 Ellis, S. D., C. K. Vermilion, and J. R. Walsh (2010), Phys. 4415
4351 Rev. D **81**, 094023. 4416
- 4352 Eskola, K. J., H. Honkanen, C. A. Salgado, and U. A. Wiede- 4417
4353 mann (2005), Nucl. Phys. **A747**, 511. 4418
- 4354 Field, R., and R. C. Group (CDF) (2005), arXiv:hep- 4419
4355 ph/0510198 [hep-ph]. 4420
- 4356 Floris, M. (2014), *Proceedings, 24th International Conference* 4421
4357 *on Ultra-Relativistic Nucleus-Nucleus Collisions (Quark* 4422
4358 *Matter 2014): Darmstadt, Germany, May 19-24, 2014*, 4423
4359 Nucl. Phys. **A931**, 103. 4424

- Fodor, Z., and S. D. Katz (2004), JHEP **04**, 050. 4425
- Fries, R. J., B. Muller, C. Nonaka, and S. A. Bass (2003), 4426
Phys. Rev. Lett. **90**, 202303. 4427
- Gelis, F., E. Iancu, J. Jalilian-Marian, and R. Venugopalan 4428
(2010), Ann. Rev. Nucl. Part. Sci. **60**, 463, arXiv:1002.0333 4429
[hep-ph]. 4430
- Greco, V., C. M. Ko, and P. Levai (2003), Phys. Rev. Lett. 4431
90, 202302. 4432
- Gubser, S. S. (2007), Phys. Rev. **D76**, 126003. 4433
- Gyulassy, M., and M. Plumer (1990), Phys.Lett. **B243**, 432. 4434
- Harris, J. W., and B. Muller (1996), Ann. Rev. Nucl. Part. 4435
Sci. **46**, 71. 4436
- Heinz, U., and R. Snellings (2013), Ann. Rev. Nucl. Part. 4437
Sci. **63**, 123. 4438
- Hocker, A., and V. Kartvelishvili (1996), Nucl. Instrum. 4439
Meth. **A372**, 469. 4440
- Horowitz, W. A., and M. Gyulassy (2008), Phys. Lett. B 4441
666, 320. 4442
- Huang, J., Z.-B. Kang, and I. Vitev (2013), Phys. Lett. **B726**, 4443
251. 4444
- Huang, J., Z.-B. Kang, I. Vitev, and H. Xing (2015), Phys. 4445
Lett. **B750**, 287. 4446
- Huth, J. E., *et al.* (1990), in *1990 DPF Summer Study on* 4447
High-energy Physics: Research Directions for the Decade 4448
(Snowmass 90) Snowmass, Colorado, June 25-July 13, 1990, pp. 0134–136. 4449
- Hwa, R. C., and C. B. Yang (2003), Phys. Rev. **C67**, 034902. 4451
- Hwa, R. C., and C. B. Yang (2009), Phys. Rev. C **79**, 044908. 4452
- Iancu, E., A. Leonidov, and L. D. McLerran (2001), Nucl. 4453
Phys. **A692**, 583. 4454
- Jeon, S., and G. D. Moore (2005), Phys. Rev. **C71**, 034901. 4455
- Jia, J. (2013), Phys. Rev. **C87** (6), 061901. 4456
- Jia, J., W. A. Horowitz, and J. Liao (2011), Phys. Rev. **C84**, 4457
034904. 4458
- Karsch, F. (2002), in *Lectures on Quark Matter*, Lecture 4459
Notes in Physics, Vol. 583, edited by W. Plessas and 4460
L. Mathelitsch (Springer Berlin Heidelberg) pp. 209–249. 4461
- Kauder, K. (2017), “star measurements of the shared mo- 4462
mentum fraction z_g using jet reconstruction in p+p and 4463
au+au”, ” Quark Matter”. 4464
- Khachatryan, V., *et al.* (CMS) (2010), JHEP **1009**, 091. 4465
- Khachatryan, V., *et al.* (CMS) (2015a), Phys. Rev. Lett. 4466
115 (1), 012301. 4467
- Khachatryan, V., *et al.* (CMS) (2015b), Eur. Phys. J. 4468
C75 (5), 237. 4469
- Khachatryan, V., *et al.* (CMS) (2016a), JHEP **02**, 156. 4470
- Khachatryan, V., *et al.* (CMS) (2016b), Eur. Phys. J. 4471
C76 (7), 372. 4472
- Khachatryan, V., *et al.* (CMS) (2016c), JHEP **01**, 006. 4473
- Khachatryan, V., *et al.* (CMS) (2016d), Phys. Lett. **B754**, 4474
59. 4475
- Khachatryan, V., *et al.* (CMS) (2017a), JHEP **04**, 039. 4476
- Khachatryan, V., *et al.* (CMS) (2017b), Phys. Lett. **B765**, 4477
193. 4478
- Khachatryan, V., *et al.* (CMS) (2017c), Phys. Rev. **C96** (1), 4479
015202, arXiv:1609.05383 [nucl-ex]. 4480
- Khachatryan, V., *et al.* (CMS) (2017d), Phys. Lett. **B768**, 4481
103. 4482
- Kodolova, O., I. Vardanian, A. Nikitenko, and A. Oulianov 4483
(2007), Eur. Phys. J. **C50**, 117. 4484
- Krohn, D., J. Thaler, and L.-T. Wang (2010), Journal of 4485
High Energy Physics **2010** (2), 1. 4486
- Kucera, V. (ALICE) (2016), in *Proceedings, 7th International* 4487
Conference on Hard and Electromagnetic Probes of High- 4424
Energy Nuclear Collisions (Hard Probes 2015).
Larkoski, A. J., S. Marzani, G. Soyez, and J. Thaler (2014),
JHEP **05**, 146, arXiv:1402.2657 [hep-ph].
Levai, P., G. Papp, G. I. Fai, M. Gyulassy, G. G. Barnafoldi,
I. Vitev, and Y. Zhang (2002), *Quark matter 2001. Pro-*
ceedings, 15th International Conference on Ultrarelativistic
nucleus nucleus collisions, QM 2001, Stony Brook, USA,
January 15-20, 2001, Nucl. Phys. **A698**, 631.
Lisa, M. A., and S. Pratt (2008).
Lisa, M. A., S. Pratt, R. Soltz, and U. Wiedemann (2005),
Ann. Rev. Nucl. Part. Sci. **55**, 357.
Lokhtin, I. P., L. V. Malinina, S. V. Petrushanko, A. M. Sni-
girev, I. Arsene, and K. Tywoniuk (2009a), Comput. Phys.
Commun. **180**, 779.
Lokhtin, I. P., L. V. Malinina, S. V. Petrushanko, A. M. Sni-
girev, I. Arsene, and K. Tywoniuk (2009b), *Proceedings,*
4th International Workshop on High p(T) physics at LHC,
PoS High-pT physics09, 023.
Majumder, A. (2007a), *Proceedings, 19th International*
Conference on Ultra-Relativistic nucleus-nucleus collisions
(Quark Matter 2006): Shanghai, P.R. China, November
14-20, 2006, J. Phys. **G34**, S377.
Majumder, A. (2007b), J.Phys.G **G34**, S377.
Majumder, A. (2012), Phys. Rev. **D85**, 014023.
Majumder, A. (2013), *Proceedings, 5th International Confer-*
ence on Hard and Electromagnetic Probes of High-Energy
Nuclear Collisions (Hard Probes 2012): Cagliari, Italy,
May 27-June 1, 2012, Nucl. Phys. **A910-911**, 367.
Majumder, A., and J. Putschke (2016), Phys. Rev. **C93** (5),
054909.
Majumder, A., and M. Van Leeuwen (2011), Prog. Part.
Nucl. Phys. **66**, 41.
Mehtar-Tani, Y., and K. Tywoniuk (2015), Phys. Lett. **B744**,
284.
Milhano, G. T. D. A. (2017), “the origin of the modification
of the z_g distribution in aa collisions”, ” Quark Matter”.
Milhano, J. G., U. A. Wiedemann, and K. C. Zapp (2017),
arXiv:1707.04142 [hep-ph].
Miller, M. L., K. Reygers, S. J. Sanders, and P. Steinberg
(2007), Ann. Rev. Nucl. Part. Sci. **57**, 205.
Moreland, J. S., J. E. Bernhard, and S. A. Bass (2015), Phys.
Rev. **C92** (1), 011901.
Muller, B. (2013), *Proceedings, 5th International Conference*
on Hard and Electromagnetic Probes of High-Energy Nu-
clear Collisions (Hard Probes 2012): Cagliari, Italy, May
27-June 1, 2012, Nucl. Phys. **A910-911**, 5.
Nattrass, C., N. Sharma, J. Mazer, M. Stuart, and A. Be-
jnood (2016), Phys. Rev. **C94** (1), 011901.
Neufeld, R. B., I. Vitev, and B. W. Zhang (2011), Phys. Rev.
C83, 034902.
Nonaka, C., and S. A. Bass (2007), Phys. Rev. **C75**, 014902.
Noronha-Hostler, J., B. Betz, J. Noronha, and M. Gyulassy
(2016), Phys. Rev. Lett. **116** (25), 252301.
Novak, J., K. Novak, S. Pratt, J. Vredevoogd, C. Coleman-
Smith, and R. Wolpert (2014), Phys. Rev. **C89** (3),
034917.
Ozonder, S. (2016), Phys. Rev. **D93** (5), 054036.
Poskanzer, A. M., and S. A. Voloshin (1998), Phys. Rev.
C58, 1671.
Pumplin, J., D. R. Stump, J. Huston, H. L. Lai, P. M. Nadol-
sky, and W. K. Tung (2002), JHEP **07**, 012.
Qin, G.-Y., J. Ruppert, C. Gale, S. Jeon, and G. D. Moore
(2009), Phys. Rev. **C80**, 054909.

- 4488 Qin, G.-Y., J. Ruppert, C. Gale, S. Jeon, G. D. Moore, and M. G. Mustafa (2008), Phys. Rev. Lett. **100**, 072301.
- 4490 Qin, G.-Y., and X.-N. Wang (2015), Int. J. Mod. Phys. **E24** (11), 1530014, [,309(2016)].
- 4492 Qiu, J.-w., and I. Vitev (2006), Phys. Lett. **B632**, 507, arXiv:hep-ph/0405068 [hep-ph].
- 4494 Qiu, Z., and U. Heinz (2012), Phys. Lett. **B717**, 261.
- 4495 Qiu, Z., C. Shen, and U. Heinz (2012), Phys. Lett. **B707**, 151.
- 4497 Ranft, J. (1999), arXiv:hep-ph/9911232 [hep-ph].
- 4498 Renk, T. (2008), Phys. Rev. **C78**, 034908.
- 4499 Renk, T. (2009), Phys. Rev. **C80**, 014901, arXiv:0904.3806 [hep-ph].
- 4501 Renk, T. (2013a), Phys.Rev. **C88** (1), 014905.
- 4502 Renk, T. (2013b), Phys. Rev. **C87** (2), 024905.
- 4503 Renk, T., and J. Ruppert (2006), Phys. Rev. **C73**, 011901.
- 4504 Ruppert, J., and B. Muller (2005), Phys. Lett. **B618**, 123.
- 4505 Salam, G. P. (2010), Eur.Phys.J. **C67**, 637.
- 4506 Sapeta, S., and U. A. Wiedemann (2008), Eur. Phys. J. **C55**, 293.
- 4508 Schenke, B., S. Jeon, and C. Gale (2010), Phys. Rev. **C82**, 014903.
- 4509 Schenke, B., S. Jeon, and C. Gale (2011), Phys. Rev. Lett. **106**, 042301.
- 4512 Sharma, N., J. Mazer, M. Stuart, and C. Nattrass (2016), Phys. Rev. **C93** (4), 044915.
- 4514 Shuryak, E. V. (1980), Phys. Rept. **61**, 71.
- 4515 Sickles, A., M. P. McCumber, and A. Adare (2010), Phys.Rev. **C81**, 014908.
- 4517 Sirunyan, A. M., *et al.* (CMS) (2017a), arXiv:1708.09429 [nucl-ex].
- 4519 Sirunyan, A. M., *et al.* (CMS) (2017b), Phys. Lett. **B772**, 306.
- 4521 Sirunyan, A. M., *et al.* (CMS) (2017c), Phys. Rev. Lett. **119** (8), 082301, arXiv:1702.01060 [nucl-ex].
- 4523 Sjostrand, T., S. Mrenna, and P. Z. Skands (2006), JHEP **0605**, 026.
- 4525 Skands, P. Z. (2010), Phys.Rev. **D82**, 074018.
- 4526 Song, H., and U. W. Heinz (2008a), Phys. Rev. **C77**, 064901.
- 4527 Song, H., and U. W. Heinz (2008b), Phys. Lett. **B658**, 279.
- 4528 Srivastava, D. K., R. Chatterjee, and M. G. Mustafa (2016), arXiv:1609.06496 [nucl-th].
- 4530 Suarez, C. (2012), *Baryon to Meson Ratio in Relativistic Heavy Ion Collisions*, Ph.D. thesis (University of Illinois at Chicago).
- 4533 Tachibana, Y., N.-B. Chang, and G.-Y. Qin (2017), Phys. Rev. **C95** (4), 044909, arXiv:1701.07951 [nucl-th].
- 4535 Tannenbaum, M. J. (2017), arXiv:1702.00840 [nucl-ex].
- 4536 Van Hove, L., and A. Giovannini (1988), Acta Phys. Polon. **B19**, 917.
- 4538 Veldhoen, M. (ALICE) (2013), *Proceedings, 5th International Conference on Hard and Electromagnetic Probes of High-Energy Nuclear Collisions (Hard Probes 2012)*, Nucl. Phys. **A910-911**, 306.
- 4542 Vitev, I. (2007), Phys. Rev. **C75**, 064906, arXiv:hep-ph/0703002 [hep-ph].
- 4543 Vitev, I., and M. Gyulassy (2002), Phys. Rev. Lett. **89**, 252301.
- 4546 Vitev, I., S. Wicks, and B.-W. Zhang (2008), JHEP **11**, 093.
- 4547 Voloshin, S. A., A. M. Poskanzer, and R. Snellings (2008), in *Relativistic Heavy Ion Physics*, edited by R. Stock, Chap. 23 (Springer Berlin Heidelberg) pp. 293-333.
- 4548 Wang, X.-N., and X.-f. Guo (2001), Nucl. Phys. **A696**, 788, arXiv:hep-ph/0102230 [hep-ph].
- 4552 Wang, X.-N., and Z. Huang (1997), Phys. Rev. **C55**, 3047.
- 4553 Wicks, S., W. Horowitz, M. Djordjevic, and M. Gyulassy (2007), Nucl. Phys. **A784**, 426.
- 4555 Wiedemann, U. A. (2000a), Nucl. Phys. **B588**, 303.
- 4556 Wiedemann, U. A. (2000b), Nucl. Phys. **B582**, 409.
- 4558 Wiedemann, U. A. (2001), Nucl. Phys. **A690**, 731.
- 4559 Wong, C.-Y. (2007), Phys. Rev. C **76**, 054908.
- 4560 Wong, C.-Y. (2008), Phys. Rev. C **78**, 064905.
- 4561 X.-N. Wang, and M. Gyulassy, (1991), Phys. Rev. D **44**, 3501.
- 4562 Zakharov, B. G. (1996), JETP Lett. **63**, 952.
- 4563 Zapp, K. C. (2014a), Phys.Lett. **B735**, 157.
- 4564 Zapp, K. C. (2014b), Eur. Phys. J. **C74** (2), 2762.
- 4565 Zardoshti, N. (ALICE) (2017), in *26th International Conference on Ultrarelativistic Nucleus-Nucleus Collisions (Quark Matter 2017) Chicago, Illinois, USA, February 6-11, 2017*, arXiv:1705.03383 [nucl-ex].
- 4566 Zhang, H., J. F. Owens, E. Wang, and X.-N. Wang (2007), Phys. Rev. Lett. **98**, 212301.
- 4567 Zhang, H., J. F. Owens, E. Wang, and X.-N. Wang (2009), Phys. Rev. Lett. **103**, 032302, arXiv:0902.4000 [nucl-th].
- 4571 Zimmermann, A. (ALICE) (2015), in *10th International Workshop on High-pT Physics in the RHIC/LHC Era (HPT 2014) Nantes, France, September 9-12, 2014*.